Mémoire

Auteur : Rosenberg, Océane
Promoteur(s) : Michel, Loïc; 29043
Faculté : Faculté des Sciences
Diplôme : Master en océanographie, à finalité approfondie
Année académique : 2024-2025
URI/URL : http://hdl.handle.net/2268.2/23915

Population Dynamics and Reproduction of Vent Ophiuroids

(Azores, Portugal)

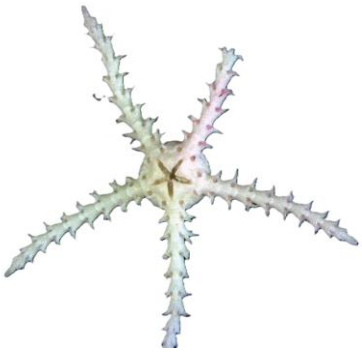

Océane Rosenberg

Promotor: Dr. Ana Colaço[1]
Co-promotor: Professor Loïc Michel[2]

A Thesis presented for the degree of Master in Oceanography

University of Liège, Belgium

Academic year 2024-2025

[1] Institute of Marine Sciences – Okeanos, University of the Azores, Horta, Portugal
[2] Laboratory of Oceanology, Freshwater and Oceanic Sciences Unit Research (FOCUS), University of Liège, Belgium

According to the rules imposed by the jury of the Master in Oceanography, this document must not exceed 50 pages in Times 12 or an equivalent font.

Acknowledgements

First, I would like to express my gratitude towards Loïc Michel and Ana Colaço for accepting my request to be my promotors and for their guidance and advice throughout this work. Their expertise, availability and constructive feedback were precious to write this thesis.

I would like to extend a friendly thank you to Luis, laboratory technician at the Okeanos, for his invaluable help in preparing the various solutions tested in the laboratory, as well as his kindness. His help greatly facilitated the progress of my experimental procedures.

I must also thank Joana and Domitila for their invaluable help in preparing my paraffin blocks. Their skill to help were essential for the successful completion of my histological work.

In addition, I would like to deeply thank Mariana and Aditi for their kindness, encouragement, and unwavering support, as well as for their advice and assistance. I would like also to express my gratitude for their warm welcome to the deep sea laboratory which created a motivating and friendly environment that made my stay all the more enriching.

A very special thank you goes also to Juliette, Anne and Moème for their unwavering friendship, support, and wise advice. Their presence has been a source of comfort, motivation, and joy.

I also would like to thank my readers, Professor Philippe Compère, Professor Stéphane Roberty and Professor Charles Troupin, for taking the time to read my thesis. I truly appreciate their interest in my work and their valuable feedback

Lastly, I would like to extend my heartfelt thanks to everyone who supported me throughout this thesis with their insights, guidance, kind words, and constructive feedback.

Abstract

This thesis studies the population dynamics and reproductive biology of *Ophioctenella acies,* a brittle star associated with deep hydrothermal systems on the Mid-Atlantic Ridge, sampled at the Broken Spur and Rainbow Pit hydrothermal sites at depths of 3,100 m and 1,900 m, respectively. Using a morphometric and histological approach, the collected specimens were analyzed to better understand their life cycle, fertility, and reproductive dynamics. The analysis of disc sized enabled the identification of multiple cohorts, indicating a pattern of annual recruitment. The results show a mixed demographic structure with the presence of young stages in the cohorts, supporting the hypothesis of regular recruitment. Histologically, the gonads showed different gametogenic stages, with no apparent synchronization, reflecting continuous reproduction throughout the year. This can be a reproductive strategy adapted to the variable conditions of extreme environments. The species *O. acies* appears to reproduce opportunistically, with high individual variability in terms of fertility and oocyte size, regardless of body size. These findings contribute to a better understanding of the adaptation of ophiuroids to hydrothermal habitats and the resilience of hydrothermal communities to environmental disturbances. This study therefore aims to understand their reproductive strategies and the adaptations that enable them to survive and reproduce in these isolated and specific extreme environments.

Résumé

Cette thèse étudie la dynamique de population ainsi que la biologie de reproduction d'*Ophioctenella acies*, une ophiure associée aux systèmes hydrothermaux profonds de la dorsale médio-atlantique, échantillonnées sur les sites hydrothermaux de Broken Spur et Rainbow Pit respectivement à 3100 m et 1900 m de profondeur. À travers, une approche morphométrique et histologique, les individus récoltés ont été analysés afin de mieux comprendre leur structure de population, leur biologie reproductive ainsi que leur dynamique de reproduction. L'analyse des tailles de disque a permis de discriminer plusieurs cohortes, montrant une structure démographique mixte avec une présence de jeunes stades appuyant l'hypothèse d'un recrutement régulier. Sur le plan histologique, les gonades présentaient différents stades gamétogéniques, sans synchronisation apparente, ce qui reflète une stratégie de reproduction adaptée aux conditions variables des environnements extrêmes. L'espèce *O. acies* semble présenter une reproduction de type opportuniste, avec une grande variabilité individuelle en termes de fécondité et de taille ovocytaire, indépendamment de la taille corporelle. Ces éléments contribuent à une meilleure compréhension de l'adaption des ophiures aux habitats hydrothermaux et des processus de résilience des communautés hydrothermales face aux perturbations environnementales. Cette étude vise donc à comprendre leurs stratégies reproductives et les adaptations qui permettent leur survie et reproduction dans ces environnements extrêmes isolés et spécifiques.

Contents

List of Abbreviations

AD	Adoral Shield
AS	Arm Spines
AUV	Autonomous Underwater Vehicles
DAP	Dorsal Arm Plate
DS	Disc Spines
HOV	Human Occupied Vehicles
MAR	Mid Atlantic-Ridge
MO	Mature Oocytes
MPA	Marine Protected Areas
MSR	Marine Scientific Research
OO	Oogonia
OP	Oral Papillae
OS	Oral Shield
PVO	Pre Vitellogenic Oocyte
ROV	Remotely Operated Vehicles
RS	Radial Shield
VAP	Ventral Arm Plate
VO	Vitellogenic Oocyte

I) INTRODUCTION

1) Background

Covering nearly 71% of Earth's surface, the ocean plays a crucial role on our planet, in sustaining life and providing the foundation for a vast range of dynamics and diverse ecosystems. Oceanic primary production, a photosynthetic activity of phytoplankton contributes to almost half of global net primary production (NPP) (Behrenfeld et al., 2006), supporting the richness and complexity of marine ecosystems. The ocean offers us an exceptional biodiversity and different types of habitats, with the vast majority of marine species still remaining undescribed by science (Mora et al., 2011).

Surface ecosystems, particularly those located in coastal areas, are among the most productive and species-rich environments. For example, tropical coral reefs host a significant proportion of the world's marine biodiversity, while mangroves and seagrass beds protect coastlines and store large quantities of blue carbon in their sediments (Alongi, 2012). These coastal ecosystems provide many essential ecosystem services, such as protection against erosion, support for fisheries and carbon sequestration (Barbier et al., 2011). Benthic habitat diversity is shaped by multiple interacting parameters, notably light availability, the physico-chemical properties of the water column (e.g., temperature, levels of dissolved oxygen, surface productivity, salinity, and ice cover), and the physical structure of the seabed, including depth, sediment grain size, and substrate morphology (Anderson et al., 2010; Huang et al., 2011). In subtidal areas, habitats range from sandy and muddy bottoms to seagrass meadows and coral reefs each hosting distinct ecological communities (Joydas et al., 2019). Intertidal environments typically include mangrove forests, sandy shores, rocky shores and protected tidal flats often linked to bays or coastal lagoons. These habitats can be both soft substrate (e.g., muddy, sandy or gravelly bottoms) and hard substrate (e.g., coral reefs, outcrops or artificial structures) which provide stable support for sessile organisms such as sponges, cold-water corals, ascidians mussels or barnacles (Bonsdorff et al., 1996; Brzana & Janas, 2016; Joydas et al., 2019). Some habitats are described as biogenic because they are created or structured by organisms themselves. These include seagrass beds, kelp forests, and tropical coral reefs. These living structures play an essential role in providing shelter, food and breeding sites for many species (Lot et al., 2019).

As you move away from the coast, in the open ocean, you encounter the oceanic pelagic zone, which is organized into different vertical superposed layers, including the epipelagic zone (0-200 m) and the deep sea from 200 m depth (Angel, 2003; Bell et al., 2025). Although local densities are often low, the extent of the high seas means that the cumulative biomass, productivity and biodiversity of oceanic pelagic areas are remarkably high on a global scale. These open waters are essential for regulating the Earth's climate and for the survival of major commercial fisheries and some small-scale artisanal fisheries. They are also essential habitats for a wide range of species such as tuna, large sharks, dolphins, whales, squid, seabirds and sea turtles (Spalding et al., 2012).

Lastly, the deep sea, the largest biome on earth, encompasses 90 % of our oceans and represents the final frontier of marine ecosystems. It comprises the pelagic environments such as the mesopelagic zone (200-1000 m), the bathypelagic zone (1000-3000 m) and the abyssopelagic zone (> 3000m) (Angel, 2003). The benthic environments, from continental shelves to abyssal plains (3000-6000m deep) and hadal depths including ocean trenches (> 6000m deep), are characterized by physico-chemical constraints. Despite extreme conditions, the seabed is home to a high level of biodiversity and communities of organisms with remarkable adaptations, revealing the amazing functional diversity of marine life (Ramirez-Llodra et al., 2010).

Benthic ecosystems play an essential role in the overall dynamics of marine environments. Infaunal invertebrates largely influence a series of essential ecological processes, including the carbon cycle and sedimentary carbon storage. These ecosystems deliver essential ecological services, yet they are becoming increasingly vulnerable to human-induced pressures such as bottom-contact fishing, mining, pollution, shipping and offshore oil and gas operations (Halpern et al., 2008; William et al., 2010; Lecours et al., 2015; Harris, 2020).

2) Deep sea benthic environments

The deep sea is the largest biome on earth, yet it remains largely unexplored and misunderstood, with only 0.01% of the ocean floor sampled and studied, and 5% explored (Bell et al., 2025). However, we do know that this environment contains the most abundant biodiversity on Earth (Tyler et al., 2003; Ramirez-Llodra et al., 2010). In these environments, mainly inaccessible to humans, the development of remote sensing mapping techniques (e.g., scanning sonar) and direct observation techniques (e.g., human-occupied vehicles (HOV's), remotely operated vehicles (ROV's), autonomous underwater vehicles (AUV's), submersibles) with ever increasing capability are making it possible to define the deep ocean floor more precisely (Greene et al., 1999; German et al., 2008; Bell et al., 2025). These technologies made it possible to observe active hydrothermal vents on the Galápagos Ridge for the first time in 1977, at a depth of approximately 2500 m, thanks to the *DSV Alvin* submersible (Corliss et al., 1979; Bell et al., 2025).

The deep-sea floor from the continental slope to the abyssal plains represents 362km^2 of the 510km^2 of the earth's surface and is formed by many geological structures such as mid-ocean ridges, canyons, seamounts, cold-water coral reefs, hydrothermal vents, methane seeps, mud volcanoes, faults and trenches (**Figure 1**; Ramirez-Llodra et al., 2010).

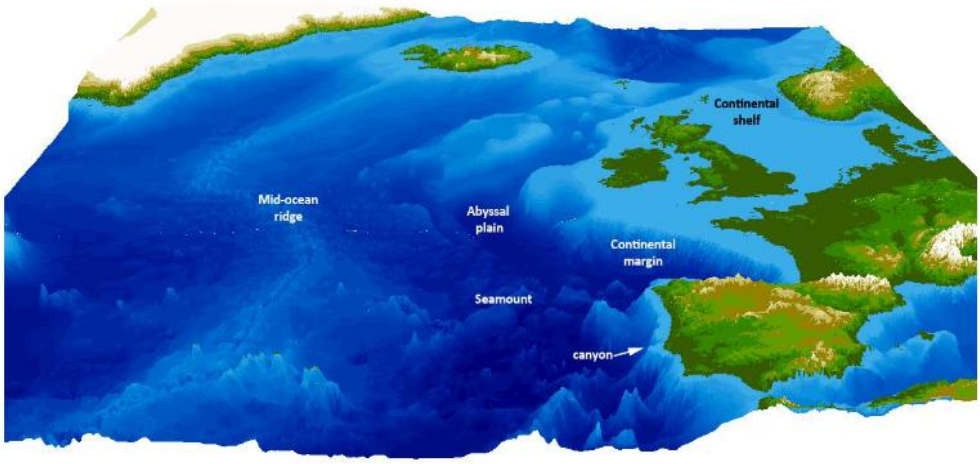

Fig. 1. Map of the North-East Atlantic showing the different ecosystems of the deep sea (Ramirez-Llodra et al., 2010; © ˚Age Høines, MAR-ECO).

Abyssal plains are estimated to cover approximately 76% of the ocean floor, making them the main benthic habitat. They are followed by continental margins (10%) and the mid-ocean ridge system (9%). Although less extensive, seamounts (2.6%) and oceanic trenches (2%) also represent a significant part of the seafloor. In contrast, other specific environments such as hydrothermal vents, cold seeps, whale carcass falls, benthic oxygen minimum zones (OMZs) and cold-water coral reefs occupy much smaller areas and remain highly localized (Ramirez-Llodra et al., 2010).

The deep ocean plays a key role in regulating the climate, particularly through carbon

sequestration (e.g., sinking of marine snow and whale fall) (Pearson et al., 2023), and contributes to the production of ~80% of the Earth's oxygen thanks to phytoplankton sustained by upwelling deep cold waters (Yamaguchi et al., 2024). It is also a major food resource, with 200 million tons of fish and seafood caught each year (Ritchie & Roser, 2021), and represents a promising reservoir of therapeutic molecules derived from marine organisms such as sponges and bacteria (Hamoda et al., 2021; Saeed et al., 2021). However, this vital ecosystem is now seriously threatened by pollution, industrial exploitation including fishing and mining and the consequences of climate change (e.g., warming, acidification, deoxygenation) (Ramirez-Llodra et al., 2010; 2011; Bell et al., 2025).

The deep ocean is a dynamic environment, not as stable and uniform as was once thought, with regular disturbances such as tidal currents and seasonal phytodetritus deposits, as well as episodic disturbances such as benthic storms (Ramirez-Llodra et al., 2010). In many cases, deep-sea environments are resource-poor, fed mainly by the constant descent of nutrient particles from surface waters. This slow fall in organic matter sustains benthic communities that may not be very productive but are particularly diverse, with a predominance of filter-feeding organisms and species that feed on deposits (Georgieva et al. 2021). The limited availability of food resources in the deep sea, both on the seabed and throughout the water column, significantly shapes the trophic organisation of the heterotrophic communities. These ecosystems are particularly well adapted to survive in low-energy conditions. In general, in these food-poor environments, the megafauna is mainly detritivorous and depends on the decomposition of organic matter. Life at depth is marked by the phenomena of dwarfism and gigantism in certain organisms, two adaptive strategies in response to a progressive reduction in food availability as depth increases. Gigantism, in particular, is thought to be encouraged by the fact that large invertebrates expend proportionally less energy per unit of mass than smaller ones (Peters, 1983; Ramirez-Llodra et al., 2010**)**, giving them an advantage in these environments where resources are limited. In contrast, habitats with hard surfaces (e.g., mid-ocean ridges, seamounts, canyon walls or coral reefs) **(Figure 1;** Ramirez-Llodra et al., 2010**)** tend to support a higher concentration of filter feeders, which thrive by extracting particles from the surrounding water. Furthermore, in reducing environments (e.g., hydrothermal vents), energy production is mainly achieved by chemoautotrophy, supported by symbiotic interactions between host organisms and chemosynthetic microbes (Ramirez-Llodra et al., 2010).

2.1) Hydrothermal vents ecosystem

2.1.1) Hydrothermal vent dynamics

In the ocean, many areas of high volcanic activity rise to hydrothermal vents which are most commonly found along the mid-ocean ridge, the world’s longest mountain chain. These vents occur at depths beyond the reach of sunlight, where superheated fluids exceeding 400 °C, rich in dissolved minerals, form the basis of unique and complex ecosystems. Although more than 300 active hydrothermal fields have been confirmed to date (Beaulieu and Szafranski, 2020), their extent remains extremely small on a global scale, representing less than 0.00001% of the planet's total surface area (Van Dover et al., 2018).

Hydrothermal vent structures are characterized by the emission of hot fluids, loaded with minerals and chemical compounds, emitted from spreading centers and formed well below the seafloor, generally at bathyal depths (Fisher et al., 2007; Georgieva et al. 2021). These thermochemical interactions mainly occur in permeable geological layers of the oceanic crust, such as the extrusive layer (0.5-1 km thick), where seawater percolates through cracks and fissures in the oceanic crust until it reaches rock heated by shallow pockets of magma. At this point, the interaction between seawater and hot rock causes the fluid to lose elements like oxygen, magnesium, and sulfates, while gaining hydrogen, carbon dioxide, methane, sulfides, silica, and

reduced metals while rising in temperature (Holden et al., 2012). When superheated fluids are discharged onto the ocean floor, they cool rapidly. This sudden change in temperature leads to the precipitation of numerous dissolved compounds and to the formation of sulfide chimneys, where complex thermal and chemical gradients then develop (Fisher et al., 2007; Holden et al., 2012). This chemical process is responsible for the formation of hydrothermal vents, mineral structures composed mainly of iron, copper, and zinc sulfides (Fisher et al., 2007). These fluids are anoxic, highly reduced, and acidic (pH from 2-4), contain significant quantities of gases, including CO_2, H_2S, H_2 and sometimes CH_4, whose composition varies according to temperature and pressure (Von Damm et al., 1995; Fisher et al., 2007; Levin et al., 2016). In addition to representing major geological formations, they are often rich in mineral resources of economic interest (Georgieva et al., 2021).

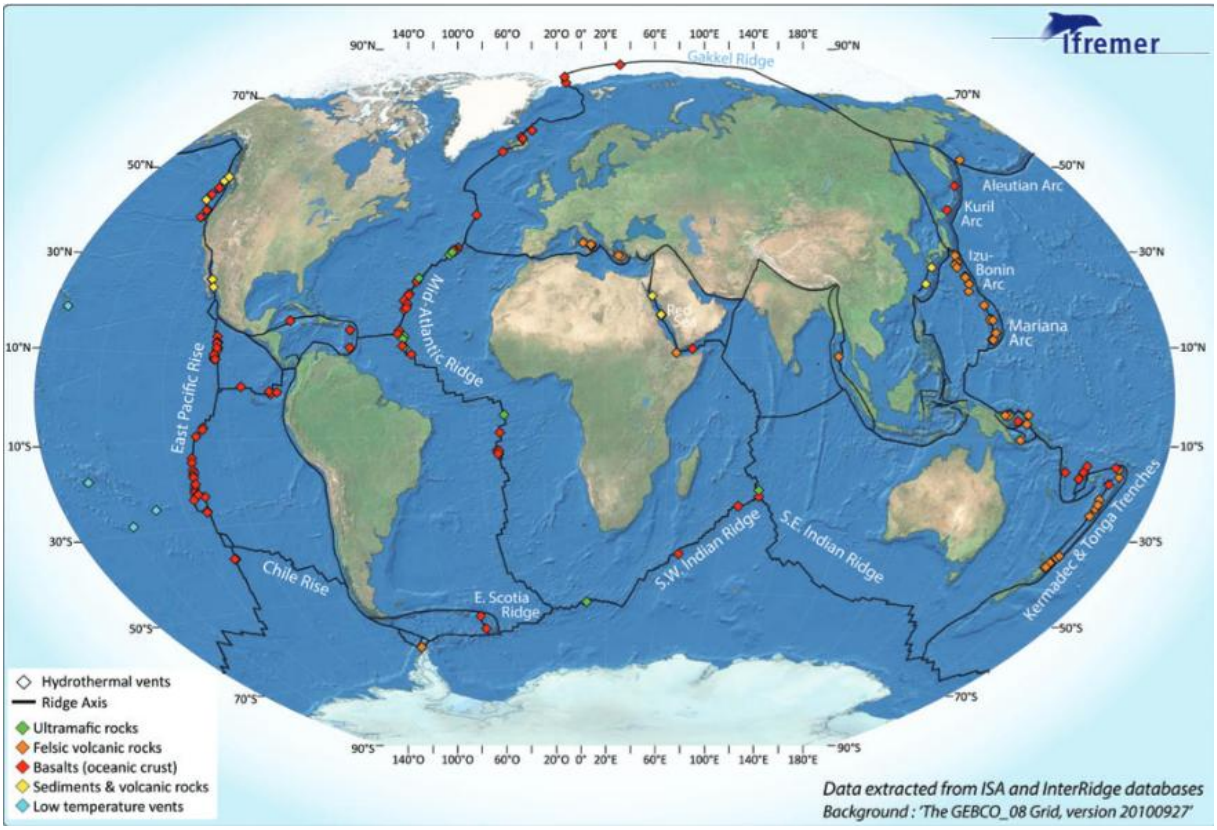

Fig. 2. Known and sampled hydrothermal vent sites located along mid-ocean ridges with their geological context (Ifremer; Konn et al., 2015)

The actual number of hydrothermal vents and locations remains unknown. A global estimate of active hydrothermal fields has been estimated at around 1060 fields. (Baker & German, 2004). About 521 vent fields have been identified in the world's oceans to date. These fields are either confirmed by direct observation (i.e., ground-truthing) or detected by hydrothermal plumes in the water column, turbidity, or chemical anomalies. They are distributed in different tectonic zones: mid-ocean ripples (52%), arc volcanoes in subduction zones (25%), back-arc spreading centers (21%) and intraplate volcanoes (2%) (Beaulieu et al., 2013; **Figure 2**).

Hydrothermal ecosystems offer a diversity of ecosystem services (Levin et al., 2016), in particular through their contribution to biogeochemical cycles and the transformation of elements such as carbon, sulfur and nitrogen (Hinrichs & Boetius, 2022). Although localised, the vents create chemical gradients and energy-rich biogeochemical zones favorable to primary

production and biomass. These environments support the active activity of oxidising microorganisms of Fe, Mn, CH_4 and NH_4+ (Holden et al., 2012). Deep-sea hydrothermal vents are attracting growing interest as potential contributors to iron (Fe) enrichment in the inner ocean. This dissolved iron from the ocean floor could be transported over long distances to regions such as the Southern Ocean (Lough et al., 2022). This phenomenon is all the more important given that iron is a limiting nutrient for primary productivity in several key ocean areas, playing a central role in regulating the global carbon cycle. On a global scale, hydrothermal inputs of dissolved iron to the deep ocean are estimated at between 3 and 4 gigamoles per year (Resing et al., 2015). Hydrothermal plumes can supply up to 25% of all the Fe dissolved in the deep ocean (Bennett et al., 2008; Holden et al., 2012).

Other ecosystem services exist, such as precipitation of sulfide minerals (e.g., iron, zinc, copper) attracting mining interest, communities offering genetic potential for biotechnology (e.g., enzymes, drugs), cultural services (e.g., art, literature, education, research) (Turner et al., 2019) and finally, the contribution to a high diversity of organisms in the deep sea and habitat creation (Levin et al., 2016).

2.1.2) Ecological role of hydrothermal vents

These structures, with their thermal and chemical gradients, also generate a wide variety of microhabitats, populated by rare and endemic species, perfectly adapted to the extreme conditions of these environments (Fisher et al., 2007; Georgieva et al. 2021).

The discovery of hydrothermal vents in 1977 revolutionized our view on oceanic primary production processes (Baker et al., 2010). Hydrothermal vent environments derive their energy from chemical reactions. This energy comes from chemoautotrophic micro-organisms capable of transforming reduced compounds, such as hydrogen sulfide (H_2S), dihydrogen (H_2), methane (CH_4) or even ferrous iron (Fe^{2+}), present in the fluids emitted by vents, into organic matter. These bacteria play a fundamental role in forming the base of the food chain. They are found either in free form in their environment in long-distance plumes, in local particles consumed by filter feeders, in microbial mats grazed by herbivores, or in symbiotic association with macro-invertebrates (Tunnicliffe, 1991). In the latter case, they may be integrated directly into the animal's tissues (endosymbiosis) or attached to their outer surface (ectosymbiosis) (Georgieva et al. 2021). In both cases, they represent the main food source that sustains the entire food chain (Tunnicliffe, 1991; Fisher et al., 2007).

Trophic structures are determined on three levels: producers with chemosynthetic or methanotrophic bacteria, primary consumers with mussels, shrimps and polychaetes, and predators with fish, crinoids and ophiuroids (Gebruk et al., 1997). Fluid chemistry and the variability of hydrothermal flow generate local heterogeneity. Around these vent structures, animal communities are organized according to a marked zonation, from the active center, very hot and rich in reduced fluids, to the colder, more stable periphery (Tunnicliffe, 1991; Gebruk et al., 1997). The distribution of organisms depends mainly on their ability to tolerate the toxicity of the chemical compounds contained in hydrothermal fluids (Chausson, 2001). Hydrothermal vent ecosystems are generally characterized by a dominance of benthic invertebrates such as vestimentiferan tubeworms, bathymodiolin mussels, vesicomyid clams, provannid snails, rimicarid shrimp, and yeti crabs that maintain symbiotic relationships with chemoautotrophic microorganisms (Van Dover, 2014). These symbiotic microorganisms rely on electron donors such as sulfide found in vent fluids, electron acceptors like oxygen present in seawater, and sources of inorganic carbon, which can include CO_2 or methane from vent emissions, as well as dissolved CO_2 in the surrounding seawater (Van Dover, 2014).

The stability of the communities depends on the lifespan of the hydrothermal structures. Furthermore, vents are active environments where catastrophic eruptions can wipe out whole communities in very short periods of time (Ramirez-Llodra et al., 2010). When a new source

appears, there is rapid colonisation and ecological succession, initially by pioneer species followed by specialised ones (Grassle, 1985). Connectivity between hydrothermal vent communities depends largely on larval dispersal, a process shaped by oceanographic conditions, the duration and behavior of the larval stage, and the dynamics of vent activity itself (Turner et al., 2019). Vents are known to act as stepping stones for species dispersal (Turner et al., 2019).

The soundscapes specific to certain deep-sea habitats such as hydrothermal vents could act as acoustic signals enabling benthic larvae to detect and reach suitable habitats for their settlement. Indeed, the dynamic activity of hydrothermal vents, including high-pressure venting and adjacent eruptions, leads to significant acoustic emissions. These structures are reported to generate unique acoustic signatures that guide the larvae as they disperse, sometimes over very long distances, towards specific, suitable habitats (Lin et al., 2019; 2021).The sounds emitted (up to 50 dB above the ambient level) vary according to the type of geological structure or biological community present (Lin et al., 2019).

2.1.3) Anthropogenic impacts

Vents are located on ridges present in all oceans, mostly in deep water away from the direct effect of variations of sea-level and climate (Tunnicliffe, 1991). Natural disturbances to hydrothermal vent ecosystems are mainly caused by volcanic eruptions, the hydrothermal cycle, tectonic activity and, to a much lesser extent, tidal fluctuations (Van Dover, 2000).

However, since their discovery over 40 years ago, marine scientific research (MSR) has been the main source of human disturbance in these environments. Although motivated by the goals of exploration and contributing to human knowledge, these activities lead to increased pressure on these sensitive ecosystems (Glowka, 2003). Most damage to hydrothermal vents is caused by Human-Occupied Vehicles (HOVs) and Remotely Operated Vehicles (ROVs) due to their sometimes clumsy maneuvers, light pollution, intensive and destructive sampling (Van Dover, 2000).

A number of legal frameworks are in place to protect these ecosystems, such as the United Nations Convention on the Law of the Sea (UNCLOS), which aims to protect rare or fragile ecosystems, and the Convention on Biological Diversity (CBD), which imposes obligations on states to conserve ecosystems and species, especially through the creation of marine protected areas (MPAs) (Glowka et al., 1994; Glowka, 2003). In October 2001, the Azores Regional Government proposed the creation of marine protected areas at the Menez Gwen and Lucky Strike hydrothermal sites along the Mid-Atlantic Ridge (Santos et al., 2003). In these cases, the boundaries of MPAs would be defined in such a way that MSR would be the only activity authorized, framed by precise zoning within hydrothermal fields, thus excluding all mining, fishing, or tourism activities (Glowka, 2003).

However, we are witnessing the emergence of the deepwater mining industry, with a growing interest in new sources of minerals and materials, particularly seafloor massive sulfides (SMS). SMS are mineral deposits enriched in metals (Fe, Cu, Zn, Pb), and are notably high in sulfur content that precipitate from hydrothermal fluid as it interacts with the cooler seawater (Hoagland et al., 2010).

Hydrothermal vents are also highly threatened by the mining of polymetallic sulfides rich in metals such as copper. Acting under the United Nations Convention on the Law of the Sea, the International Seabed Authority (ISA) oversees the exploration and exploitation of seabed resources in international waters, with the mandate to ensure these activities serve the interests of humankind (Gollner et al., 2021). The ISA has therefore awarded several member states research and exploration contracts for polymetallic sulfides on hydrothermal sites. These ecosystems are vulnerable because they are rare and fragmented habitats covering a very small area (<50 km^2 worldwide) with assemblages of specific and endemic communities whose resilience remains highly uncertain (Van Dover et al., 2018; Gollner et al., 2021). In order to protect

these environments on a regional and global scale, the International Seabed Authority (ISA) has organized a mining code and established a research program aimed at improving existing plans for the spatial management of vent ecosystems. Some areas where hydrothermal sites are found are already protected by effective measures within certain Exclusive Economic Zones (EEZs) and continental shelves or by conventions and measures such as Marine Protected Areas (MPAs) (Rona et al., 2010; Abecasis et al., 2015; Menini & Van dover, 2019). In the North-East Atlantic, four hydrothermal sites have been recognized as EBSA's (Ecologically or Biologically Significant Areas) by the Convention on Biological Diversity (CBD). A marine area is considered an EBSA when it holds exceptional ecological and/ or biological value, such as serving as a critical habitat a vital food source, or a breeding site for specific species (Convention on Biological Diversity, 2012). They are also characterised as Vulnerable Marine Ecosystems (VMEs) by the Food and Agricultural Organization (FAO).

To date, mining remains the only human activity to threaten hydrothermal vent ecosystems. The ability of these environments to recover naturally from a single mining disturbance mainly depends on immigration, larval recruitment, and colonization. Deep mining activities generate excessive noise that masks natural geophony (i.e., sounds produced by geological or geophysical activities such as volcanic eruptions) and biophony (i.e., sounds generated by organisms intentionally or unintentionally, depending on behavioral contexts, species and even populations) and make habitats “invisible” to larvae (Lin et al., 2019; Duarte et al., 2021). This noise alters the connectivity between habitats, affecting ecological resilience and potentially disrupting recolonisation cycles following damage (Lin et al., 2019). Understanding the ecological and biological processes and dynamics that govern life-history stages could be crucial to reduce and mitigate the long-term consequences of mining operations (Van Dover, 2014).

3) Deep sea hydrothermal vent fauna

The success and dense biomass of vent ecosystems are fuelled by a constant source of energy and symbiotic partnerships between chemoautotrophic microorganisms and their animal hosts. These flourishing and diverse communities are in stark contrast to the sterile seabed that surrounds them (Ramirez-Llodra et al., 2010).

Around 600 species have been identified worldwide in hydrothermal vent ecosystems, many of the invertebrates that host chemoautotrophic bacteria and are endemic to the vents (Desbruyères et al. 2006). These adapted organisms can withstand extreme temperatures and high concentrations of heavy metals and toxic substances (Grassle, 1985). In hydrothermal vents, biodiversity is low, but abundance and biomass are high, and the communities are dominated by a few species (Ramirez-Llodra et al., 2010). In fact, some species are endemic to hydrothermal systems. Such is the case of the shrimp *Rimicaris exoculata*, widespread along the mid-Atlantic ridge (MAR), which is found in dense aggregations in the immediate proximity of hot fluid emissions. They draw their energy from the symbiotic bacteria that colonize their gills and mouthparts, using the hydrogen sulfide present in the fluids to produce organic matter (Van Dover et al., 1988; Gebruk et al., 1997). Other species live in symbiosis, such as the emblematic vestimentiferan of hydrothermal vents of the East Pacific Rise, the giant tubicolous worms *Riftia pachyptila*, which have no mouth or anus when they reach adulthood and are housed in chitinous tubes (Grassle, 1985).

Anomurans associated with hydrothermal vents mainly belong to the families Galatheidae, Chirostylidae, Lithodidae, Kiwaidae and Parapaguridae. They are generally observed in greater abundance at the periphery of hydrothermal vents. These crustaceans have a wide variety of reproductive strategies, life cycles and dispersal capacities, ranging from pelagic egg-laying to direct development (Segonzac & Desbruyères, 1997). The yeti crab (*Kiwa hirsuta*), discovered in 2005 on the Pacific-Antarctic Ridge, lives near active hydrothermal vents. Its morphology is adapted to this extreme habitat, with atrophied eyes (partially or totally blind)

and appendages covered in long setae that host symbiotic filamentous bacteria (Macpherson et al., 2005).

Polychaetes come in various forms, including fireworms, chaetopterans and alvinellids. *Alvinella pompejana*, a thermophilic worm endemic to the East-Pacific Ridge, lives directly attached to the walls of active hydrothermal vents, where temperatures can exceed 80°C. It is considered to be one of the most thermotolerant metazoans known. This species constructs protective tubes made of chitin and proteins, providing a barrier against extreme temperatures and heavy metals. Temperatures measured in these tubes vary on average between 30 and 68°C, with peaks of up to 81°C (Grassle, 1985; Le Bris & Gaill, 2007).

The mussel *Bathymodiolus thermophilus* is a mytilid bivalve of deep hydrothermal vents, harbouring chemotrophic symbionts while retaining a functional digestive tract. This species exhibits marked sexual dimorphism, with females generally being larger than males, and possible successive hermaphroditism, with males becoming females after spawning (Berg et al., 1985; Tunnicliffe, 1991). Its long and planktotrophic larval development favors a high dispersal capacity, which is an important adaptive advantage for the colonization of new hydrothermal sites (Van Dover, Berg & Turner, 1988; Tunnicliffe, 1991).

Vesicomyiid clams, often referred to as the "giant clams" of mid-ocean ridges, live buried in the cracks of basalt near hydrothermal vents. Their muscular feet insert deep into these crevices to capture dissolved sulfide, which is then transported by the vascular system to symbiotic bacteria located in their gills (Fisher et al., 1988; Tunnicliffe, 1991).

Although fish are significantly less abundant than invertebrates in hydrothermal environments, some species, particularly those in the family Zoarcidae, are closely associated with them. The genera *Thermarces* and *Pachycara* are largely dominant, accounting for nearly 50% of the fish species recorded at hydrothermal vents and cold seeps. However, strictly vent-dependent fishes remain rare, with only 21 species identified to date from approximately 50 hydrothermal fields, reflecting both limited species diversity and high endemism within these extreme ecosystems (Biscoito et al., 2002).

Molluscs (36.1% of all vent animals), arthropods (34.3%), and polychaetes (18.1%) dominate this environment because they possess protective structures (i.e., shells, tubes, exoskeletons) that are useful against chemical toxicity and suspended particles. These groups are also the most tolerant of extreme conditions in other marine environments. 83.4% of known species are strictly endemic to vents. This high endemism suggests that hydrothermal vents function as isolated biogeographic islands, favoring rapid speciation and lineages obligately associated with these extreme environments (Wolff, 2005). Other species can be found such as anemones, gastropods, barnacles and even octopods in hydrothermal vents in the Southern Ocean, along the East Scotia Ridge (ESR) (Rogers et al., 2012).

Among the echinoderms, a group poorly represented in hydrothermal vents, holothuroids have been identified, notably *Chiridota hydrothermica*, endemic to active hydrothermal sites in the Pacific, found in direct contact with hot fluids (Smirnov et al., 2000). A seven-armed starfish, belonging to the Stichasteridae family and endemic to hydrothermal vents, has been observed both in the immediate proximity of smokers and on the periphery, in areas of low diffusion and low temperature. This species appears to feed on organisms typical of vents, including the Kiwa n. sp. crab and barnacles. (Rogers et al., 2012). And finally, we identify ophiuroids like the dominant and very abundant species *Ophiocten gracilis* and *Amphioplus daleus* at the vents of the Mohn Ridge in the North Atlantic (Schander et al., 2010).

3.1) Ophiuroids

3.1.1) Ecology

Ophiuroid species richness varies depending on the type of habitat, whether hydrothermal vents, seamounts, abyssal plains, deep ocean floor or cold-water coral reefs (Schmidt et al., 2024). According to available data for 1,512 species of ophiuroids, 37% live at depths of less than 100 m, 39% between 100 and 1000 m, and 24% at depths greater than 1000 m (Hendler & Tran, 2001). Ophiuroids, which represent the most abundant megafaunal taxon in non-reducing deep-sea environments (Gage & Tyler, 1991), have also been reported from several hydrothermal sites (Tyler et al., 1995; Stöhr & Segonzac, 2006; Rodrigues et al., 2011). Hydrothermal vents located on the East Pacific Ridge and the Pacific-Antarctic Ridge support the endemic species *Spinophiura jolliveti* (Ophiuridae), while *Ophiolamina eprae* **(**Ophiacanthidae) is present in vents in the East Pacific. The latter is rarer than *S. jolliveti*, probably because it lives hidden in crevices or on other animals. It is found at depths of around 2590 m, associated with the fixed and mobile fauna of the vents. *S. jolliveti* is associated with Bathymodiolus mussel beds present in hydrothermal diffusion zones and is also observed on substrates colonised by chemosynthetic bacteria (Stohr & Segonzac, 2006).

The seafloor between and around the mounds was home to ophiuroids and crinoids, settled on sulfur blocks and outcrops. These ophiuroids were observed in close proximity to the hydrothermal vents, coexisting with typically event-dependent species, such as *Ridgeia sp*., at a Northeast Pacific spreading center (Juiniper et al., 1992).

The density of ophiuroids observed in the Central Bransfield Basin (Antarctica) in the immediate vicinity of the active hydrothermal area (approximately 15 individuals/m²) was not higher than that of another ophiuroids bed located at a depth of more than 700 meters, on the slope of the ridge, outside the active area (Aquilina et al., 2013).

The ophiuroids *Ophiolimna antarctica* was observed at a depth of 1546 m in the Kemp's Caldera, an active volcanic structure located in the South Sandwich Islands Arc, near hydrothermal vents. Its average density reaches 17 individuals per square meter, with a distribution in localized aggregates on bare basalt or weakly covered by sediment. This population could belong to the peripheral fauna associated with hydrothermal vents. Omnivorous, *O. antarctica* consumes a variety of elements: crustacean fragments, organic detritus, fish scales, and partially digested tissues and spines of other ophiuroids. This diet reflects an opportunistic strategy combining necrophagy, occasional predation, and selective detritivory (Boschen et al., 2013).

Species found in North Atlantic hydrothermal vents include *Ophiolycus purpureus*, *Ophiosemnotes clavigera*, *Ophiactis abyssicola,* and *Ophioctreta spectabilis*. These species are not endemic to chemosynthetic habitats such as hydrothermal vents and are also found in other habitats such as cold-water coral reefs and ocean ridges (Schmidt et al., 2024). *Ophiactis abyssicola* is a suspension-feeding species and generally inhabits pillow lava and inserts itself into cracks (Eichsteller et al., 2022). The lack of endemism in these species suggests that they are probably opportunistic species, with high density, or accidental species present at low density (Rodrigues et al., 2011).

Located on the Mid-Atlantic Ridge (MAR), the endemic ophiuroid *Ophioctenella acies* is present in the majority of the hydrothermal vent fields at the North Mid-Atlantic Ridge such as Broken Spur, Lucky Strike, Rainbow, Snake Pit, TAG and Logatchev (Boschen and Colaço, 2021) and in some vent fields largely dominates the community. In the Logatchev vent field, they can reach densities of 2390 individuals per litter of mussels, thus representing 81% of the macrofauna sampled (Van Dover & Doerries, 2005). This species appears to be well adapted to these reducing environments and is commonly found in association with mytilid bivalves (Segonzac & Desbruyères, 1997; Stöhr & Segonzac, 2005). The species *Ophiactis tyleri sp*.,

Ophiocten centobi Paterson, Tyler & Gage, 1982, *Ophiomitra spinea* Verrill, 1885 and *Ophiotreta valenciennesi rufescens* Koehler, 1896 are also present in hydrothermal vents. However, they are not endemic to these environments, as they have also been observed in other bathyal habitats. Their abundance is generally lower than those of strictly endemic species (e.g., *O. acies*, *Spinophiura jolliveti* and *Ophiolamina eprae*) (Stöhr & Segonzac, 2005; Rodrigues et al., 2011). *O. tyleri* was observed near a translucent smoker, on an isolated sulfide rock colonised by attached mussels. The area was also home to a diverse fauna including the crab *C. affinis*, polychaetes, gastropods, copepods, numerous amphipods, shrimps and a galatheid crab (Stöhr & Segonzac, 2005). *O. centobi* ophiuroids were collected in an abyssal environment, mainly on basalt fragments, among mytilid bivalves, pteropod shells, dead coral, and basaltic gravels. Some specimens come from areas with little or no visible hydrothermal emission, in association with sponges and pedunculated crinoids (Stöhr & Segonzac, 2005). An individual of *O. spinea*, measuring 8 mm disk diameter (dd), was collected near an active hydrothermal vent, in oxidised sediments, among mussel shells, live mussels, the hydrothermal shrimp *Mirocaris fortunata* and chaetopterid polychaetes. A second, larger specimen (14 mm dd) was collected outside the hydrothermal influence, 400 m from the active field, on a wall colonised by a fixed fauna composed of sponges, corals, comatulas and asteria. Collected at an ambient temperature of 3.2°C, the species appears to be able to tolerate conditions specific to hydrothermal environments (Stöhr & Segonzac, 2005). A specimen of *Ophiotreta valenciennesi rufescens* was collected from a block of white sulfides located one meter from the base of an active hydrothermal edifice (296°C), close to *Bathymodiolus azoricus* mussels, in a diffusion zone. The block was colonised by sponges, hydrozoans and serpulid polychaetes (Stöhr & Segonzac, 2005).

3.1.2) Reproduction and development

Although they are numerous, varied, and widespread, the larval development mode has been described for only 4% of ophiuroid species, and data on deep-sea species are particularly rare (Hendler & Tran, 2001). In deep-sea environments, the majority of marine organisms exhibit a bipartite life cycle, characterized by a planktonic larval phase playing a key role in their distribution within marine systems (Arbizu et al., 2014). Due to their poor swimming ability and small size, the dispersal of these larvae depends mainly on ocean currents and the duration of their larval development (Schmidt et al., 2024). The reproductive mode of deep-sea ophiuroids is still poorly understood and is often inferred indirectly from the size of the oocytes, in relation to the type of larval development. In general, species with small oocytes produce planktotrophic larvae, capable of feeding in the water column. Those with medium-sized oocytes give birth to lecithotrophic larvae, which live thanks to their reserves. Finally, species with large oocytes incubate their embryos and release fully formed young. However, this classification remains approximate because oocyte sizes are distributed continuously, making it difficult to accurately predict the mode of reproduction based only on oocyte diameter (Hendler & Tran, 2001). Reproductive cycles are generally associated with habitats where environmental factors, such as day length or temperature which vary in predictable ways. However, a continuous mode of reproduction has been proposed for certain species of echinoderms, particularly those living near the equator or in deep waters, where seasonal variations are less pronounced such as hydrothermal vents (Hendler, 1991; Brogger et al., 2013).

3.1.3) *Ophioctenella acies*

Distribution and ecology

Ophioctenella acies is an ophiuroid closely associated with the reducing environments of the North Atlantic, it has never been observed at depths below 1600 m and reaches its highest densities above 3000 m (Stöhr & Segonzac 2005; Madeira et al., 2019). *O. acies* has been observed in active hydrothermal vents on the Mid-Atlantic Ridge such as Lucky Strike (Desbruyères et al., 2001), Logatchev (Gebruk et al., 2000, 2010; Van Dover & Doerries, 2005), Rainbow Strike (Desbruyères et al., 2001), Broken Spur (Tyler et al. 1995), Snake Pit sites except Menez Gwen, often associated with beds of *Bathymodiolus spp* (Van Dover & Doerries, 2005) mussels, hydrothermal sediments and a diverse fauna (polychaetes, crustaceans, gastropods, cnidarians). The species is also present in non-hydrothermal reducing environments, such as the cold seeps of Barbados, Blake Ridge, and Florida Escarpment, always in association with mussels, vestimentiferans and other species typical of these habitats (Stöhr & Segonzac, 2005). *O. acies* appears to be endemic to the Atlantic, which is consistent with the fact that almost 85% of bathyal echinoderms are found in just one ocean (Vinogradova, 1979).

At Broken Spur, *O. acies* colonises the solid surfaces of chimneys, mounds and altered sulfide deposits in the immediate vicinity of active vents (Tyler et al., 1995). The densities recorded for this species, reaching 30 individuals/dm², are comparable to those measured at the TAG and Snake Pit sites where they can reach up to 20 individuals ± 2 (Tyler et al., 1995; Copley et al., 1997). It has also been observed at the base of hydrothermal structure BX16, at the Broken Spur site, in the shimmering water zone, where it cohabits with chaetopterid polychaetes and white anemones (Gebruk et al., 1997). Individuals are most abundant between 10 and 15m from the active vent of a black smoker and in areas of diffuse flow (Tyler et al., 1995).

This species can also live with vesicomyid clams (*Calyptogena*) (Gebruck et al., 2000) or on hydrothermal substrates rich in heavy metals. It can therefore tolerate a wide range of chemical conditions, including toxic fluids rich in copper, lead or cadmium with temperatures ranging from 4 to 168°C (Desbruyeres et al., 2000).

Its diet is thought to be of the deposit-feeding type, with the species taking advantage of organic matter from neighbouring communities, in particular pseudo-feces rich in dissolved organic carbon discharged by mussels in the medium (Tyler et al., 1995; Stöhr & Segonzac, 2005). *O. acies* has also been observed remaining positioned on the open siphons of these mussels, probably to capture these nutrient discharges directly (Stöhr & Segonzac, 2005). In addition, the isotopic compositions of organic carbon also indicate that *O. acies* adopts an opportunistic behavior, exploiting various sources of organic matter (Gebruk et al., 2000; Van Dover & Doerries, 2005). Also, the dental morphology of *O. acies* indicates that it has adapted to a detritivorous diet, enabling it to collect organic particles and filamentous bacteria present on the surfaces of hydrothermal deposits (Tyler et al., 1995).

The unusual distribution of the species, covering both hydrothermal vents and cold seeps, suggests a wide ecological range and low speciation, unlike associated genera such as *Bathymodiolus*. The question of genetic connectivity between the populations of the western Atlantic (seeps) and those of the MAR (vents) remains open. Hypotheses include larval transport by deep Atlantic currents or ancient dispersal, followed by isolation and a lack of morphological diversification (Van Dover et al., 2002; Stöhr & Segonzac, 2005). Although larval dispersal is probable (the youngest stages are very small, suggesting planktotrophic development), uncertainties remain about larval lifespan, characteristics of axial currents, larval losses at transform faults. The continuous presence of juveniles in the samples indicates regular recruitment, but it is not known if the larvae remain local or disperse widely.

Reproductive studies and molecular analyzes are needed to clarify these aspects (Stöhr & Segonzac, 2005).

4) Objectives

The main objective of this study is to improve our understanding of the population structure and reproductive biology of brittle stars associated with hydrothermal vent ecosystems, focusing specifically on the species *Ophioctenella acies* found in the Broken Spur vent field (magmatic environment) and Rainbow pit site (ultramafic environment) (Mid-Atlantic Ridge). Given the ecological importance and vulnerability of these deep-sea environments, this research aims to contribute to our understanding of their biology and functional dynamics. With a view to gaining a better understanding of their life cycle and the potential resilience of these fragile ecosystems, which are facing ever-increasing pressure from human activity (e.g. deep sea mining). Indeed, the main aim is to study the population dynamic and reproductive biology of hydrothermal echinoderms using morphometric and histological analyzes of the gonads. It includes tissue preparation and analysis of gametic stages. To determine the potential size threshold that exists for sexual maturity, which will lead to a better understanding of their life cycle characteristics and the timing of reproductive capacity. And finally, to contribute to a better understanding of the adaptation of brittle stars to extreme environments, particularly in reducing ecosystems such as hydrothermal vents.

II) METHODOLOGY

1) Areas studied

1.1) The Broken Spur hydrothermal vent site – Mid-Atlantic Ridge (MAR)

Regional characteristics

The Mid-Atlantic Ridge is characterised by 13 active fields, including Menez Gwen (850m max depth), Lucky Strike (1700m), Rainbow (2300m), TAG (3670m), Snake Pit (3500m), Broken Spur (3100m), Logatchev (3000m), Pobeda, Irinovskoye, Semyenov, Ashadze (4200m), Lost City (850m) and Moytirra (2085m) (**Figure 3;** Boschen-Rose & Colaço, 2021).

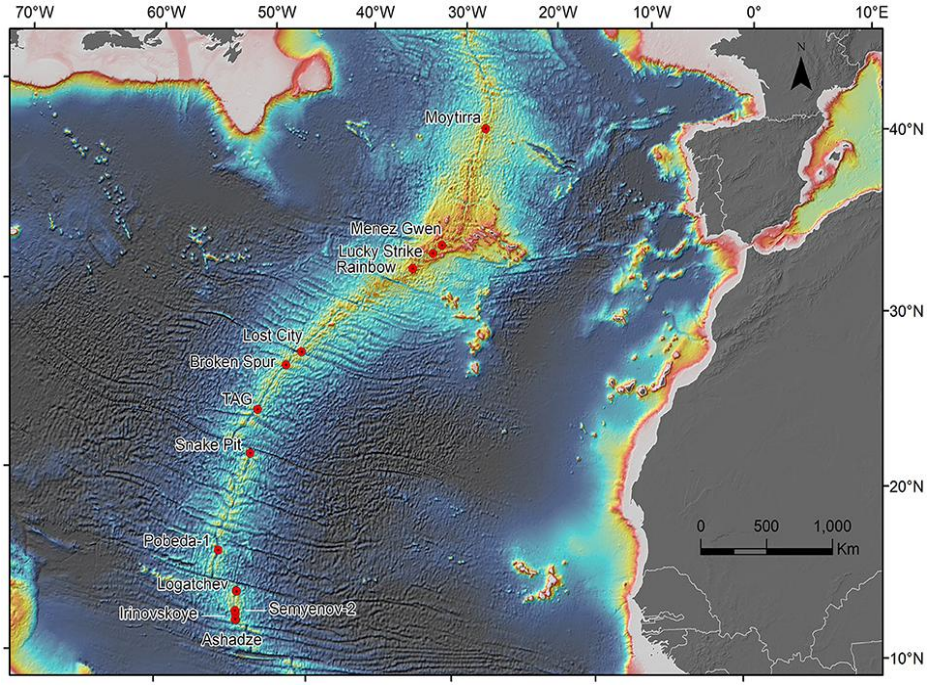

Fig. 3. Location of hydrothermal vent fields along the Mid-Atlantic Ridge (MAR) (Boschen-Rose & Colaço, 2021).

Along the Mid-Atlantic Ridge (MAR), the Broken Spur hydrothermal field discovered in 1993 (Murton et al., 1994) at 29°10'N, 43°10.4'W from 3050 to 3875 m deep (Gebruk et al., 1997; Cruz et al., 2018) occupies an axial summit graben that runs along the top of a volcanic ridge. The presence of recent lava flows within this structural depression provides clear evidence of recent volcanic activity in the area (Murton et al., 1995; Copley, 1997). Broken Spur comprises ten hydrothermal edifices with 5 main active structures (e.g., Bogdanov, Saracen's Head, Spire, Wasp's Nest and White Mushroom) (**Figure 4**). Rising from the volcanic basement of the axial ridge the hydrothermal structures take the form of chimneys measuring between a few meters and several tens of meters in height, with diameters reaching a few meters (Copley et al., 1997). Since the time of its discovery, the Broken Spur field exhibited sulfide compositions, fluid geochemistry and levels of hydrothermal activity comparable to those observed at other sites along the Mid-Atlantic Ridge (Murton et al., 1995).

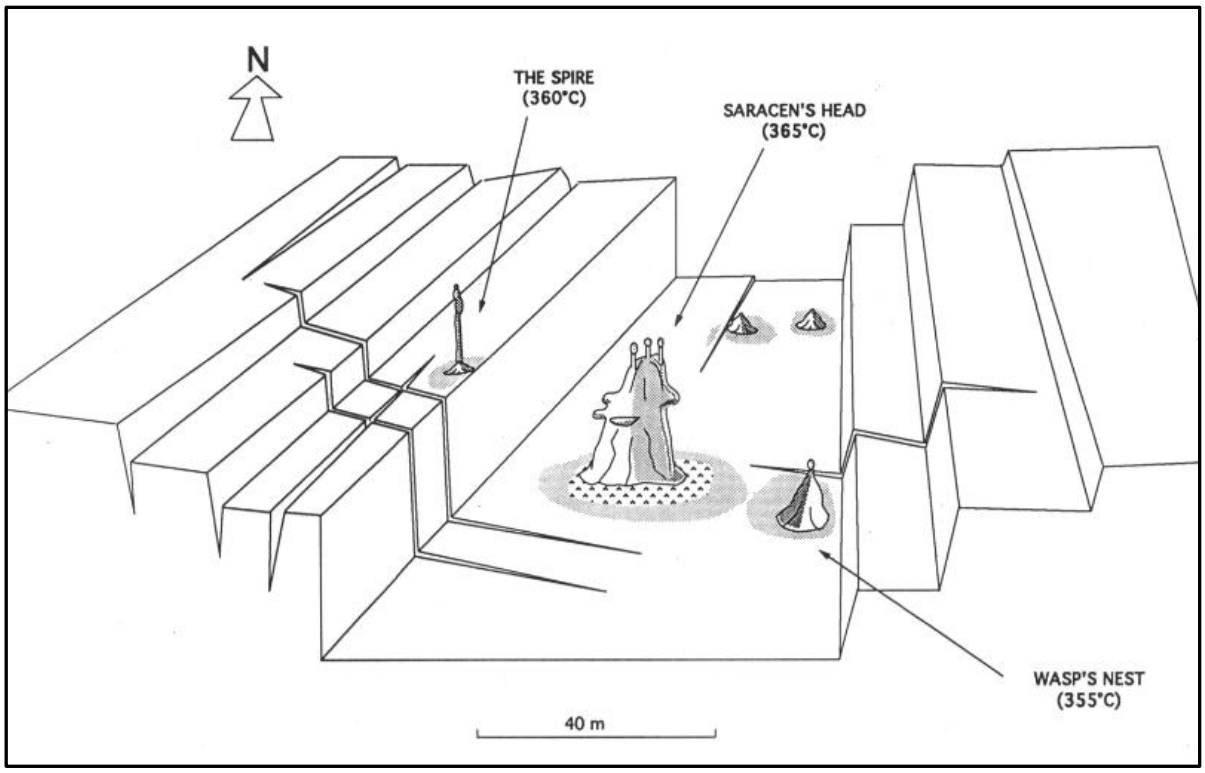

Fig. 4. Morphology of the Broken Spur vent site and position of the various chimneys (e.g., The Spire, Saracen's Head and Wasp's Nest) (Dover, 1995).

The presence of extensive sulfide mounds, associated with weathered debris and oxyhydroxide-rich sediment deposits, suggests that Broken Spur is a geologically mature hydrothermal field that has probably been active for several thousand years (Murton et al., 1995). The high level of activity in the black smokers, combined with the presence of low-temperature microhabitats potentially suitable for invertebrate settlement, suggests that the hydrothermal system is not in a terminal phase.

In February 2018, Poland signed a 15-year contract with the International Seabed Authority (ISA) for polymetallic sulfide exploration on a section of the Mid-Atlantic Ridge including two active hydrothermal fields (i.e., Broken Spur and Lost City). The contract requires the collection of environmental data, particularly on benthic communities, which are the most vulnerable to mining (Radziejewska et al., 2022).

Ecology of the Broken Spur vent field

The Broken Spur vent field shares ecological similarities with hydrothermal vent sites along the MAR. This site is characterised by a zoned distribution of species: *bresiliid* shrimps dominate the areas close to the black smokers, while towards the periphery there are mainly worms, mussels, ophiuroids and anemones. The latter are found at the base of the sulfide mounds. Crabs, whose density is highest on platform structures, and fish, a more mobile species, are found both near active structures and in more remote areas (Murton et al., 1995; Copley et al., 1997). Unlike the hydrothermal vents in the Pacific, the Broken Spur site has neither vestimentiferan tubeworms nor alvinellid polychaetes (Murton et al., 1995). In addition, each hydrothermal structure at Broken Spur seems to harbour a specific fauna, organized according to its own zonation (Gebruk et al., 1997).

Species found on the site include the bresiliid shrimps (*Rimicaris exoculata* and *Chorocaris fortunata*), the brachyur crab *Segonzacia mesatlantica*, decapods of the genus *Munidop-*

sis, and the ophiuroids *O. acies*. The site is also home to bivalves (*Bathymodiolus sp.*), gastropods (*Phymorhynchus moskalevi*), polychaetes (*Ampharetid sp.*, *Chaetopterid sp.*), anemones (*Actinian sp.*) and *Pachycara thermophilum* and *Synaphobranchid* fish (Copley et al., 1997; Gebruk et al., 1997; Biscoito et al., 2009).

The low-temperature mounds are covered with sulfide sediments and rocky debris, colonised by white anemones measuring around 15 mm, with a high-density of one anemone per 15 cm². Swimming polychaetes are also present in the water column, with a density of one individual per 2 to 3 m³. While high-temperature mounds, such as Saracen's Head, have at their base a sediment deposit colonised by tubes of 20 to 30 mm long fluted worms, fixed perpendicularly to the substrate with a regular distribution. The solid surfaces of these structures are occupied by ophiuroids, brachyuran crabs, Munidopsis squat-lobsters and bresiliid shrimps. On the Wasp's Nest mound, crabs are particularly abundant, reaching a density of 1 individual per 10-15 cm². Colonies of living mussels, stained with iron oxide (a sign of very slow growth), lodge in the crevices of structures like The Spire (Murton et al., 1995).

Broken Spur represents the only known hybridization zone in the Atlantic between two mussel species, *B. azoricus* and *B. puteoserpentis*, where they coexist and can interact genetically, producing viable offspring. However, this hybrid zone remains transient and unstable due to local environmental constraints. Nevertheless, this location makes it a unique site for studying hybridization and larval dispersal processes in extreme deep-sea environments (O'Mullan et al., 2001; Won et al., 2003).

During the TRANSECT cruise in July 2018 (DOI: 10.17600/18000513; **Figure 5**), which studied the Broken Spur vent field (Le Bris et al., 2018). Ophiuroids were collected on 27 July 2018 during biological sampling dives (TRANSECT VICTOR dive 692/9; **Figure 5**) using the remotely operated vehicle (ROV) *Victor 6000*. This ROV was equipped with a claw, a manipulator arm, and an HD video camera (Sony FCB-H11) to perform video transect surveys. After collection, specimens were fixed in 4% formaldehyde to preserve cell structures, then transferred to 70% ethanol for reproductive analysis.

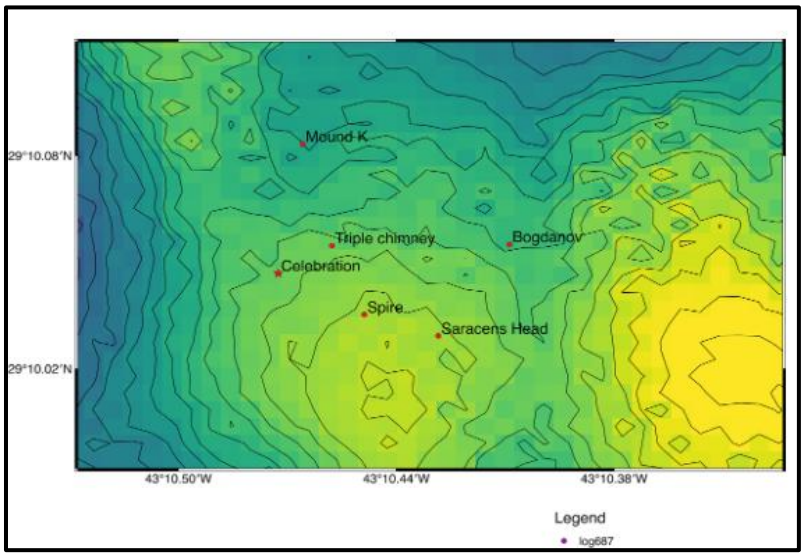

Fig. 5. Map illustrating the Broken Spur hydrothermal field, including the main structures sampled during the TRANSECT campaign

(Le Bris et al., 2018; https://doi.org/10.17600/18000513). Produced using Q-GIS 2.18.20 software, it combines bathymetric data for the site and the locations of hydrothermal edifices (Cruz et al., 2022).

The ophiuroids collected were found in association with anemones.

1.2) The Rainbow Pit hydrothermal vent site – Mid-Atlantic Ridge (MAR)

The Rainbow Pit hydrothermal vent site was discovered in May 2022 during the Arc-en-Sub'22 french oceanographic campaign exploring the Rainbow Massif, an ultramafic structure located at 36°14'N on the Mid-Atlantic Ridge (Escartin and Andreani, 2023). Due to their proximity to the hot Rainbow vents, it is assumed that the pits are part of the Rainbow hydrothermal system. The Rainbow Pit site has not yet been described, so there is no related information or data available.

These ultramafic environments are mainly located at slow mid-ocean ridges such as the Mid-Atlantic Ridge (MAR), particularly at sites such as Rainbow, Logatchev, Ashadze, and Lost City, where the interaction of seawater with mantle rocks such as olivine and pyroxene produces hydrogen (H_2) through serpentinization. These environments are highly reducing, promoting abiotic reactions such as the formation of methane (CH_4) and simple organic molecules favorable to chemosynthesis and microbial life. The conditions of ultramafic hydrothermal systems are analogous to early Earth environments (i.e., reducing, rich in H_2, CH_4, Fe, Ni, moderate to high temperatures) (Konn et al., 2015). At Rainbow Pit, hydrothermal fluids reach a maximum temperature of around 95°C and emerge as clear, shimmering water from discrete cracks in the seafloor. During this campaign, brittle stars were collected on May 12, 2025, at a depth of 1,900 m using the M210 ROV at the east of the Rainbow Pit site, in the diffusion zone. Ophiuroids were found in association with *Bathymodiolus* mussels.

2) Population Dynamics

Disc Diameter

First, the samples covered in organic detritus were carefully cleaned using a Leica MZ125 binocular loupe, distilled water, and fine forceps. They were then stored in 70% ethanol in the refrigerator. Only individuals with an intact disc were used for the reproduction analyses. The disc diameter of each brittle star was measured and photographed (7.12x zoom) using the Leica MC190HD camera associated with the Leica MZ16FA binocular loupe, using Leica Application Suite V4.12 software (**Figure 6, A**). The disc was measured from the distal edge of the disc to the opposite end (**Figure 6, B**). The length of the arms of each brittle star was also measured using the ImageJ application; only intact (unbroken) arms were taken into account, and an average was calculated for each individual. Finally, each brittle star was placed in a numbered Eppendorf tube and stored in 70% ethanol. Measurements were then rounded to the nearest millimeter.

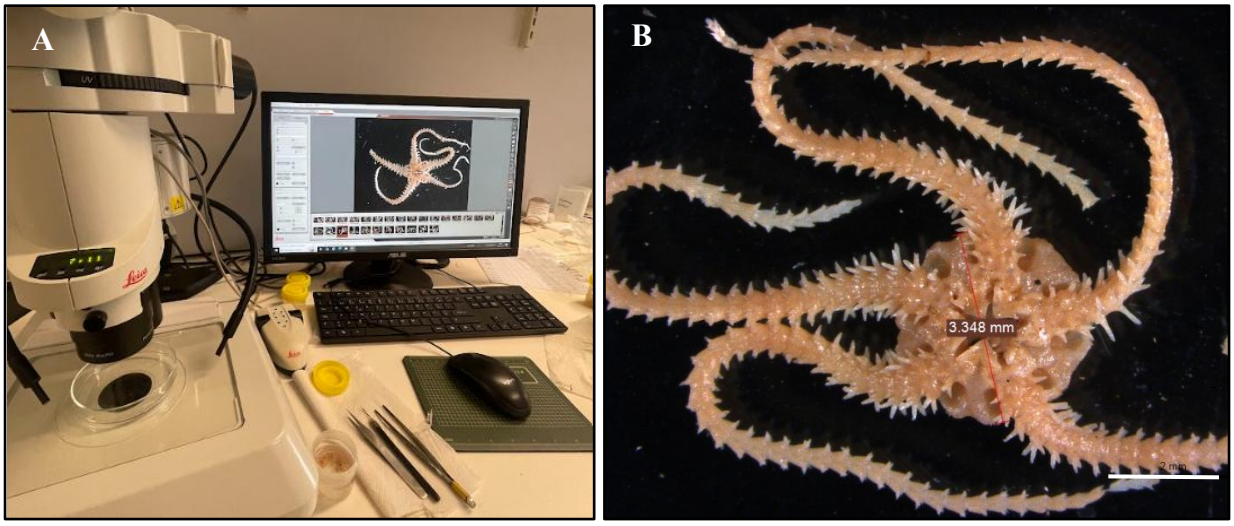

Fig. 6. A. Measurement under a Leica MZ16FA binocular loupe equipped with a Leica MC190HD camera and Leica Application Suite V4.12 software, used to photograph the ophiuroid; **B.** Ophiuroid measured (3.348 mm dd) using Leica Application Suite V4.12 software (2mm scale at bottom right in black at bottom of photo)

Cohort Analysis

In order to determine the optimal number of cohorts present in the samples with the disc diameter, several statistical models were tested. The aim was to better visualise the age classes (juveniles vs. adults) in order to understand the demographic structure, recruitment dynamics and life cycle of the individuals. To obtain a biologically consistent estimate of the number of cohorts, the "mixtools" package was selected. Cohort decomposition analysis was thus performed using the "mixtools" package (*Tools for Analyzing Finite Mixture Models*, version 2.0.0.1; Benaglia et al., 2010), under the R Statistical programming environment software (version 2024.09.1 +394). The "mixtools" package enables very robust analyses of biological and environmental data in order to decompose populations into sub-groups (e.g., age classes) (Benaglia et al., 2010). The normalmixEM() function has been used to mix univariate normals. The AIC (Akaike Information Criterion; Akaike, 1973) and BIC (Bayesian Information Criterion; Schwarz, 1978) criteria were calculated for 1 to 9 models reflecting the cohorts. The AIC aims to identify the model offering the best fit to the data while penalising complexity. The lower its value, the better the compromise between fidelity and simplicity. The BIC, on the other hand, applies a stricter penalty for complexity in order to limit the risks of over-interpretation; a lower BIC also indicates a model that is statistically more parsimonious and relevant.

3) Species identification

With the aim of identifying the species present in our samples, photos of a few individuals were taken using the Leica MC190HD camera with the Leica 10447101 Planapo 2.0x zoom lens and the Leica Application Suite V4.12 software in order to observe characteristic features. A detailed search was carried out through books and scientific articles to compare morphological similarities with previously described species from hydrothermal sites. Among the samples, only one species was identified: *Ophioctenella acies*.

Table 1. Systematics of *O. acies*

Phylum	class	order	Family	Genus	species
Echinodermata	Ophiuroidea	Ophiurida	Ophiuridae	Ophioctenella	acies

Brittle stars *O. acies* can be recognized by the presence of three spicules on the arms, as well as spicules in the shape of a circle around the mouth. They also have a very hexagonal dorsal plate. According to Tyler (1995), the autapomorphy (i.e., an evolved character unique to a species or taxon) of the species *O. acies* is characterised by a jaw with a sharp arrow-shaped outer edge, long teeth, contiguous radial shields over most of the length, and the dorsal plate of the arms with a distinctive proximal notch. Other characters such as 3 and very occasionally 4 arm spines with the ventral ones hooked, the oral shield is also arrow-shaped or the ventral arm plates are small and separate (**Figure 7**).

Juveniles can be recognized by their dorsal plate, which is covered with small, round, entangled plates similar to a cauliflower (**Figure 7, A**). This characteristic fades as the individual grows (**Figure 7, D**), giving way to 5 radial shields (**Figure 7, E**).

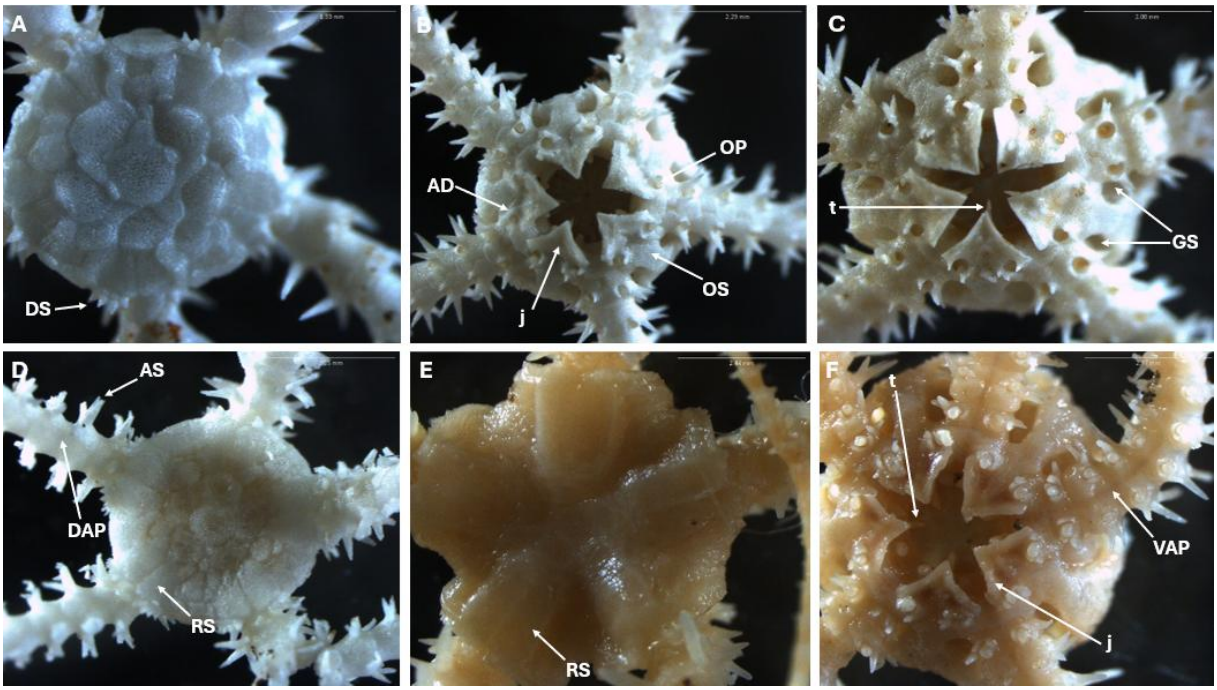

Fig. 7. Morphological characteristics of *Ophioctenella acies*, **A**. Dorsal view of juvenile; **B**. Ventral view; **C**. Ventral view; **D**. Dorsal view; **E**. Dorsal view; **F**. Ventral view. AD : adoral shield; AS : arm shield; DAP : dorsal arm plate; GS : genital slits; j : jaw; OP : oral papillae; OS : oral shield; RS : radial shield; t : teeth; VAP : ventral arm plate. (scale top right).

4) Histology procedure and microscopy examination

Decalcification

Before any handling in the laboratory, particularly in the presence of acid, a lab coat and gloves are required. In brittle stars, the central disc is small and highly calcified, considerably limiting the space available for the viscera. The viscera, compressed into narrow zones, frequently extend into the arms, making handling them delicate and subject to severe damage. The presence of a rigid calcareous skeleton is a major obstacle to detailed anatomical examination, restricting possible methods of study. However, traditional acid decalcification techniques have often preserved the overall anatomy and morphology, while largely preserving the internal structures. Several decalcification protocols have been tested on brittle stars, using different acids (e.g., EDTA, Bouin's solution, Nitric Acid or HCl) at varying concentrations and durations according

to articles (Märkel & Röser, 1985; Dobson & Turner, 1989; Byrne, 1991; Sumida et al., 2001; Hendler & Tran, 2001; Falkner & Byrne, 2003; Laming et al., 2021). Nitric acid was chosen as the decalcifying agent, as specimens treated with this solution were in a better state of preservation. A sample representing 10% of each of the five cohorts was selected for treatment. The brittle stars were decalcified using a solution of 3% nitric acid and 70% ethanol (Dobson & Turner, 1989; Wilkie et al., 2016; Laming et al., 2021). To do this, 200 mL of solution was prepared by mixing 6 mL of nitric acid, 140 mL of ethanol and completing with 54 mL of distilled water. Afterwards, the decalcifying solution is added to a beaker, then withdrawn using a clean 5 ml pipette and added to the test tube containing the brittle star. The test tube was then placed on a tube holder in the presence of a weight, and the whole set was gently shaken (~ 112rpm) on a Heidolph Promax 2020 orbital shaker for 7 days (**Figure 8**). This procedure was repeated for each ophiuroid.

The brittle stars were then gently and thoroughly cleaned with distilled water and placed in an Eppendorf in the presence of 4% formalin. To achieve the best possible results when decalcifying tissue, it is very important to determine the point at which decalcification is complete. Incomplete decalcification can lead to tissue distortion and damage to the microtome when cutting the tissue. To ensure that the decalcification is complete, the brittle star is placed under a binocular loupe to analyse the rigidity, color and texture of the membrane, in order to confirm that there is no longer any calcium carbonate. To see if an ophiuroid is completely decalcified, it can also be placed in acid to see if there are any bubbles or effervescence. If bubbles are present, then $CaCO_3$ remains. In addition, the tissues must be completely soft with no calcified structure. We can try removing the membrane from the ophiuroid and removing the gonads respecting tissue integrity, if there is any resistance, then the tissues are still calcified. This precise and time-consuming procedure is carried out under a binocular magnifying glass using forceps and the finest needles possible, given the very small size of brittle stars. The gonads are located between the base of the arms, on the oral side of the disc at the level of the genital slits.

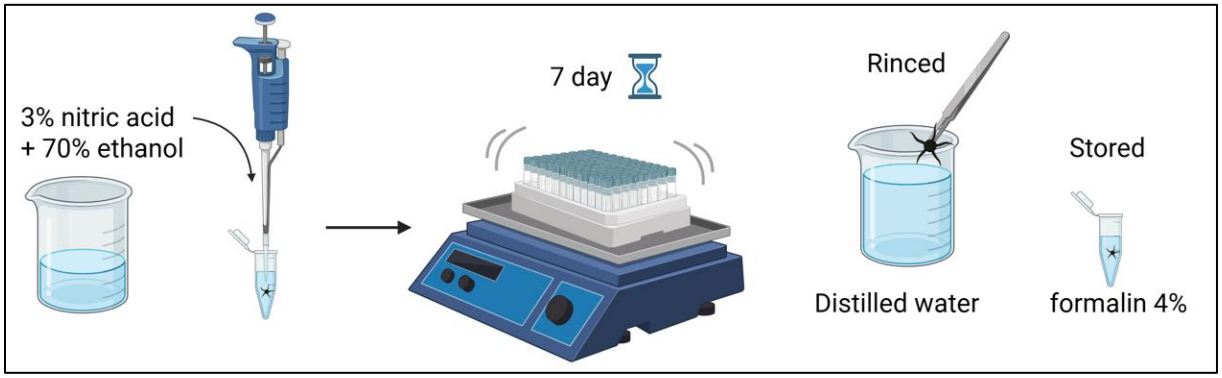

Figure 8 : Schematic diagram illustrating the stages of decalcification. (Illustration created with *BioRender.com*)

Dehydration

Dehydration replaces the water in the sample with the embedding medium. As the paraffine wax is not miscible with water, the fixed parts will have to be dehydrated in alcohol baths with a series of solutions composed of increasing percentages of ethanol (70%, 80%, 90%, 96%, 100%) to gradually remove water.

Prior to dehydration, samples were rinsed with ultrapure water (Milli-Q water ®, Merck Millipore) and then transferred to Eppendorf tubes with 50% ethanol overnight. Following to the protocol of Rakka (2024), tissues were transferred into 70% ethanol for 30 minutes in a

vacuum chamber (Binder Vacuubrand CVC 2000) with the aim of removing any bubbles that were created during decalcification. In the absence of a vacuum chamber, air bubbles prevent solutions from penetrating tissues, resulting in procedure failure. All the following baths will follow the same process and be put into vacuum chamber; the Eppendorf's must remain open. The samples were transferred in 80% ethanol for 30 minutes, followed by 90% ethanol for 15 minutes, then 95% ethanol for another 15 minutes. Complete dehydration was achieved by transferring the tissues through three successive baths of 100% ethanol, each lasting 20 minutes. After dehydration, the ethanol was replaced by a paraffin-miscible solvent (Xylene). The samples were transferred into clean vial with xylene and also put into the vacuum chamber for 20 minutes to ensure thorough clearing prior to paraffin infiltration. Afterwards, tissues are transferred into paraffin wax and left in the oven for 1 hour at 50°C in the oven (**Figure 9**).

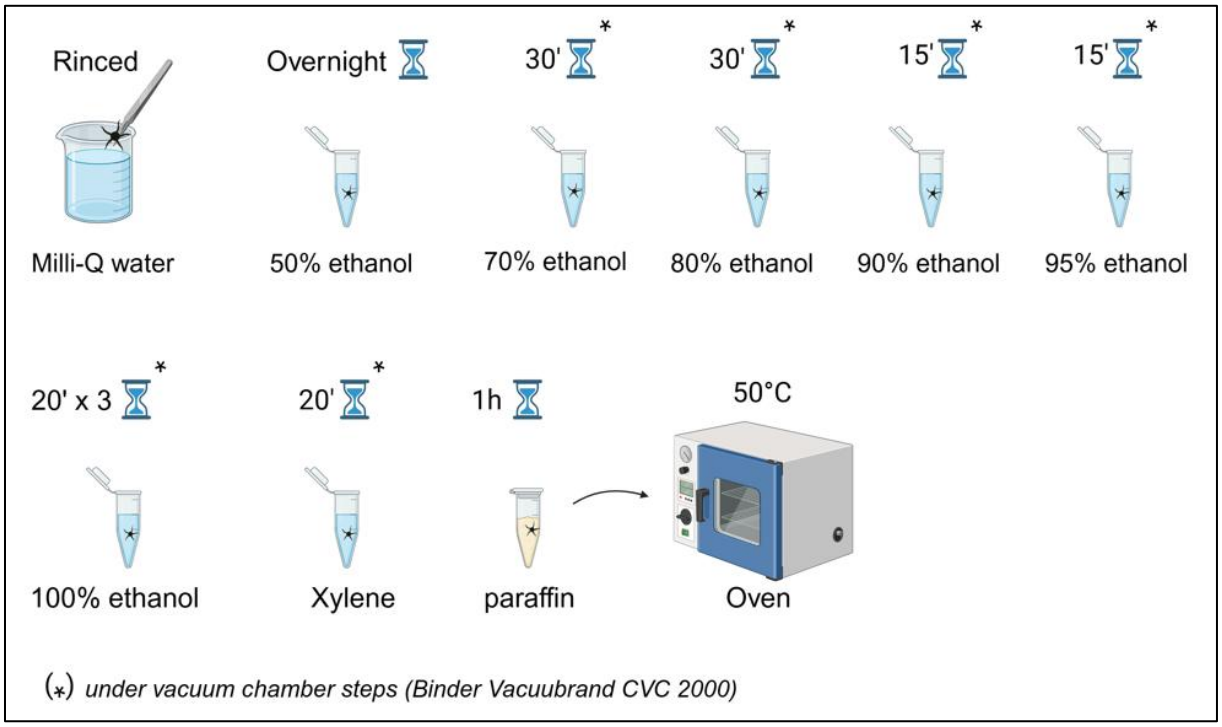

Fig. 9. Tissue dehydration protocol after decalcification. Dehydration steps are performed in a vacuum chamber (Binder Vacuubrand CVC 2000) to avoid bubble formation. (Diagram created with *BioRender.com*).

Inclusion and microtomy

Above all, the arms of the brittle stars have been removed for better handling and fixing of the discs. Prior to embedding, paraffin wax, molds and forceps were preheated in the oven at 50°C at least for 5-6 hours to ensure consistent thermal conditions. Molten paraffin was then maintained at 50°C on a magnetic stirring hot plate, with the stirrer set to low speed to maintain a homogeneous temperature. A small amount of warm paraffin was then poured into the mold. The tissue sample (disk) was then carefully and horizontally positioned in the mold using fine and preheated forceps. This step has to be fast to prevent the paraffin from cooling when transferring the disk to the mold. After allowing the paraffin wax to cool slightly at room temperature and stabilize the sample, additional paraffin wax was poured in to fill the mold completely. Care was taken to eliminate any air bubbles during this step. When the paraffin block has solidified a little, the labels are gently immersed in the melted paraffin and added to the cooling block

(**Figure 10**). The mold was then transferred to a cold surface, followed by placement in a refrigerator and then put for no more than 5 minutes in the freezer until the paraffin block was fully solidified. Once hardened, the block was gently removed from the mold using the edge of a knife. You have to be careful not to hurt yourself.

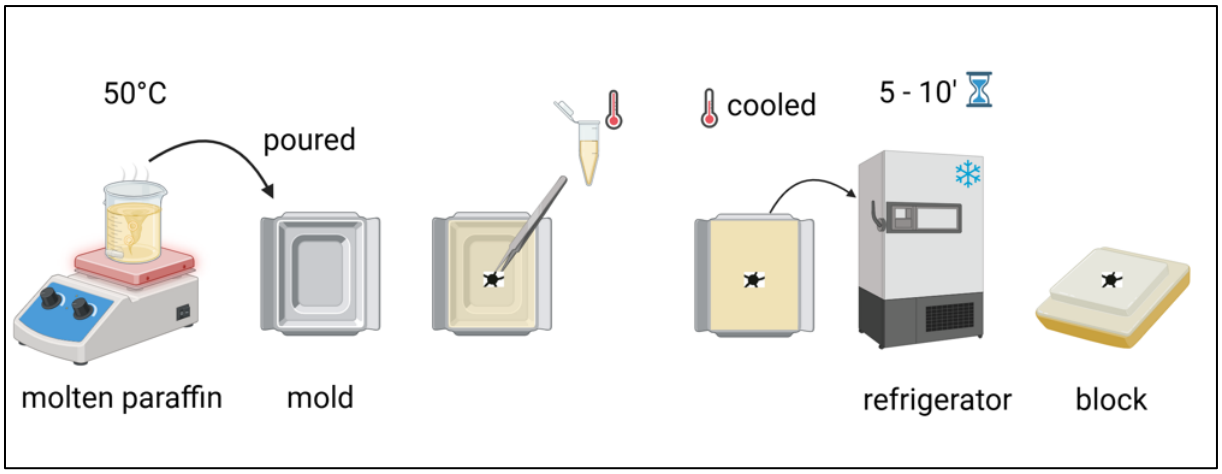

Fig. 10. Embedding of ophiuroid discs in paraffin for histological processing (Diagram created with *BioRender.com*).

The cutting process begins with the preparation of the Leica RM2035 microtome, followed by the installation of a cold water bath and a hot water bath filled with distilled water maintained at around 39-40°C. Each histological slide is labelled with a pencil to ensure correct identification and avoid getting lost, as there are several slides per sample. The paraffin block has to be placed as straight as possible. The paraffin block is then cut until the area to be sectioned is clearly exposed. Using the manual rotary microtome, 5 µm-thick cross-sections are made, forming a ribbon of serial sections. This ribbon is carefully detached with a scalpel and gently manipulated, preferably with round-tipped forceps. It is first placed in the cold water bath to relax the ribbon, then transferred to a histological slide. The slide is then placed in the hot water bath to stretch the ribbon, taking care not to lose the sample in the water or leave it submerged for too long. Finally, the slides are left to dry overnight.

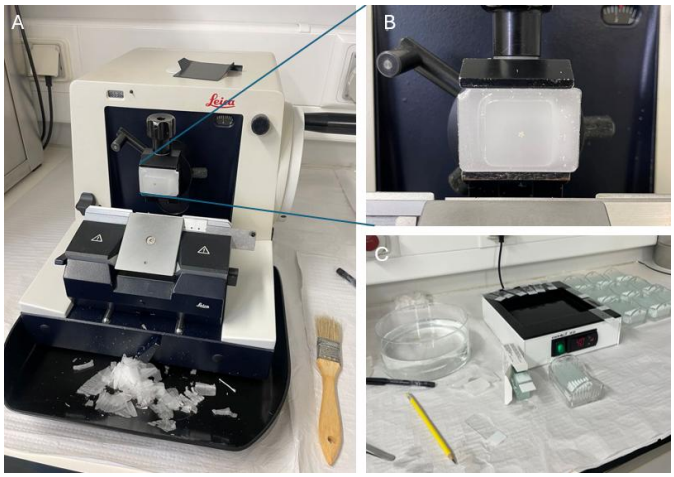

Fig. 11. Cutting set up; **A**. the manual rotary microtome Leica RM2035, **B**. paraffin block with the disk positioned at its center, C. cold water bath and hot water bath set to 40°C, along with slides.

Staining and microscope observation

For histological staining, the tissues are highlighted with stains (Hematoxylin & Eosin), for differentiation of cell structures.

First, we have to prepare the staining table where each staining vial is labelled with its contents and, ideally, the immersion time for each step also.

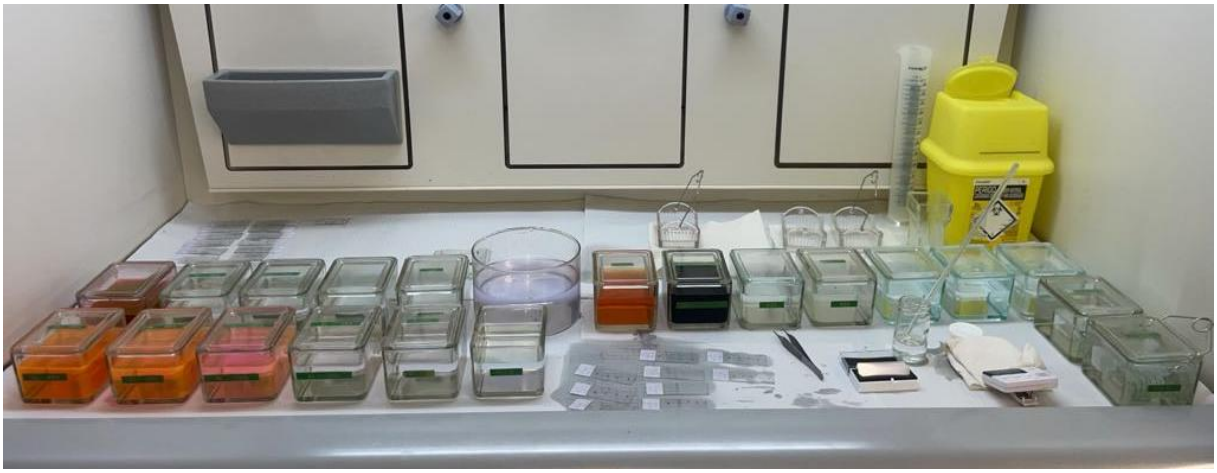

Fig. 12. : Staining set up. The different baths to be carried out from right to left for coloring.

The slides are placed in the oven at 50°C for 5 minutes to help remove any remaining paraffin wax. The reverse dehydration process is performed. Slides are then immersed in xylene for 20 minutes, followed by sequential rehydration steps : 5 seconds in 100% ethanol, then 5 seconds in 95% ethanol and finally 5 seconds in 70% ethanol. The slides are then rinsed twice in distilled water for 5 second each to complete the rehydration process.

For the staining, the slides are transferred in Harris haematoxylin for 5 minutes, followed by a brief rinse (10 s) in 1% HCl and washing with hot tap water (10s) until the tissue turns blue. The hot tap water must be changed after each use following staining with Harris haematoxylin. The slides are then rinsed twice in distilled water for 5 seconds each time. They are then passed through 70% ethanol for 5 seconds and 95% ethanol for also 5 second before being immersed in eosin for 2 minutes and 30 seconds. Differentiation continues with two quick rinses in 95% ethanol, followed by two rinses in 100% ethanol and two xylene passages to lighten the tissue. The last xylene treatment should also last 2 minutes and 30 seconds. Next, excess xylene is gently blotted off with a paper towel and the coverslips are mounted using DPX (Distyrene Plasticizer and Xylene). DTX protects the histological section from moisture, scratches and degradation over time. It provides adequate transparency, which is super-important for observing tissue under the microscope. If the DTX does not completely cover the tissue with the coverslips, the tissue will not be visible properly. Finally, slight pressure is applied on slides with the forceps and guide bubbles to the margins of the coverslip. It is important to ensure that no bubbles remain on the tissue to guarantee optimal visualization and long-term preservation of the section.

Fig. 13. Final histological preparation of the slides

Tissue slides are then analyzed and photographed using the Leica DFC340FX camera in association with the Leica DM600B optical microscope and the software Leica to establish sex ratio (females/males) and count oocytes. For each sample, gametic stages were analyses (spermatogonia, spermatocytes, vitellogenic oocytes, etc.) and the oocyte diameters were measured only for the ones with a nucleus (vitellogenic stages) (**Figure 22**). The counting process of gamete proportions was established at each stage to assess development synchronization.

III) RESULTS

1) Population Dynamics

There is a significant positive linear relationship between the diameter of the discs and the length of the arms of *O. acies* (**Figure 14**). This means that individuals with larger discs also have longer arms, suggesting proportional allometric growth of body structures.

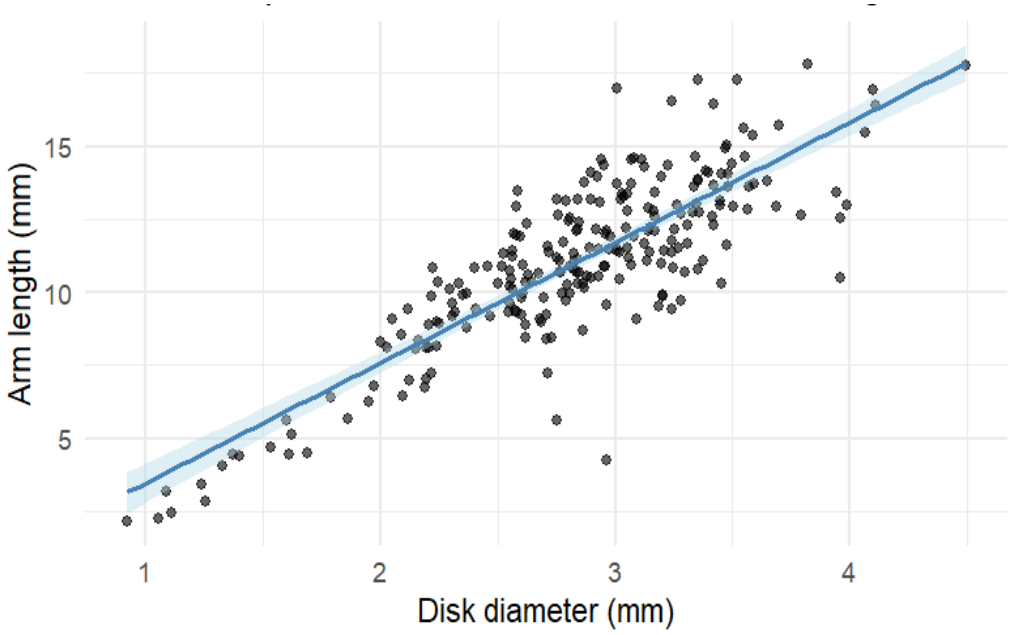

Fig. 14. Relationship between disc diameter (mm) and arm length (mm) of *Ophioctenella acies* for the population find at broken spur vent field. Each point represents an individual, the blue line indicates the linear regression model, and the shaded area represents the 95% confidence interval around the regression model.

There is a general tendency for an increase in disc diameter to be accompanied by an increase in arm length. This reflects a positive correlation between these two variables. The linear model reflects this trend well and can therefore be used to estimate arm length from disc diameter or vice versa.

Cohort analysis

The Gaussian Mixture Model (GMM) using the Bayesian Information Criterion (BIC) suggested the presence of two clusters, while the silhouette score method indicated nine potential cohorts. However, the latter result appears biologically unrealistic. The Expectation-Maximization (EM) algorithm implemented in the *mixtools* package was used which provided a more suitable cohort estimation. The chosen model represents a compromise between statistical relevance and biological plausibility. This approach allowed us to identify a cohort structure that is both model-supported and interpretable in a biological context.

The smallest BIC, indicating the best fit according to this criterion, is obtained for model 2 (corresponding to two cohorts). However, this model seems insufficient to faithfully represent the complexity of the biological data. We therefore prefer model 5 (5 cohorts) (**Figure 15 & 16**), whose AIC is closest to that of model 2, but which offers a more realistic representation of the cohorts observed.

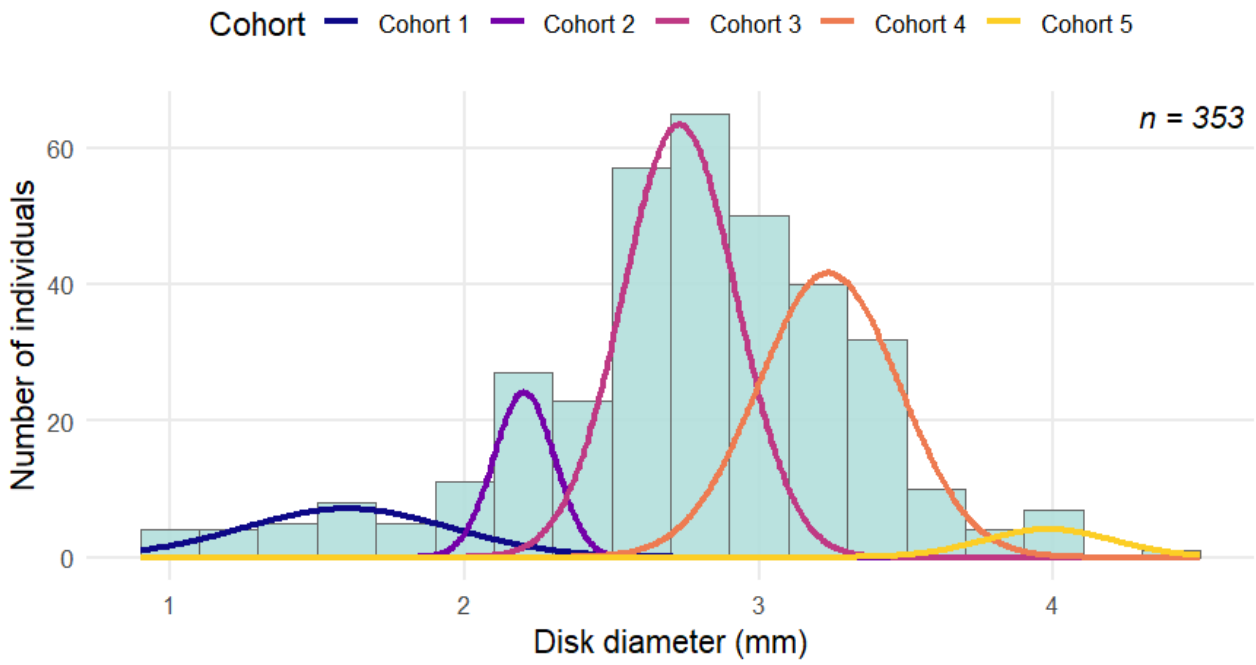

Fig. 15. Modal decomposition of *Ophioctenella acies* disc diameter of the Broken Spur population sampled in july 2018 in a 5-cohort model (EM estimation, using *mixtools*).

Each cohort corresponds to a group of individuals of the same age or of the same recruitment. The curves correspond to the normal distributions estimated by the model and corresponding to the five cohorts assumed in the population analyzed.

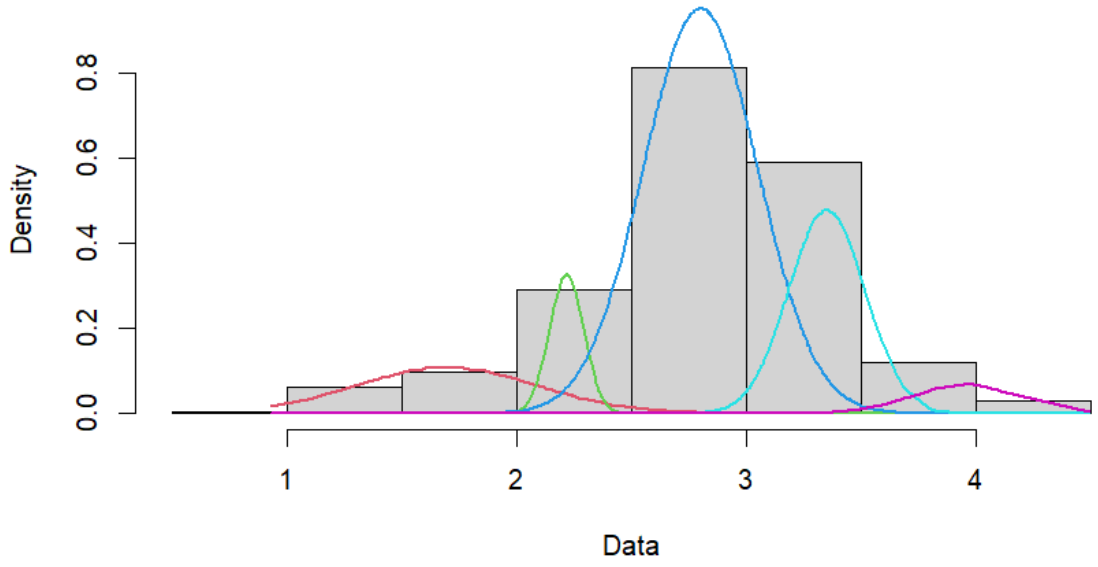

Fig. 16. Distribution of *Ophioctenella acies* disc diameters from the Broken Spur site in july 2018 modeled using a 5-component Gaussian mixture analysis (cohorts), performed with the *mixtools* package in R software. The histogram represents the density of the observed data, while the colored curves indicate the estimated densities for each cohort.

This graphic illustrates the distribution of *O. acies* disc sizes measured in millimeters across all samples collected at Broken Spur. The analysis was performed using the *mixtools* package, which allows the population structure to be modeled as mixtures of normal distributions. Five

distinct cohorts are identified, each represented by a colored density curve. This modeling suggests a structured population dynamic, potentially linked to successive episodes of recruitment of the species.

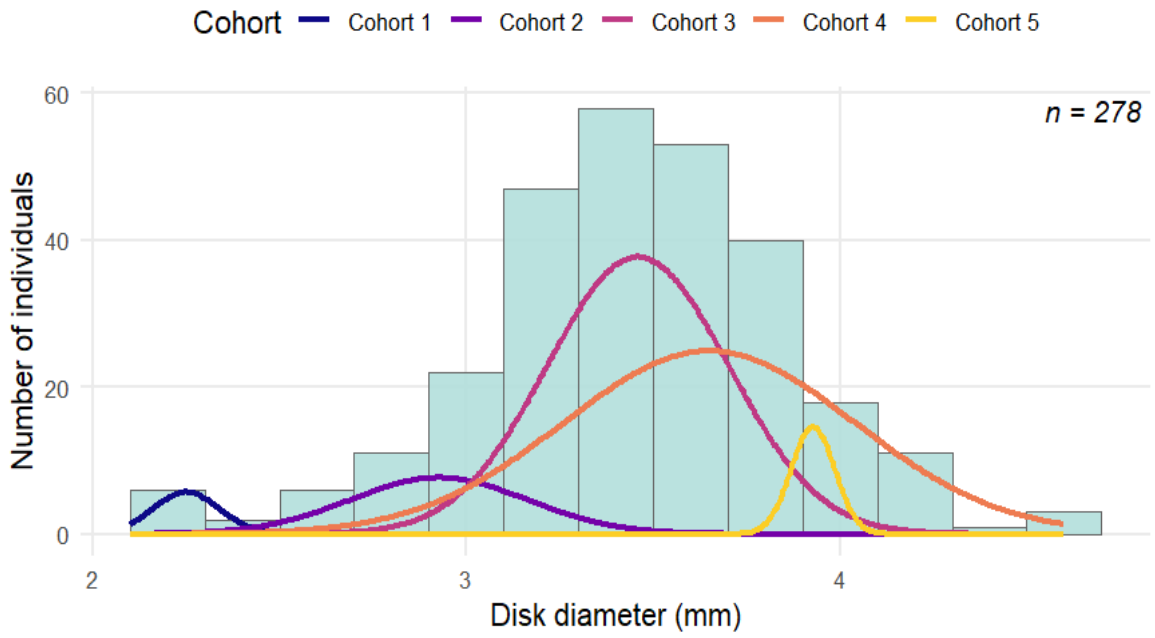

Fig. 17. Modal decomposition of the diameters of *O. acies* discs collected at the Rainbow Pit site in May 2025. The 5-cohort model was estimated using the EM estimation method using the *Mixtools* package. The histogram shows the distribution of measured individuals (n= 278) and the colored curves indicate the estimated densities for each cohort.

The central cohorts (pink and orange) comprise the majority of individuals, while the smaller cohorts at the extremes may reflect recent juveniles or older adults.

The modal distributions of disc diameters show distinct population dynamics between the two samples. The Rainbow Pit population (n=278) has a dominant cohort centered around 3.3 mm, accompanied by smaller or larger individuals, reflecting a relatively stable population structured around a main age class. In contrast, the Broken Spur population (n=353) reveals two small cohorts (< 2.5 mm), indicating one or more recent recruitment events. The tighter structure of the cohorts and the abundance of juveniles suggest that this population may be more active. The individuals found at Rainbow Pit were generally larger than those found at Broken Spur (**Figure 17).**

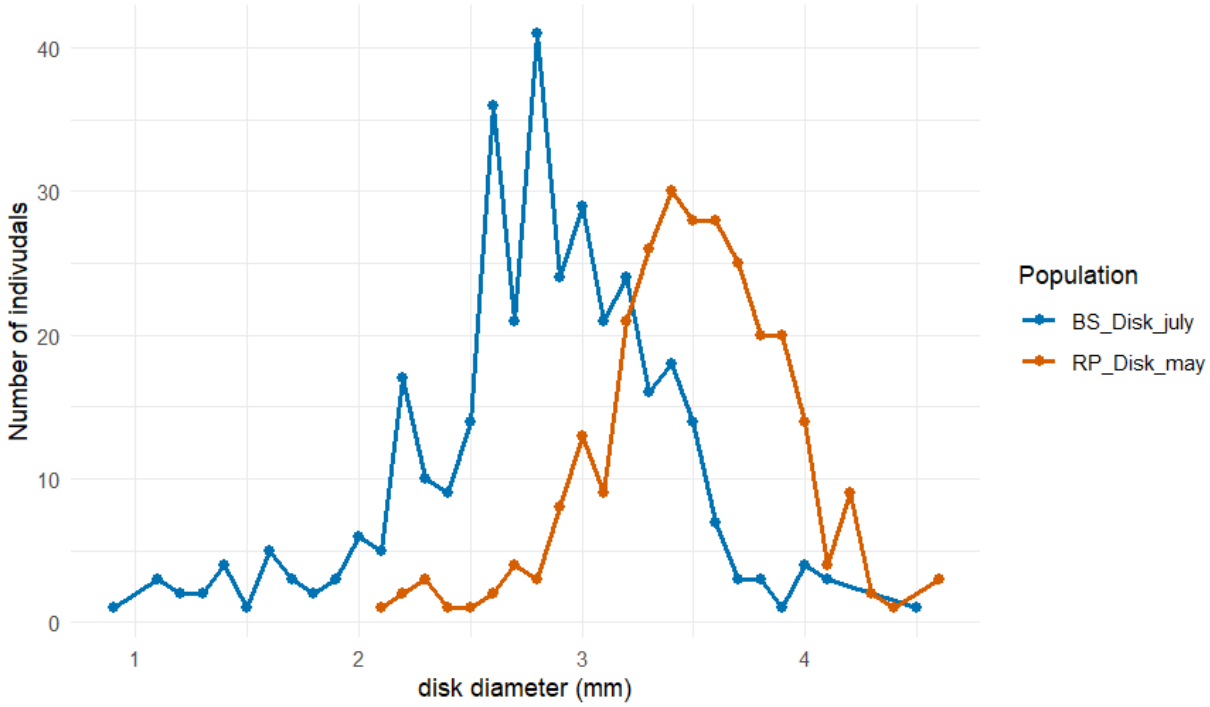

Fig. 18. Comparison of the distribution of O. acies disc diameters between two populations collected at two different sites: the Broken Spur hydrothermal site in July 2018 (blue) and the Rainbow Pit site in May 2025 (orange). Each point represents the number of individuals measured for a given size class.

At Broken Spur, the population sampled in July shows a dominance of small diameters (2.6 - 3.2 mm dd). The maximum peak number of individuals reaches 40 in a relatively small size class (~ 2.9 mm dd). The presence of very small individuals (< 2 mm dd) probably suggests continuous recruitment. At the Rainbow Pit site, the distribution appears more symmetrical and unimodal, centered around 3.4 and 3.6 mm dd with a maximum peak of about 30 individuals. The proportion of small individuals is lower than at Broken Spur, suggesting either an older cohort, a lack of recent recruitment, higher post-larval mortality, or sampling bias. The profiles show a marked difference in the demographic structure between the two samples, with a higher proportion of small individuals in July suggesting more recent or more intense recruitment.

2) Reproduction

2.1) Sex-ratio

Brittle stars from each cohort were selected for histological analysis of gametes in order to verify the presence or absence of gametes and gametic stages. The sex was identified for each individual, as well as the sex ratio for each population.

Table 2. Sex distribution of sexed individuals collected at the Broken Spur and Rainbow Pit hydrothermal sites.

Site <chr>	sexe <chr>	n <int>	proportion <dbl>
Broken Spur	female	8	0.2666667
Broken Spur	male	22	0.7333333
RainbowPit	female	3	0.3000000
RainbowPit	male	7	0.7000000

The proportions shown correspond to the relative fractions of males and females in the populations at each site. Ophiuroids from each cohort were selected for histological analysis of gametes in order to verify the presence or absence of gametes and gametic stages. The sex was identified for each individual, as well as the sex ratio for each population.

Analysis of the sex ratio of individuals collected at the Broken Spur and Rainbow Pit sites reveals a dominance of males at both sites. At Broken Spur, of the 30 individuals sexed, 73% are males compared to only 27% females (n=30), indicating a strongly unbalanced sex ratio in favor of males. This imbalance is also observable at Rainbow Pit, although less markedly, with 70% of 10 sexed individuals being males and 30% females (n=10) (**Table 2**). However, these proportions should be interpreted with caution, as they are based on a relatively small number of sexed individuals. It is therefore possible that the observed imbalance is the result of sampling and analysis bias. An increase in the number of individuals analyzed would be necessary to confirm the existence of a true sex imbalance in these populations. No hermaphrodites were observed among the brittle stars analyzed.

The disc diameter of *O. acies* ranged from 2.217 mm to 4.109 mm in females and from 2.052 mm to 4.491 mm in males. The disc diameter of males of Broken Spur ranged from 2.052 mm to 4.491 mm and from 2.217 mm to 4.109 mm for females. Regarding the Rainbow Pit vent field the disc diameter of females ranged from 3.072 mm to 3.421 mm and from 3.167 mm to 4.122 mm for males. At Broken Spur, there is no marked difference between the sexes, although males have a slightly wider distribution and are larger. At Rainbow Pit, males have a higher median diameter than females (**Figure 19**). However, these results should be interpreted with caution given the sex ratio in favor of males. In addition, disc sizes at Rainbow Pit were larger than those at Broken Spur regardless of sex. This may be due to environmental differences between the sites (e.g., food availability, substrate).

The Shapiro-Wilk normality test showed that all distributions did not differ significantly from a normal distribution ($p > 0.05$) in any group (Broken Spur females: $W = 0.948$, $p = 0.689$; Broken Spur males: $W = 0.972$, $p = 0.751$; Rainbow Pit females: $W = 0.837$, $p = 0.206$; Rainbow Pit males: $W = 0.949$, $p = 0.723$). Disc diameter was therefore considered to be normally distributed in both sexes at both hydrothermal sites. T-tests were performed to compare sexe differences at Broken Spur and Rainbow Pit, as well as males and females between sites. The disc diameter of *O. acies* were not significantly different between sexes at Broken Spur (mean ± SE: females = 3.08 mm, males = 3.05 mm; *Welch's t-test*, $t = 0.09$, $df = 12.46$, $p = 0.928$). At Rainbow Pit, although males appeared to be larger on average (females = 3.20 mm, males = 3.60 mm), the difference was only marginally non-significative ($t = -2.36$, $df = 6.77$, $p = 0.0512$). No significative difference was observed between sites in terms of female disc diameter ($t = -0.55$, $df = 9.00$, $p = 0.599$), while males were significantly different ($p < 0.05$) with larger males at Rainbow Pit than at Broken Spur ($t = -3.10$, $df = 18.05$, $p = 0.0062$). These results indicate potential site-specific variation in male growth or recruitment dynamics, while female size remains more consistent across sites.

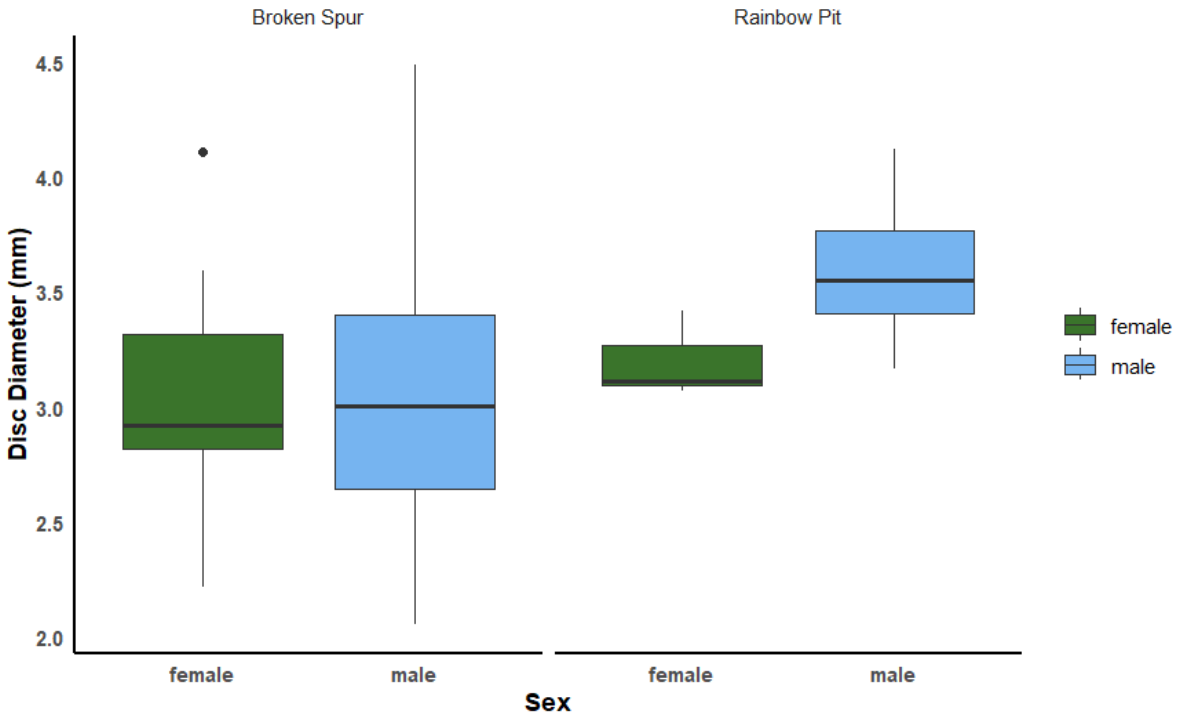

Fig. 19. Distribution of disc diameter (mm) of male and female *O. acies* individuals from the two hydrothermal sites (Broken Spur and Rainbow Pit).

The presence of gametes was observed in all cohorts of the Broken Spur population (the main population analyzed), with the exception of the first (< 2 mm disc diameter), for which excessive tissue degradation prevented any observation.

2.2) Analysis of gametic stages

Spermatogenesis

Spermatogenesis is the process of sperm formation from germline stem cells. In *O. acies*, this process takes place in the gonads, located at the base of the arms, at the end of the central disc, and may extend slightly into the arms. There are several stages of development during spermatogenesis. The identification of development stages in this study follows the visual recognition of spermatogenesis stages guided by Brogger et al. (2013).

Stage I corresponds to the presence of spermatogonia (sg), germ stem cells recognizable by their small size and dense nucleus; they are located at the periphery of the gonadal lobes (Grange et al., 2004; Borges et al., 2009) (corresponding to the dark cells observed in **Figure 20 B, C, D**). In stage II, larger spermatocytes (sc) with less dense nuclei are observed (**Figure 20 A, B, D**). Stage III is characterized by spermatids which are smaller and round, often organized into "sperm strings" toward the center of the lobe, present in clusters, then gradually organized into rows (Grange et al., 2004; Laming et al., 2021) (**Figure 20 A, B, C, D**). This stage is characterized by the sperm production, where the peripheral spermatocyte layer has visibly shrunk (Grange et al., 2004). Stage IV marks the beginning of the release of spermatozoa into the gonadal lumen and testes have increased in size (Grange et al., 2004; Laming et al., 2021), forming spiral or cluster structures. Finally, in stage V, the gonadal lobe is completely filled with mature, elongated, flagellated, and functional spermatozoa. Towards the end of this phase, a "whorl" (or spiral cluster) of spermatozoa forms from the remaining testicular mass. It gradually detaches and accumulates in the center of the testicles. This last part of the stage

precedes the emission of gametes (Grange et al., 2004).

The cells are arranged in a characteristic centrifugal gradient: spermatogonia are located at the periphery of the gonad, while the most differentiated cells (spermatozoa) are found toward the central lumen of the gonad lobe.

In the male individuals observed, the majority of gonads were immature or in the early stages of maturation, with an abundance of spermatogonia. However, some lobes showed more advanced stages of differentiation, with centrally organized spermatids and spermatozoa (**Figure 20 A, B, C, D**), suggesting asynchronous development within the gonads.

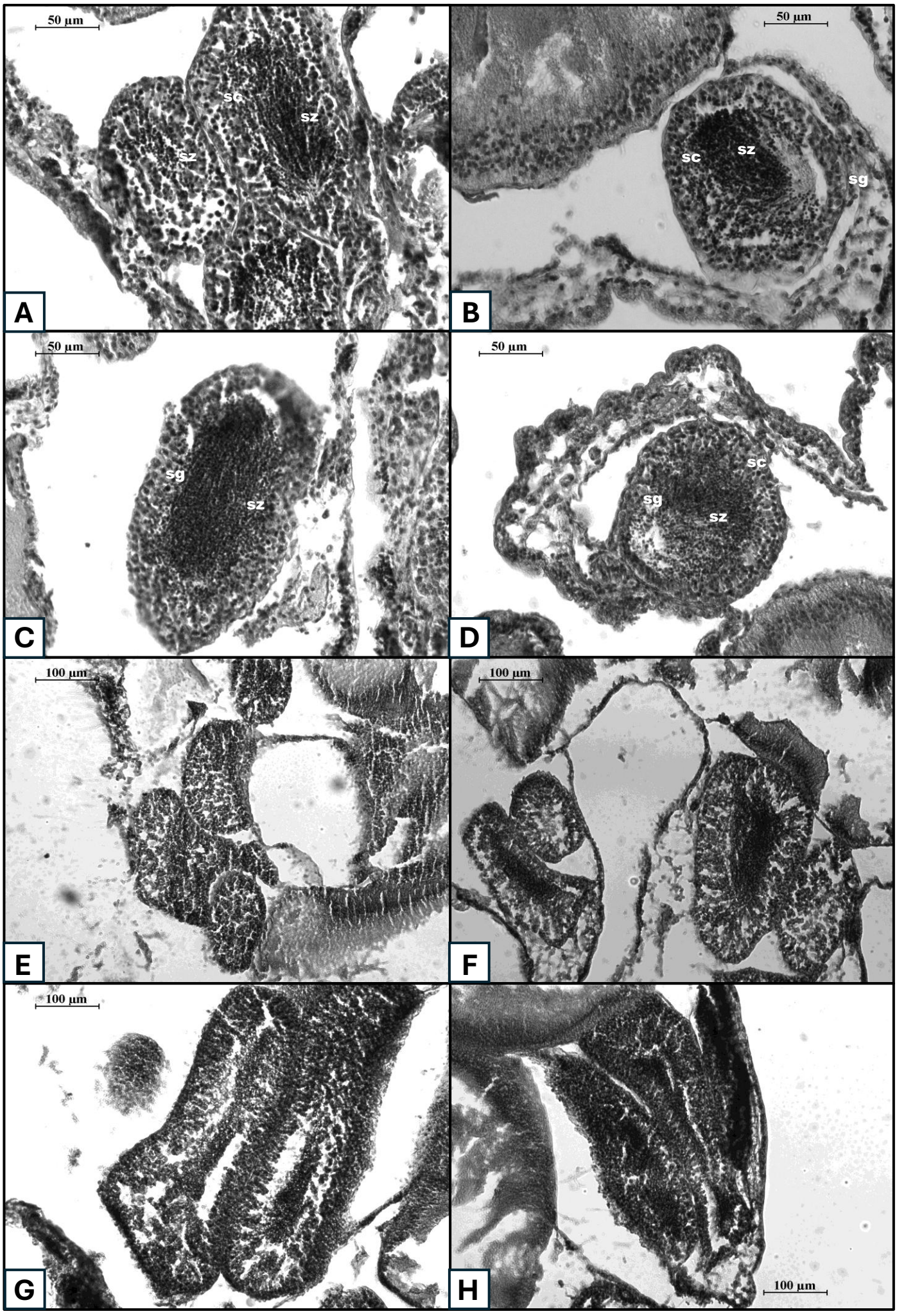
50 µm
sc
sz
sz
A
50 µm
sc
sz
sg
B
50 µm
sg
sz
C
50 µm
sc
sg
sz
D
100 µm
E
100 µm
F
100 µm
G
100 µm
H

Fig. 20. *Ophioctenella acies.* Histology of the testes. (sc) spermatocytes; (sg) spermatogonia; (sz) spermatozoa. Scale bars: A, B, C, D = 50 µm; E, F, G, H = 100 µm

Oogenesis

Oogenesis is the process by which oocytes are formed from germline stem cells. In *O. acies*, this process takes place in the female gonads, which, like in males, are located at the base of the arms at the end of the central disc. There are several successive stages in the development of female germ cells. The number of stages of oogenesis in ophiuroids (including deep-sea species) is not always universally established, it often depends on each study. However, most studies, including those on deep-sea species, generally describe between 4 and 6 stages, based on oocyte size, morphology, yolk content (vitellus), and its histological reaction (staining).

According to certain literature (Byrne, 1991; Selvakumaraswamy & Byrne, 1995; Borges et al., 2009; Laming et al., 2021), ophiuroid oogenesis comprises four main categories: previtellogenic oocytes, early-vitellogenic oocytes, mid-vitellogenic oocytes and late-vitellogenic oocytes. The stages of oogenesis have been described in detail for the deep-sea brittle stars *Ophiosphalma glabrum* and *Ophiacantha cosmica,* with three additional stages: the asymmetric vitellogenic stage (AS), which precedes the germinal vesicle breakdown (GVBD) marking the start of meiosis I; the polar bodies (PB), where meiosis has begun; and the mature stage (M), the final stage where the oocyte is ready for spawning (Laming et al., 2021). These stages were not observed in our samples. Borges et al. (2009) and Selvakumaraswamy & Byrne (1995), observed respectively for the species *O. januarii* and *Ophionereis schayeri,* five different gonadal stages in the gametogenic cycle: recovering (after spawning, including pre and early-vitellogenic oocytes), growing (including early and mid-vitellogenic oocytes), mature (late-vitellogenic oocytes), partly spawned and empty (Borges et al., 2009). In our data, the last two steps were not observed.

The identification of developmental stages in this study follows the criteria described in the previously cited articles, with visual recognition of oocyte stages guided by Brogger et al. (2013). First, we observed the stage (I) with pre-vitellogenic oocyte (PV), characterized by a lighter nucleus, cytoplasm that is in the process of organizing and cytoplasm not yet enriched in yolk (Laming et al., 2021) (**Figure 21 E, G**). Stage (II) corresponds to early-vitellogenic oocyte (EV) stage, representing the onset of yolk accumulation (Laming et al., 2021). Stage (III), the mid-vitellogenic oocytes (MV) follow, with active accumulation of vitellus in the cytoplasm, giving them a granular appearance (**Figure 21 A, C, D, E, F, G**). These oocytes are significantly larger. Finally, stage (IV) with late-vitellogenic oocytes (LV) which reach their maximum size, their cytoplasm is densely filled with reserves (Laming et al., 2021), and their nucleus sometimes becomes eccentrically located (**Figure 21 B, C, E, F, G**).

The analyses of the histological sections showed that the majority of females were in an advance development stage (i.e., mid and late-vitellogenic oocytes), almost reaching maturity. In the females observed, it was not possible to detect a massive accumulation of mature oocytes at the end of vitellogenesis, suggesting that there were no gravid females at the time of sampling. The gonads contained a range of oocyte sizes reflecting continuous but asynchronous gametogenic activity. The gonads of *O. acies* comprise two sacs : an outer sac and an inner sac (**Figure 21**).

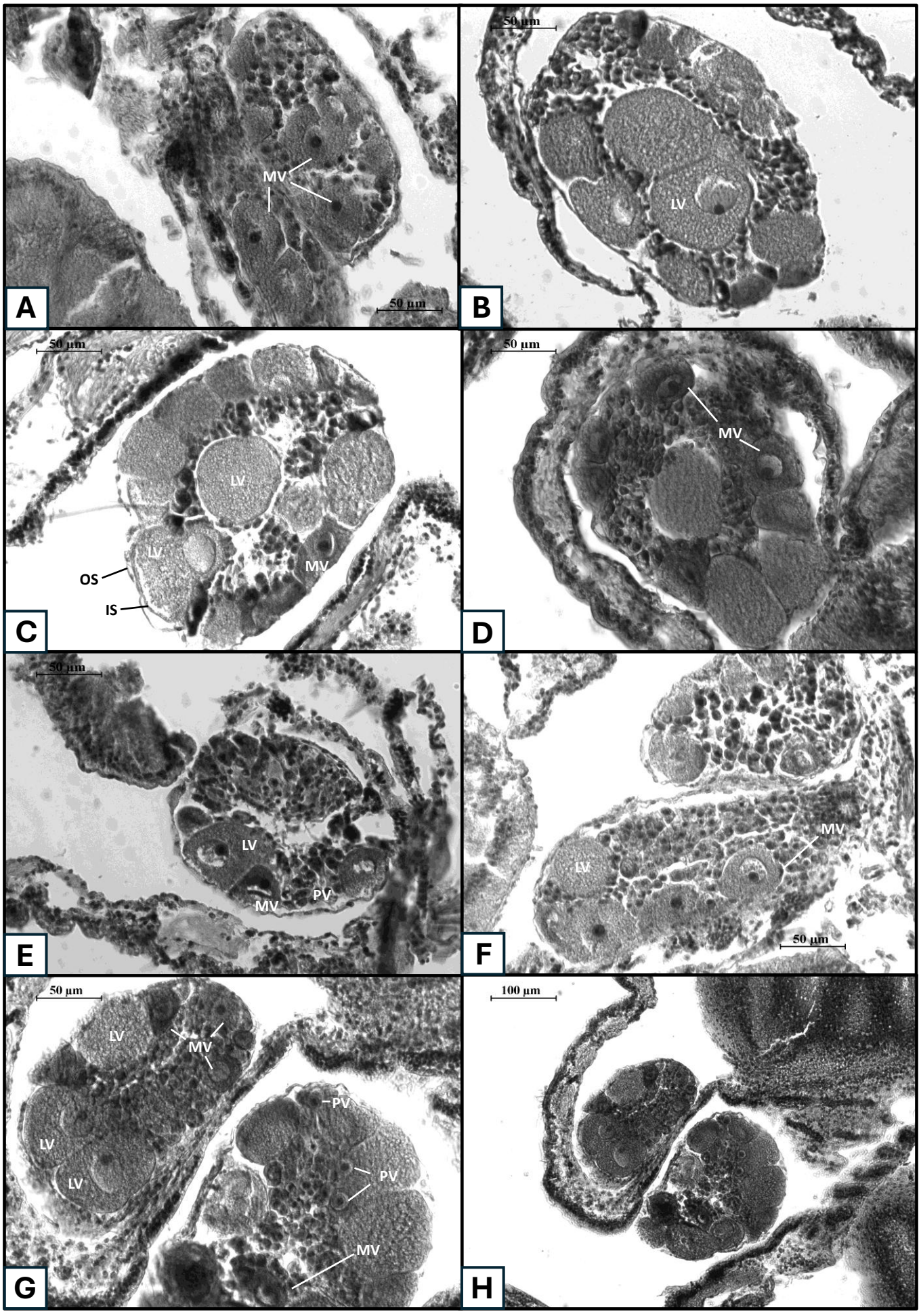
A
MV
50 µm
B
50 µm
LV
C
50 µm
LV
LV
OS
IS
MV
D
50 µm
MV
E
50 µm
LV
MV
PV
F
LV
MV
50 µm
G
50 µm
LV
MV
PV
LV
LV
PV
MV
H
100 µm

Fig. 21. *Ophioctenella acies*. Histology of the ovaries with various stage of development; the outer sac (OS), the inner sac (IS), late-vitellogenic oocytes (LV); mid-vitellogenic oocytes (MV) pre-vitellogenic oocytes (PV). Scale bars: A, B, C, D, E, F, G = 50 µm; H = 100 µm

Oocyte size frequency

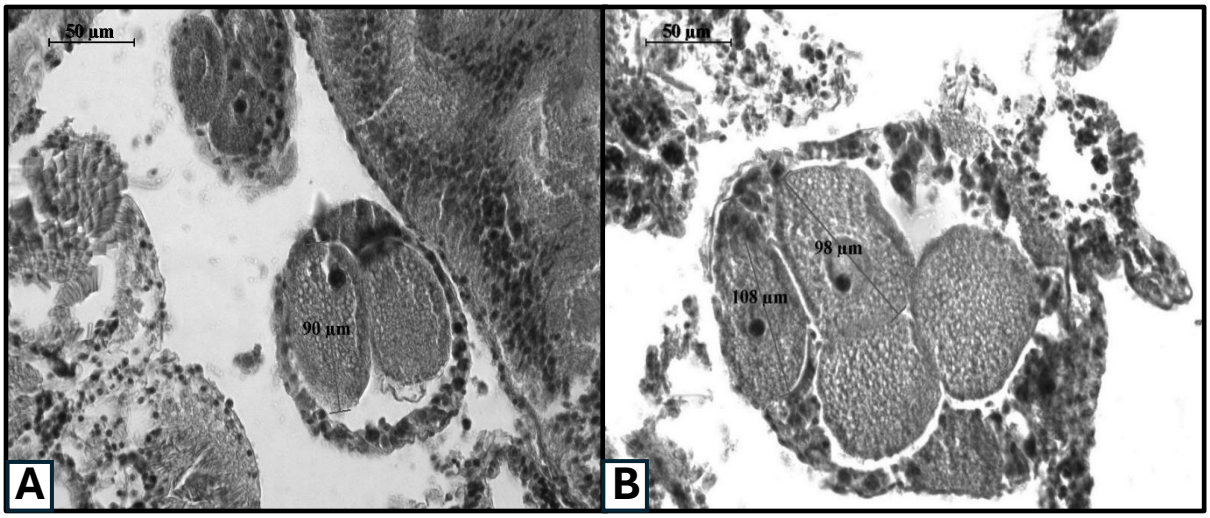

Fig. 22. Histological sections of *Ophioctenella acies* ovaries observed and measured with Leica software under an optical microscope after staining, showing oocytes in advanced vitellogenesis. **A.** Ovarian extract showing oocytes measuring approximately 90 µm in diameter. **B.** Ovarian containing large oocytes (98–108 µm) with clearly visible nuclei and granular cytoplasm typical of the vitellogenic stage. Scale: 50 µm

Only oocytes with a nucleus were measured. The measured diameter is the Feret diameter, i.e., the longest axis measurable diameter of the oocyte regardless of its orientation (Laming et al., 2021). They are then assigned to specific stages of oocyte development.

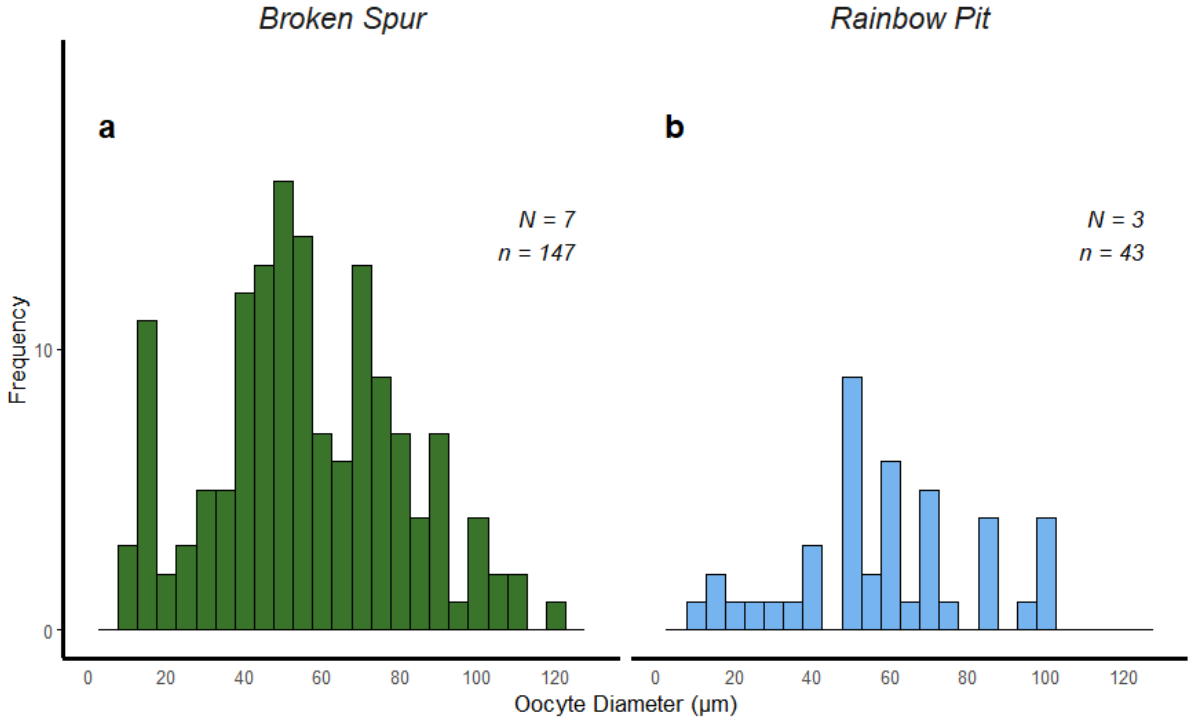

Fig. 23. Oocyte size-frequency histograms. (a) Distribution for individuals of *O. acies* collected from Broken Spur hydrothermal vent. (b) Distribution for individuals of *O.acies* collected from Rainbow Pit hydrothermal vent. N: number of individuals and n: number of oocytes

The oocyte diameter distributions observed for both populations at Broken Spur (a) and Rainbow Pit (b) are broadly unimodal, characterized by a wide range of sizes, from small oocytes (~1- 20 µm) to more developed oocytes (>100 µm). In both histograms, there is a continuous spread of frequencies across diameter classes, with no distinct, multiple peaks that would indicate the presence of clearly defined oocyte cohorts (**Figure 23**).

At Broken Spur, the distribution shows a relatively symmetrical bell curve centered around 50 µm, but with a long peak extending towards smaller (~15 µm) and larger (~ 70 µm) diameter classes. This suggests that females at this site have oocytes at different stages of development, from the pre-vitellogenic stage to the fully vitellogenic stage. The high frequency of intermediate-sized oocytes reinforces the idea of a regular and continuous maturation process rather than a synchronized wave of development.

At Rainbow Pit, although the sample size is smaller (N = 3 females), the pattern remains consistent with the Broken Spur population. The histogram shows a relatively uniform distribution, although slightly more irregular with no sign of multimodality. The presence of early-stage and late-stage oocytes also confirms an asynchronous reproduction pattern.

The absence of clearly separated modes in both distributions indicates that there is no synchronization in oocyte maturation between individuals or within individual gonads. This is incompatible with seasonal reproduction, which is typically characterized by a multimodal distribution resulting from the development of oocytes by cohorts in response to environmental signals (e.g., temperature or food availability). In contrast, the coexistence of oocytes of all sizes and the absence of a clear cohort structure strongly suggest a continuous reproduction strategy, in which oogenesis occurs gradually throughout the year. This implies that females are capable of producing and releasing gametes over long periods of time, without a marked reproductive rest phase. Such a strategy is often observed in deep-sea or hydrothermal vent species, where environmental conditions are relatively stable throughout the year and do not favor seasonal spawning.

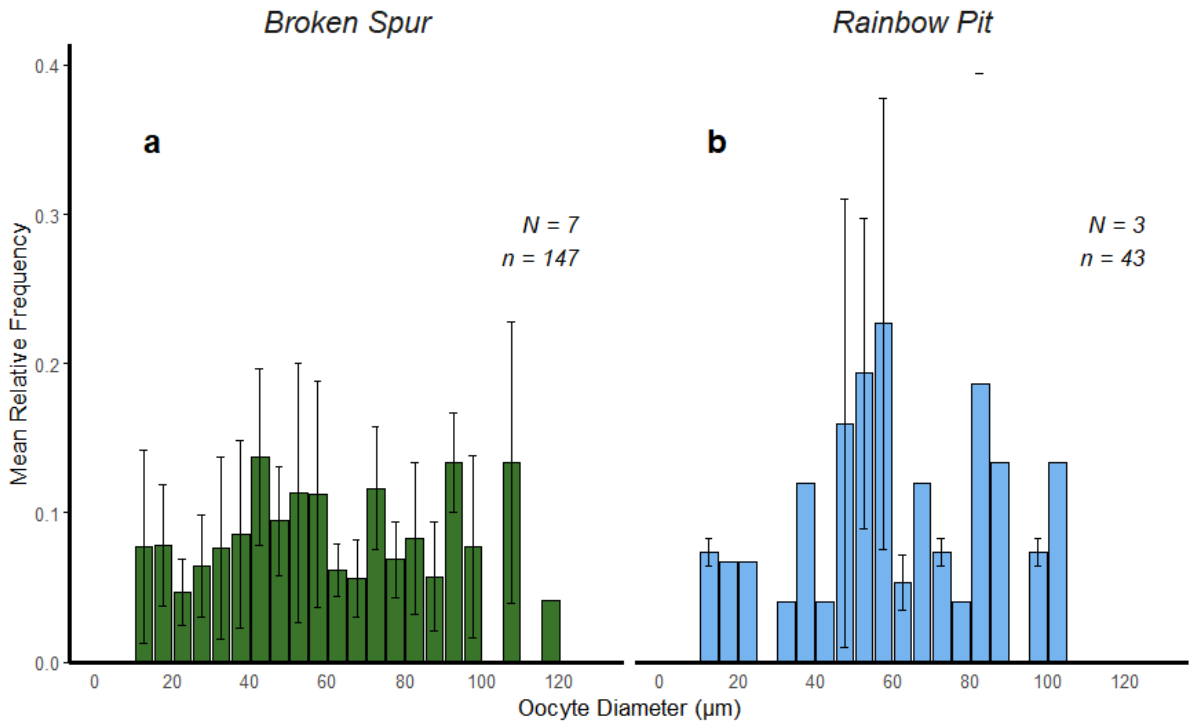

Fig. 24: Mean (± SD) Oocyte size-frequency histograms. (a) Distribution for individuals of *O. acies* collected from Broken Spur hydrothermal vent. (b) Distribution for individuals of *O.acies* collected from Rainbow Pit hydrothermal vent. N: number of individuals and n: number of oocytes

A relative frequency average was calculated for each oocyte diameter class, taking individuals one by one into account to prevent those with more data from biasing the distribution. For each individual, the relative frequency of oocytes in each diameter class was calculated by dividing the number of oocytes of an individual in a class by the total number of oocytes of the individual. The frequencies were then averaged for each diameter class, representative of the average behavior of individuals. This approach prevents an individual with many oocytes from overwhelming the others. It thus gives a better idea of the average reproductive structure, particularly for observing patterns such as oocyte cohorts. In these graphs, no cohort stands out. This analysis is much more robust when the number of oocytes is uneven between individuals. The error bars (SD) indicate the interindividual variability for each oocyte diameter class.

This graph shows the average relative frequencies of *O. acies* oocyte diameters. At Broken Spur, there were 7 females (N = 7) with 147 oocytes measured (n = 43), and at Rainbow Pit, there were 3 females (N = 3) with 43 oocytes measured (n = 43) (**Figure 24**). Regarding the Broken Spur hydrothermal vent site, the distribution is relatively homogeneous across a wide range of diameters (10-110 µm) with similar frequencies for all classes. The absence of a clear peak in oocyte diameter and the spread distribution of oocyte sizes confirm asynchronous reproduction without a dominant cohort. The large error bars show variability between individuals, which is consistent with a continuous strategy where females are not all at the same stage of development. For the Rainbow Pit hydrothermal vent, the distribution shows a very slight bimodal trend, with a more pronounced concentration around 50-70 µm. However, the error bars are very high due to the small number of females analyzed (N = 3), which greatly limits interpretation. Despite this, the presence of small, medium, and large oocytes also suggests continuous reproduction, although the visible peaks could reflect sampling bias or an effect of the small sample size measured. The distribution of oocyte sizes and the variability observed in

both populations support the hypothesis of continuous reproduction in *O. acies*. No oocyte development pattern consistent with synchronized seasonal reproduction is apparent. Females appear to produce oocytes throughout the year, at varying individual rates.

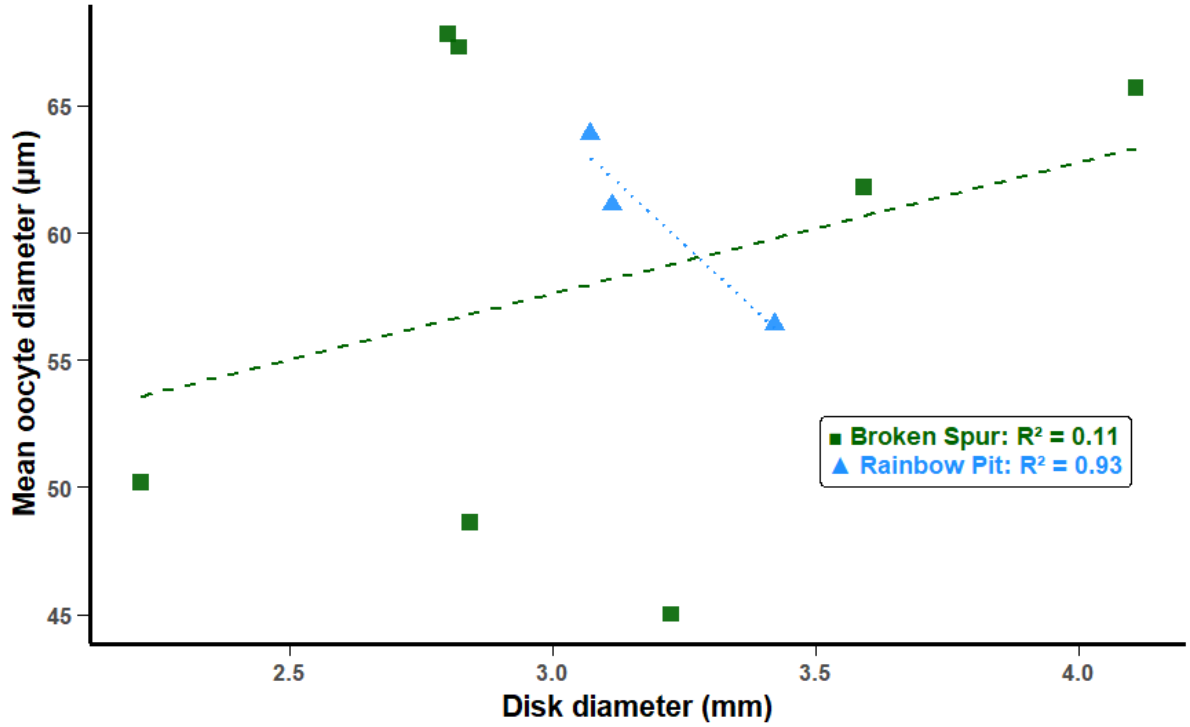

Fig 25. Relationship between disc diameter (mm) and mean oocyte diameter (µm) in *O. acies* from two hydrothermal sites in the North Atlantic (Broken Spur &Rainbow Pit). Data are presented for two populations: Broken Spur (green squares) and Rainbow Pit (blue triangles). The dotted lines represent linear regressions for each site, with R^2 values indicating the quality of the fit.

Regarding the Broken Spur site, the regression shows a very weak positive relationship between disc diameter and average oocyte diameter ($R^2 = 0.11$). This suggests that oocyte size is not strongly related to individual size at this site, or that the variability is too great to detect a clear pattern with this small sample. Conversely, Rainbow Pit data show a strong negative correlation ($R^2 = 0.93$). between disc size and oocyte diameter. This could indicate that smaller individuals have more developed oocytes, or that individuals at different stages of reproduction are present at this site.

The marked difference between the two sites could reflect environmental, temporal (reproductive phenology), or demographic (population structure) differences. In fact, these two groups come from two different hydrothermal sites that are not located at the same depth and are therefore ecologically different. The sample size is small, particularly at Rainbow Pit (3 points), which greatly limits the statistical scope of the analysis.

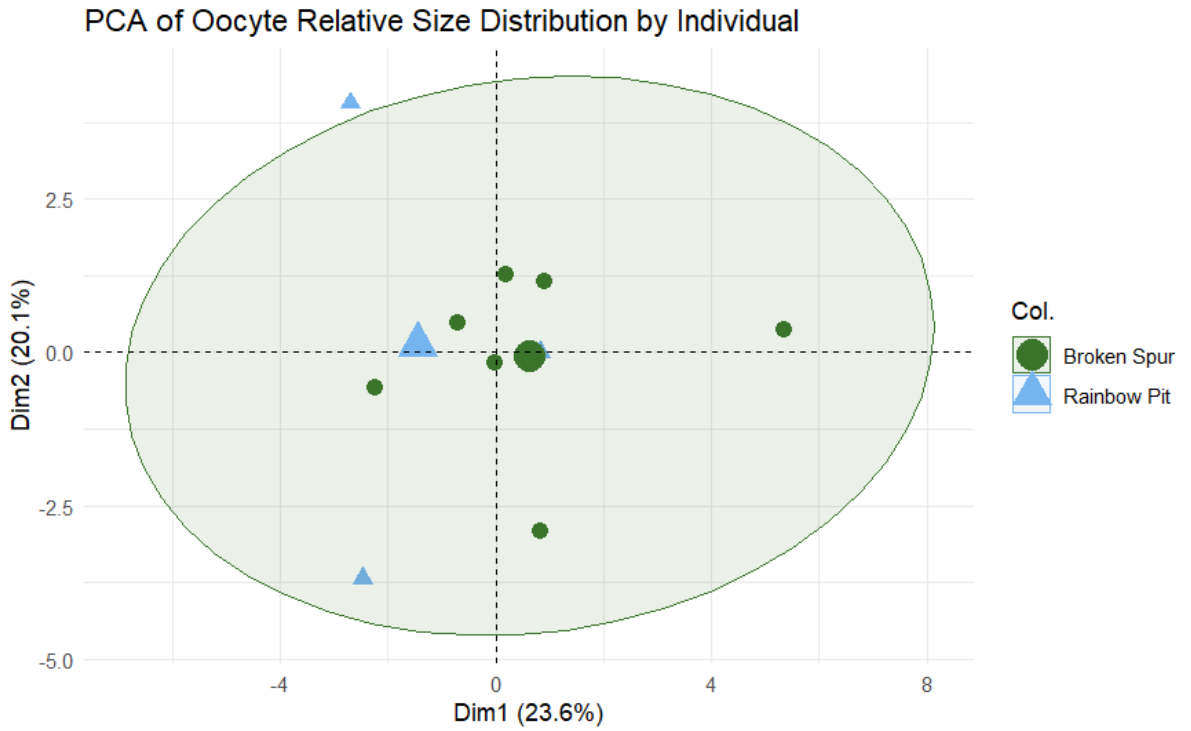

Fig. 26. Principal component analysis (PCA) of *O. acies* individuals based on the relative distribution of their oocytes by diameter class (5-micrometer bins). Each point represents an individual, with the shape indicating the site of origin: green circles for Broken Spur and blue triangles for Rainbow Pit. The ellipses represent the 95% confidence intervals for each population.

For each female individual, the relative frequency of oocytes in each diameter class (5 µm intervals) was used to perform a principal component analysis (PCA). The first dimension (Dim1) summarizes 23.6% of the variability between individuals, and the second (Dim2) summarizes 20.1%, for a total of 43.7% of the variance explained by the two axes (**Figure 23**). Each point represents an individual, whose position reflects the similarity of its oocyte profile to others: points that are close together correspond to similar profiles, and conversely, points that are further apart correspond to more different profiles. The size of the symbols indicates the quality of representation of individuals in the plane, and the ellipse represents a 95% confidence interval for all observations.

This analysis allows individual variability to be visualized independently of the site of origin. No clear separation between individuals from Broken Spur and those from Rainbow Pit is observed, suggesting that, despite slight differences in the overall distributions (histograms), oocyte profiles remain broadly comparable and similar at the individual level between the two sites.

Fecundity

The most advanced stage observed in the gonads of females was considered for the stage of development.

Table 3. *Ophioctenella acies*. Fecundity parameters. (DD disc diameter; - no data)

Site	DD (mm)	Fecundity (total no. eggs)	Mean egg size (µm)	Max. egg size (µm)	Development stage
Broken Spur	2.823	112	67.3 (SD = 26.87)	108	Stage III
Broken Spur	3.593	10	61.8 (SD = 28.91)	99	Stage II
Rainbow Pit	3.421	284	56.4 (SD = 21.76)	97	Stage III
Broken Spur	2.843	159	48.6 (SD = 18.38)	107	Stage IV
Broken Spur	3.225	169	45.0 (SD = 24.35)	81	Stage IV
Broken Spur	4.109	35	65.7 (SD = 27.54)	106	Stage II
Broken Spur	2.217	44	50.2 (SD = 13.13)	76	Stage III
Broken Spur	2.801	249	67.8 (SD = 22.58)	118	Stage III
Rainbow Pit	3.113	221	61.1 (SD = 28.83)	85	Stage II
Rainbow Pit	3.072	60	63.9 (SD = 18.47)	84	Stage II
Broken Spur	3.0	7	–	–	Stage III

The female individuals collected at Broken Spur show high morphometric and reproductive variability. The disc diameter varies between 2.217 mm and 4.109 mm, while fertility ranges from 7 to 249 oocytes. The developmental stages observed range from stages II to IV, indicating a population with heterogeneous reproductive maturity. The average size of the oocytes is between 45.0 µm and 67.8 µm, with maximum sizes reaching up to 118 µm. In comparison, individuals from Rainbow Pit have more homogeneous disc sizes (between 3.072 mm and 3.421 mm) and fecundities ranging from 60 to 284 oocytes. Only stages II and III are represented. The average oocyte sizes are mainly between 56.4 µm and 63.9 µm, with maximum sizes slightly lower than those observed at Broken Spur (between 84 µm and 97 µm). These results suggest differences in population structure and reproductive dynamics between the two sites. We can observe that there is no obvious correlation between disc size (mm) and individual fertility (e.g., the largest individual, 4,109 mm, has only 35 oocytes). Nevertheless, these data should still be treated with caution despite the small number of females analyzed.

IV) DISCUSSION

Recruitment and population structure

The two populations were sampled at two distinct hydrothermal sites: Broken Spur in July 2018 and Rainbow Pit in May 2025. These two sites have vastly different environmental characteristics, particularly in terms of depth, hydrothermal regime, and productivity resulting in significantly different population structures.

Analysis of the demographic structure of the *O. acies* population at Broken Spur revealed the presence of five distinct cohorts based on disc diameter (**Figure 15**). This dynamic suggests continuous recruitment in the study population. Polymodality and distinct peaks indicate discontinuous recruitment (Marticorena et al., 2020). The numerical dominance of cohort 3 (~3 mm dd) indicates a high proportion of subadult or young adult individuals, potentially in the process of sexual maturation. Cohort 4 (~3.5 - 4 mm dd) probably includes mature adults, while cohorts 1 and 2 (~1 - 2.5 mm dd) could correspond to juveniles from recent recruitment. The fifth cohort, which is less well represented, could correspond to older individuals. These results could reflect a relatively continuous or non-seasonal reproductive strategy, which could be the result of adaptation to hydrothermal ecosystems where colonization is rapid. In addition, the presence of individuals of different sizes might contribute to population resilience in unstable environments. However, since no relation was found between individual size and oocyte developmental stage in this study, other factors such as asynchronous reproduction strategies might be involved. Similar observations have been made in other hydrothermal species such as certain bivalve, gastropod and crustacean species such as *Ctenopelta porifera* and *Lepetodrilus tevnianus*, showing also quasi-continuous reproduction with frequent recruitment (Bayer et al., 2011). These two species reproduce almost continuously, mature rapidly, and have high fecundity, which is typical of opportunistic species and consistent with the reproductive cycles of other vent molluscs (Tyler et al., 2008; Bayer et al., 2011). It is also possible that spatial variability within sites (e.g., proximity to an active vent or a diffuse zone) influences the growth and size structure observed.

The analysis of disc sizes in *O. acies* at the Rainbow Pit site shows five cohorts, although the distribution appears to be more compacted overall than at Broken Spur (**Figure 17**). The diameters are mainly concentrated between 2.5 and 4 mm dd, with two dominant cohorts around 3.2 mm (cohort 3) and 3.6 mm (cohort 4), suggesting a population composed largely of subadult to mature individuals. Unlike Broken Spur, where very small individuals (< 2 mm dd) were present, young juveniles are few in number in this site, which could reflect older or less recent recruitment. The notable presence of a well-defined adult cohort around 3.6 mm combined with a less represented post-mature or senescent cohort could suggest local stability in recruitment over time. However, the absence of a clear juvenile mode could suggest sampling bias or higher mortality in the early stages under the physical and chemical conditions of Rainbow Pit (e.g., ultramafic environment, fluids rich in H_2, CH_4, and Fe). This distribution pattern suggests that the Rainbow Pit population is generally more homogeneous in terms of size, with a smaller spread of diameters compared to Broken Spur. This could reflect a more stable population structure, older colonization dynamics, or partial synchronization of development linked to specific environmental constraints (i.e., fluid composition, substrate type, or density of associated communities such as mussels or anemones). Temporal monitoring and the addition of genetic analyses would provide a better understanding of whether the differences observed between Rainbow Pit and Broken Spur are ecological, site-dependent, or demographic in nature, with connectivity between populations and colonization.

These differences between the two populations could reflect distinct colonization conditions, more recent or more active recruitment at Broken Spur, or environmental constraints specific to Rainbow Pit related to its ultramafic substrate. This suggests adaptation and development strategies that may be modulated by the geochemical nature, stability, and specific ecological characteristics of the sites.

Cohorts allow us to determine whether the population is dominated by juveniles (recent recruitment) or adults (aging population). The identification of five cohorts suggests a varied age structure within the population, potentially linked to successive recruitment events. This could reflect continuous reproduction or episodes of colonization favored by moderate hydrothermal fluids. A similar population dynamics pattern was observed by Comtet & Desbruyères (1998) in bivalves of the genus *Bathymodiolus* found at the Lucky Strike and Menez Gwen hydrothermal sites on the Mid-Atlantic Ridge. The authors observed clearly polymodal size distributions, reflecting several successive recruitment events. Statistical analysis of these distributions identified between five and seven distinct cohorts, revealing discontinuous recruitment over time.

The results obtained show a marked difference in the size dynamics of males between the two hydrothermal sites studied. While no significant size difference was detected between males and females at Broken Spur, males at Rainbow Pit are significantly larger on average than their counterparts at Broken Spur ($p < 0.05$). Conversely, female size remained relatively consistent between the two sites, suggesting either greater morphometric stability in females or stricter regulation of their growth. This male-specific difference could reflect several biological or ecological processes, such as site-specific environmental conditions (e.g., temperature, food availability, water chemistry), differences in reproductive strategies, or variation in recruitment timing. In the hydrothermal crab *Kiwa tyleri*, significant variation in size between males and females has been observed, as well as differences between hydrothermal sites (Thatje et al., 2015). Males in particular show more pronounced growth, with more developed claws than females, which could be linked to competitive behaviors or differentiated reproductive strategies. This morphological and spatial differentiation suggests the existence of distinct ecological and behavioral strategies between the sexes, potentially influenced by competition or access to trophic resources (Thatje et al., 2015).

For instance, larger males at Rainbow Pit could indicate earlier recruitment, faster growth, or delayed sexual maturation compared to Broken Spur. Additionally, the observed patterns might point to distinct population structures between the two sites, possibly involving a cohort lag or an asymmetry in population dynamics (e.g., due to differences in larval dispersal, migration or connectivity). Supporting this, individuals at Broken Spur displayed smaller disc diameters than those at Rainbow Pit. The differences observed in male size between the two sites could be influenced by local environmental conditions, particularly temperature. Indeed, several studies have highlighted a close link between the distribution of hydrothermal species and temperature gradients. For example, Bates et al. (2005) demonstrated that in hydrothermal gastropods, spatial distribution and behavioral preferences were directly related to substrate temperatures. Some species, such as *Lepetodrilus fucensis*, actively select habitats with moderate and relatively stable temperatures, while others, such as *Provanna variabilis*, are more associated with colder, peripheral areas. These thermal preferences influence colonization, growth, and competition dynamics, and could thus contribute to different population structures between sites (Bates et al., 2005). By analogy, the presence of larger male individuals at Rainbow Pit could reflect a local thermal regime that is more favorable to prolonged or accelerated growth, or even delayed sexual maturation. The dominance of intermediate to large-sized individuals at Rainbow Pit could correspond to a cohort that has persisted over a longer period, with little or no recent recruitment during the sampling period, potentially giving rise to a new

juvenile cohort in the near future. Among hydrothermal shrimp, *Rimicaris hybisae* from the Von Damm Vent Field (2,294 m) were significantly larger than specimens from the Beebe Vent Field (4,944 - 4,972 m), which could be due to differences in structure between the sites. Furthermore, this study shows that the largest individuals were those that were sexually active and mature, indicating future reproduction (Nye et al., 2013). It is also important to note that the two sites were not sampled at the same time, which could introduce some temporal bias into the comparison. However, given the depth and relatively stable conditions of hydrothermal environments, seasonal variations are likely to have minimal influence (Van Dover, 2000). Nevertheless, short-term fluctuations in vent activity or episodic recruitment events cannot be ruled out as potential factors contributing to the observed differences.

Reproductive biology

Ophioctenella acies is a gonochoric species with no evident sexual dysmorphism. It is not possible to sex individuals physically by the external structure. However, no hermaphroditism was observed among the individuals analyzed, a condition that is less frequently observed in ophiuroids than gonochorism (Boschen et al., 2013). Gonads are composed of multiple lobes situated at the base of each arm in both males and females. Based on the histological analysis of *O. acies* a cyclic pattern with typical gametogenic stages could not be distinguished. This species appears to show asynchronous maturation, with several stages coexisting within the same gonad. A similar configuration is observed in *Ophioplocus januarii*, a species living in shallow temperate waters north of Patagonia. This species reproduces continuously and aperiodically, characterized by the simultaneous presence of gametes at different stages of maturation (Brogger et al., 2013). Continuous reproduction is generally associated with warm-water species and deep-sea species, although some deep-sea species exhibit reproductive seasonality (Hendler, 1991; Brogger et al., 2013). This is the case for the species *Ophiocten gracilis*, also found in the North Atlantic at depths of up to 1,000 m, reproduces seasonally and synchronously (Sumida et al., 2000). This species reproduces in early spring, which could allow the larvae to reach the surface layers of the water before the water column stratifies (Sumida et al., 2000). In the same case, deep sea ophiuroid such as *Ophiocten histatin, Ophiocten gracilis*, and *Ophiura ljungmani* produce small oocytes, have a planktotrophic development, and synchronized reproduction (Tyler & Gage, 1980; Tyler, 1986; Gage et al., 2004). Some species of deep sea ophiuroids also do not exhibit seasonality in their reproduction. This is the case with *Ophiacantha bidentata*, which reproduces asynchronously (Tyler et al., 1982), and *O. lymani*, in which no annual reproductive periodicity has been observed despite seasonal annual recruitment (Gage and Tyler, 1982). Some other species of MAR events have seasonal reproduction, as evidenced in the bivalve *Bathymodiolus azoricus* (Colaço et al., 2006).

Histological observations of the male gonads of *O. acies* revealed well-structured spermatogenesis, characterized by a centrifugal arrangement. Spermatogonia are located on the periphery of the gonadal lobes, while mature, flagellated spermatozoids accumulate in the center of the lobe, forming spiral structures. This organization reflects continuous gamete production with an orderly progression through the stages of differentiation: spermatogonia, spermatocytes, spermatids, and spermatozoids. The sperm morphology in *O. acies* is similar to that of other ophiuroid species such *as O. januarri* (Brogger et al., 2013). This mode of structured spermatogenesis, combined with the observation of lobes entirely filled with functional cells, suggests sustained spermatogenic activity compatible with a continuous reproduction strategy (Brogger et al., 2013). This pattern is consistent with the species hydrothermal habitat, where reproductive opportunities may arise occasionally and where maintaining a permanent reserve of mature gametes increases the chances of fertilization in an unstable environment. Males from the Rainbow

Pit population sampled in May had a large gamete reserve, supporting the idea that males were in full reproductive activity at the time of sampling. This observation could indicate a change in the reproductive cycle, suggesting either an earlier peak in spermatogenic activity at Rainbow Pit, or that males were taking advantage of the spring peak in primary production at the surface, a phenomenon that may not be exploited at Broken Spur in July. The geothermal nature, which differs between sites, could enable more stable conditions with a supportive environment for rapid gamete maturation. At Rainbow Pit, the ultramafic environment rich in reduced compounds promoting microbial productivity would allow for this maturation (Sevgen et al., 2025). Conversely, Broken Spur has potentially been marked by recent instability or recolonization, hosting a population in transition or recovery (Dover, 1995; Sevgen et al., 2025). Monthly monitoring would be necessary to distinguish seasonal effects related to the type of hydrothermal site.

Histological observations of the female gonads of *O. acies* show continuous oogenesis marked by the coexistence of several stages of oocyte development within the same individual (**Figure 22**). The ovaries could contain pre-vitellogenic, mid-vitellogenic, and late-vitellogenic oocytes. Vitellogenic oocytes showed differences in granularity, likely reflecting varying levels of yolk reserves to end to be ready to be thrown into the ocean. This mixture of maturation stages indicates asynchronous development, characteristic of species that reproduce continuously or opportunistically when conditions are favorable. The presence of several mid-vitellogenic and late-vitellogenic oocytes suggests active activity even in the absence of an accumulation of mature oocytes. The absence of ovaries completely filled with LV ready to be expelled could indicate either fractionated ovulation, harvesting just before spawning, or a prolonged spawning strategy. Thus, *O. acies* appears to maintain constant egg production without a marked peak in reproduction, probably in order to maximize its chances of reproductive success in an unstable habitat for reproduction. The presence of oocytes at different stages of development in the ovaries has also been observed in gastropods endemic to hydrothermal systems, such as *Lepetodrilus atlanticus* and *Ifremeria nautilei* (O'Hara et al., 2014). Furthermore, the smallest individuals observed with gametes measured 2.052 mm in males and 2.217 mm in females, suggesting that the size at first reproduction is around these respective sizes.

The reproduction of ophiuroids in deep hydrothermal vents is influenced by a combination of phylogenetic, abiotic, and biotic factors. Although many aspects of gametogenesis are constrained by phylogeny, factors such as habitat stability and food availability can modulate the quantity and quality of oocytes produced (Ramirez-Llodra, 2002). The ability of a population to adapt and recover after natural or anthropogenic disturbances is thus closely linked to its reproductive characteristics, such as age at sexual maturity, gametogenesis, fertility, and oocyte size (Marticorena et al., 2020). In species living in hydrothermal environments, the almost continuous nature of gametogenesis suggests a stable energy supply, probably provided by the constant production of biomass by chemoautotrophic microorganisms (Tyler et al., 1994). This particular ecological context favors a reproductive strategy focused on continuous oocyte production, allowing for prolonged or spread-out reproduction.

Egg size

Analysis of the distribution of oocyte diameters reveals differences between the female populations of *O. acies* from Broken Spur and Rainbow Pit (**Figure 23**). The correlation between actual fertility and body size reflects ovarian growth. The size at which the first vitellogenic oocytes appear corresponds to the size at which spermatozoa are detected in the seminal receptacle (Tyler et al., 2008).

At Broken Spur (**Figure 23a**), the distribution appears spread out, with a wide range of

oocyte diameters (~10 to over 110 µm) and a relatively homogeneous distribution. This high variability indicates asynchronous gametogenesis with the simultaneous presence of numerous stages of maturation as previously mentioned, reflecting continuous and unsynchronized reproduction. Conversely, individuals sampled at Rainbow Pit (**Figure 23b**) show a more concentrated distribution around 60-70 µm with a peak frequency and fewer very young or very mature oocytes. This structure suggests either stronger synchronization of oocyte development or a sampling time closer to a peak in ovarian maturation. However, the small number of individuals (N=3) limits the validity of the conclusions. Rainbow Pit, with its ultramafic conditions and potentially more stable conditions in May, could favor concentrated oogenesis where oocytes mature at the same time, while Broken Spur, which is more unstable or in a phase of recolonization in July, would host a continuously developing population. The small variations observed between populations in the size of oocytes may reflect local environmental changes or variations in larval recruitment, but do not indicate any real change in the mode of reproduction (Bayer et al., 2011).

O. acies have an average oocyte size ranging from 45 µm to 67.8 µm. Given the small size of the oocytes observed, planktotrophic larval development is probable. This type of larval development is generally associated with smaller oocyte diameters (< 150 µm) and tends to have a long pelagic period with the potential for long dispersal (Shanks, 2009; Byrne et al., 2024). In this context, larval survival is highly dependent on food availability in the water column. Thus, local or seasonal variability in trophic inputs whether hydrothermal, detrital, or related to surface flows could act as a filter on potentially continuous recruitment. This mode of development with geographical dispersion allows, depending on the larval phase duration (LPD), genetic flow between separate populations, colonization of new habitats, and reduction of intraspecific competition. However, the risk of larval mortality is high, particularly due to their vulnerability to currents and planktonic predators (Viegas et al., 2024). The planktotrophic larvae of ophiuroids, called ophiopluteus, have well-developed arms and a functional digestive system, allowing them to actively feed on plankton. Their development can follow two types of metamorphosis. In type I, the ophiopluteus transforms directly into a juvenile, as observed in *Ophiactis resilens* (Byrne et al., 2024). In contrast, type II, which is rarer, involves the transformation of the ophiopluteus into a secondary larva without arms, called a vitellaria, before the final metamorphosis, this type is particularly observed for the Ophiocomidae (Byrne et al., 2024). Many other species of ophiuroids have planktotrophic larvae (e.g., *Ophiocten histatin, Ophiocten gracilis, Ophiura ljungmani, Ophiactis resiliens, Ophioctrix spiculata, Ophiocoma dentata, Ophionereis fasciata,* etc.) (Tyler & Gage, 1980; Tyler, 1986; Gage et al., 2004; Falkner et al., 2015; Byrne et al., 2024), with planktotrophy being considered the ancestral plesiomorphic state in echinoderms (Byrne et al., 2024). The oocyte of *O. acies* remain small compared to other deep-sea ophiuroid species which faces lecithotrophic development such as *A. carchara*, with an average diameter of 0.45 mm and ranging up to 1.24 mm (Handler & Tran, 2001) or *Ophiacantha cosmica* and *Ophiosphalma glabrum*, two species frequently found in the Clarion-Clipperton Zone (CCZ) with vitellogenic oocyte feret diameters exceeding 250 µm and substantial yolk reserves, enabling them to disperse under food-impoverished conditions (Laming et al., 2021). Transitions to lecithotrophy and direct development are often associated with deep habitats with low temperatures or poor food supplies. Deep-water ophiuroid therefore adopt a lecithotrophic mode of development because the survival of larvae is often compromised, but this requires a greater energy investment than planktotrophy (Laming et al., 2021).

In hydrothermal vent species, early maturation is considered an advantageous life history trait characteristic of opportunistic species (Bridges et al., 1994). The minimum size for sexual maturity corresponds to the size at which the first mature oocytes appear (MacNeil et al., 2025).

Fecundity

Analysis of fertility parameters in *O. acies* reveals significant interindividual variability in both the total number of oocytes and their average size. Fertility values range from 7 to 284 oocytes per individual, with no obvious direct correlation with disc diameter. For example, an individual from Broken Spur with a disc diameter of 2.80 mm had 249 oocytes, while another with a diameter of 3.59 mm had only 10. This variability suggests that body size does not necessarily predict fertility, at least under the extreme conditions of hydrothermal vents. Similarly, average oocyte sizes vary considerably (from ~ 45 to 68 µm), with maximum sizes exceeding 100 µm. This heterogeneity could reflect differences in ovarian maturation stage, as evidenced by the stages II to IV observed, but also individual physiological responses to the environment. At Rainbow Pit, fertility appears to be higher on average, with two individuals exceeding 200 oocytes, although the number of individuals there is lower. This is consistent with previous histological and morphometric observations and could indicate a more active or synchronized reproductive phase at Rainbow at the time of sampling. These results support the idea that *O. acies* adopts a flexible reproductive strategy: variable oocyte numbers, larger oocyte sizes, and progressive development without strict synchronization. This mode of reproduction, common among several deep-sea species, maximizes the chances of reproductive success in a habitat characterized by variable resources, high environmental risks, and potentially limited connectivity (Laming et al., 2021). It would be appropriate to study the food resources of the species at different sites to see if there is an influence on fertility. These results suggest that ophiuroid have evolved toward flexible and continuous reproduction, enabling them to colonize unstable and spatially dispersed habitats.

Ecological association

The association of *O. acies* with substrates rich in sulfides and heavy metals, as well as ecological association with symbiotic communities (*bathymodiolus* mussels, polychaetes), suggests a high physiological tolerance to extreme chemical conditions. This supports the idea of ecological specialization. Difference in the ecological area of study at Broken Spur with anemones and in Rainbow Pit with *bathymodiolus* mussels.

Reproduction in Ophiuroidea clearly exhibits a wide variety of strategies, often varying greatly from one species to another. The absence of reproductive periodicity in *O. acies* observed in hydrothermal systems in the North Atlantic clearly illustrates this variability. In this species, it is possible that environmental seasonality, which influences primary production, is reflected not in gametogenic cyclicity, but in a seasonal cycle of larval survival, thus determining annual recruitment. A similar phenomenon has been described by Gage and Tyler (1982) in *Ophiomusium lymani*, a species living in deep waters in the Northeast Atlantic, where recruitment also appears to depend on seasonal fluctuations in the downward flux of particulate organic matter, rather than on an annual reproductive rhythm.

Other hydrothermal species have adopted the same strategy as *O. acies*, such as the gastropod species *Cocculina enigmadonta* and *Cocculina aurora*, which have asynchronous reproduction, quasi-continuous gametogenesis, discontinuous recruitment, and low fertility. The maximum oocyte size (< 185 µm) suggesting planktotrophic development. Low fertility could limit the resilience of populations in the event of disturbance, but their abundance at the site suggests sufficient reproductive capacity under stable conditions (MacNeil et al., 2025). In numerous studies, discontinuous recruitment has been proposed for hydrothermal vent invertebrates (MacNeil et al., 2025) as well as for *Pseudorimula midatlantica* (Marticorena et al., 2020).

In the depths of the ocean, where food is scarce, the amount of detrital organic matter, which is the main source of food, can vary throughout the year. If this is the case, the survival of post larvae, which are produced continuously, could follow the same seasonal pattern, with a delay linked to the fecundity of females and the time required for larval development (Gage and Tyler, 1982). Based on this hypothesis in the hydrothermal context, it is conceivable that the population sampled at the Rainbow Pit site in May, a period corresponding to peak phytoplankton production in the North Atlantic is just beginning to benefit from the first marine snowfall, improving the survival conditions of recently metamorphosed larvae. Thus, for the Broken Spur population sampled in July, we would logically expect to observe a higher proportion of juveniles, having survived better thanks to a more established trophic input. This scenario is consistent with our observations, which reveal the presence of individuals smaller than 2 mm (**Figure 16**), suggesting active recruitment. This would support the idea that recruitment is not governed by a seasonal reproductive cycle, but rather by larval survival, which is itself influenced by seasonal environmental factors. However, it is important to note that the two populations studied come from distinct hydrothermal sites at different depths, which limits the direct comparative scope of this interpretation.

Although hydrothermal vents do not depend directly on primary production at the surface, several local mechanisms could nevertheless generate periodic variability in trophic availability. On the one hand, variability in hydrothermal activity, such as changes in the intensity or chemical composition of fluids, can affect the activity of chemotrophic bacterial communities, and thus the amount of organic matter available to larvae. On the other hand, local circulation and the deposition of pelagic particles may play a role in certain contexts, particularly in more peripheral hydrothermal systems or those located near margins. Finally, indirect seasonal factors, such as variations in temperature, pressure, or plankton productivity at the surface, may indirectly modulate deep currents and sedimentation around the vents, thereby influencing the trophic conditions of the benthos. Therefore, even in the absence of a direct link to surface production, the larval survival of *O. acies* could be modulated by periodic local variation, whether chemical, thermal, or trophic.

Hydrothermal vent ecosystems are mainly composed of benthic invertebrates that are sessile or have very limited mobility in adulthood. These species use various modes of reproduction and life cycle strategies, which play a key role in their dispersal capacity and success in colonizing new habitats (Mullineaux et al., 2018). Many species found in hydrothermal vents and cold seeps adopt diverse reproductive strategies, ranging from continuous and highly fertile reproduction to more specialized and sporadic modes. Larval dispersal is a key mechanism for colonizing new habitats, which are often located far apart from one another. Thus, life cycles and larval dispersal potential play a decisive role in the resilience and renewal capacity of communities in these deep environments (Tyler et al., 2008). Continuous reproductive activity can promote both rapid local recolonization following persistent disturbances and long-distance dispersal after large-scale catastrophic events, as part of the population remains reproductive at all times, ensuring a constant supply of larvae. The dispersal capacity of larvae is determined by various biological factors, such as the feeding mode of the larvae, the duration of the larval stage, physiological and behavioral characteristics, and by physical parameters, including ocean currents, hydrothermal plume dynamics, and water column stratification. Planktotrophic larvae, which feed in the water column, are particularly well adapted to prolonged pelagic periods, increasing their chances of finding a suitable colonization site (Mullineaux et al., 2018). It is generally believed that deep-sea ophiuroids adopt one of three main reproductive strategies: gametogenesis synchronized with seasonal peaks in particulate organic carbon (POC), continuous reproduction throughout the year, or an asynchronous pattern. In ecosystems with short

lifespans but characterized by stable and consistently high energy availability, continuous reproduction is often favored as a reproductive strategy (Tyler et al., 2008). The observation of multiple stages of oocyte development in the same individual suggests continuous oocyte production, a characteristic typical of organisms living in relatively stable but nutrient-poor environments, such as low-activity hydrothermal vent systems. For *O. acies*, this continuous mode of reproduction could be advantageous in dealing with environmental unpredictability associated with fluctuations in thermal and chemical conditions.

Understanding the reproductive strategies and life cycle characteristics of organisms living in hydrothermal vents is essential for interpreting dispersal patterns, population structure, and ecosystem dynamics. As observed in other ecosystems, the ability of communities living in hydrothermal vents to colonize new habitats is strongly influenced by reproductive production, larval development and transport, as well as recruitment and movements from surrounding environments (Mullineaux et al., 2018; Cruz et al., 2022). It is particularly important to better understand the early stages of development of these species in order to interpret the mechanisms that govern the formation and maintenance of vent populations (Tyler et al., 1999).

Ophiuroid from hydrothermal vents remain poorly studied, and it is important to conduct further research, especially since there are still hydrothermal vents and species yet to be discovered. To better understand the reproductive dynamics of *O. acies*, it would be useful to supplement this study with a temporal analysis (samples collected in different seasons) and molecular approaches (expression of genes linked to reproduction, barcoding to verify connectivity between wind/seep populations). Understanding reproduction is crucial for assessing recovery capacity after natural or anthropogenic disturbances (e.g., mining) (MacNeil et al., 2025). Indeed, the study by Lin et al. (2021) highlighted the role of research platforms (ship noise, platforms) in altering the soundscapes of offshore sites. These disturbances could interfere with the ability of larvae to perceive the acoustic signals necessary for their settlement. Each site has a distinctive soundscape, which can potentially be used as an indicator of habitat quality or a signal of larval colonization. The impact of human underwater activities (particularly mining) on these soundscapes can be significant and long-lasting, affecting biodiversity on a large scale.

Methodological limitations and recommendations

Handling the specimens proved difficult due to their small size (1 - 5 mm dd), which limited the precision of certain steps such as dissecting the gonads to verify the decalcification protocol and positioning the discs during paraffin embedding. The decalcification protocol required adjustments, as certain acid concentrations caused tissue deterioration. The final choice (3% nitric acid and 70% ethanol) offered a good compromise between efficiency and histological preservation. However, during the cutting process, many ophiuroid perforated the paraffin strips, probably due to poor decalcification. It would therefore be more advisable to increase the decalcification time beyond 7 days. During the various processes, the brittle star tissues suffered extensive damage, making microscopic analysis of the gonads more difficult. It is also preferable to preserve ophiuroid in formalin rather than ethanol for better tissue preservation. Measurements are probably slightly underestimated, as tissues preserved in ethanol tend to shrink.

V) CONCLUSION AND PERSPECTIVES

This study highlights the reproductive and demographic characteristics of *Ophioctenella acies*, an emblematic species of deep hydrothermal environments in the North Atlantic. The results reveal a complex population structure, consisting of several cohorts coexisting simultaneously, as well as high interindividual variability in terms of fertility. This demographic and reproductive diversity could reflect an adaptive strategy that allows the species to persist in habitats characterized by chemical, thermal, and geological instability.

The presence of different gametogenic stages within the studied populations, without any real synchronization, suggests continuous and opportunistic reproduction, supported by the constant supply of organic matter in hydrothermal vent areas. The observed fertility, although variable, does not seem to be directly correlated with body size, which could reflect flexible energy allocation, adapted to resource availability and local environmental conditions. This plasticity could be a major asset for colonization and resilience to natural or anthropogenic disturbances.

In addition, the comparison of populations from two different geological contexts, magmatic (Broken Spur) and ultramafic (Rainbow Pit), provides valuable insight into possible intraspecific variations related to abiotic conditions. Although limited by the scarcity of data on Rainbow Pit, these initial observations lead the way for future research exploring the physiological responses of *O. acies* depending on the geochemical context.

From a methodological point of view, this study highlights the value of combining detailed observation techniques (microscopy, histology) with statistical tools to better characterize demographic structures in deep environments. The decalcification methodology tested here, although experimental, allowed for sufficient tissue preservation for usable histological analysis, despite technical constraints related to the small size and calcification of the specimens.

In a context where hydrothermal ecosystems are increasingly threatened by human activities, particularly deep-sea mining, this study highlights the importance of deepening our knowledge of the biological strategies of key species. Understanding the mechanisms of reproduction, recruitment, and dispersal is essential for assessing their resilience and guiding conservation efforts. *O. acies*, with its unique ecology and adaptability, thus appears to be a relevant model for better understanding the functional dynamics of deep-sea benthic communities. Due to the gaps in our understanding of deep-sea biodiversity and how these ecosystems function, combined with the unique life-history traits of many deep-sea organisms such as their slow growth rates and late reproductive maturity, it is crucial for scientists to collaborate closely with industry, conservation groups, and policymakers to design strong and effective strategies for conservation and sustainable management. This study therefore represents a first step toward a more integrated understanding of the reproductive dynamics of hydrothermal ophiuroids, such as *O. acies* and recommends continued efforts in observation, experimentation, and modelling in these unique environments.

Références bibliographiques

Abecasis, R. C., Afonso, P., Colaço, A., Longnecker, N., Clifton, J., Schmidt, L., & Santos, R. S. (2015). Marine conservation in the Azores: Evaluating marine protected area development in a remote island context. *Frontiers in Marine Science*, *2*, 104. https://doi.org/10.3389/fmars.2015.00104

Alongi, D. M. (2012). Carbon sequestration in mangrove forests. *Carbon management*, *3*(3), 313-322. https://doi.org/10.4155/cmt.12.20

Anderson, M., Greene, J., Morse, D., Shumway, C., & Clark, M. (2010). Benthic habitats. In *The Northwest Atlantic Marine Ecoregional Assessment: Species, Habitats and Ecosystems*. *Phase One* (pp. 88–144). The Nature Conservancy, Eastern US Division.

Angel, M. V. (2003). The pelagic environment of the open ocean. *Ecosystems of the World*, 39-80.

Akaike, H. (1973). Maximum likelihood identification of Gaussian autoregressive moving average models. *Biometrika*, *60*(2), 255-265. https://doi.org/10.1093/biomet/60.2.255

Aquilina, A., Connelly, D. P., Copley, J. T., Green, D. R., Hawkes, J. A., Hepburn, L. E., ... & Tyler, P. A. (2013). Geochemical and visual indicators of hydrothermal fluid flow through a sediment-hosted volcanic ridge in the Central Bransfield Basin (Antarctica). *Plos One*, *8*(1), e54686. https://doi.org/10.1371/journal.pone.0054686

Arbizu, P. M., Khodami, S., Stöhr, S., & Laakmann, S. (2014). Molecular species delimitation of Icelandic brittle stars (Ophiuroidea). *Polish Polar Research*, *35*, 243-260. doi: 10.2478/popore−2014−0011

Baker, E. T., & German, C. R. (2004). On the global distribution of hydrothermal vent fields. *Mid-Ocean Ridges: Hydrothermal Interactions Between the Lithosphere and Oceans, Geophys. Monogr. Ser*, *148*, 245-266.

Baker, M. C., Ramirez-Llodra, E. Z., Tyler, P. A., German, C. R., Boetius, A., Cordes, E. E., ... & Warén, A. (2010). *Biogeography, ecology, and vulnerability of chemosynthetic ecosystems in the deep sea* (pp. 161-183). John Wiley & Sons.

Bates, A. E., Tunnicliffe, V., & Lee, R. W. (2005). Role of thermal conditions in habitat selection by hydrothermal vent gastropods. *Marine Ecology Progress Series*, *305*, 1-15. https://doi.org/10.3354/meps

Bayer, S. R., Mullineaux, L. S., Waller, R. G., & Solow, A. R. (2011). Reproductive traits of pioneer gastropod species colonizing deep-sea hydrothermal vents after an eruption. *Marine biology*, *158*, 181-192. https://doi.org/10.1007/s00227-010-1550-1

Beaulieu, S. E., Baker, E. T., German, C. R., & Maffei, A. (2013). An authoritative global database for active submarine hydrothermal vent fields. *Geochemistry, Geophysics, Geosystems*, *14*(11), 4892-4905. https://doi.org/10.1002/2013GC004998

Beaulieu, S. E., & Szafrański, K. M. (2020). InterRidge global database of active submarine hydrothermal vent fields version 3.4.

Behrenfeld, M. J., O'Malley, R. T., Siegel, D. A., McClain, C. R., Sarmiento, J. L., Feldman, G. C., ... & Boss, E. S. (2006). Climate-driven trends in contemporary ocean productivity. *Nature*, *444*(7120), 752-755. https://doi.org/10.1038/nature05317

Beliaev, G. M., & Brueggeman, P. L. (1989). Deep sea ocean trenches and their fauna.

Bell, K. L., Johannes, K. N., Kennedy, B. R., & Poulton, S. E. (2025). How little we've seen: A visual coverage estimate of the deep seafloor. *Science Advances*, *11*(19), eadp8602. https://doi.org/10.1126/sciadv.adp8602

Benaglia, T., Chauveau, D., Hunter, D. R., & Young, D. S. (2010). mixtools: an R package for analyzing mixture models. *Journal of statistical software*, *32*, 1-29. 10.18637/jss.v032.i06

Bennett, S. A., Achterberg, E. P., Connelly, D. P., Statham, P. J., Fones, G. R., & German, C. R. (2008). The distribution and stabilisation of dissolved Fe in deep-sea hydrothermal plumes. *Earth and Planetary Science Letters*, *270*(3-4), 157-167. https://doi.org/10.1016/j.epsl.2008.01.048

Berg Jr, C. J., & Van Dover, C. L. (1987). Benthopelagic macrozooplankton communities at and near deep-sea hydrothermal vents in the eastern Pacific Ocean and the Gulf of California. *Deep Sea Research Part A. Oceanographic Research Papers*, *34*(3), 379-401. https://doi.org/10.1016/0198-0149(87)90144-0

Biscoito, M., Segonzac, M., Almeida, A., Desbruyeres, D., Geistdoerfer, P., Turnipseed, M., & Van Dover, C. (2002). Fishes from the hydrothermal vents and cold seeps-An update. *CBM-Cahiers de Biologie Marine*, *43*(3-4), 359-362.

Biscoito, M., Briand, P., & Almeida, A. J. (2009). First record of Pachycara thermophilum (Pisces, Zoarcidae) from Ashadze Hydrothermal Vent Field (Mid-Atlantic Ridge, 13 N). *International Research*, *18*, 18-21.

Bonsdorff, E., Diaz, R. J., Rosenberg, R., Norkko, A., & Cutter Jr, G. R. (1996). Characterization of soft-bottom benthic habitats of the Åland Islands, northern Baltic Sea. *Marine Ecology Progress Series, 142*, 235-245. https://doi.org/10.3354/meps142235

Borges, M., Yokoyama, L. Q., & Amaral, A. C. (2009). Gametogenic cycle of *Ophioderma januarii*, a common Ophiodermatidae (Echinodermata: Ophiuroidea) in southeastern Brazil. *Zoologia* (*Curitiba*), *26*, 118-126. https://doi.org/10.1590/S1984-46702009000100018

Boschen, R. E., Tyler, P. A., & Copley, J. T. (2013). Distribution, population structure, reproduction and diet of *Ophiolimna antarctica* (Lyman, 1879) from Kemp Caldera in the Southern Ocean. *Deep Sea Research Part II: Topical Studies in Oceanography*, *92*, 27-35. https://doi.org/10.1016/j.dsr2.2013.02.005

Boschen-Rose, R. E., & Colaco, A. (2021). Northern Mid-Atlantic Ridge hydrothermal habitats: A systematic review of knowledge status for environmental management. *Frontiers in Marine Science*, *8*, 657358. https://doi.org/10.3389/fmars.2021.657358

Brogger, M. I., Martinez, M. I., Zabala, S., & Penchaszadeh, P. E. (2013). Reproduction of *Ophioplocus januarii* (Echinodermata: Ophiuroidea): a continuous breeder in northern Patagonia, Argentina. *Aquatic Biology*, *19*(3), 275-285. http://dx.doi.org/10.3354/ab00537

Brzana, R., & Janas, U. (2016). Artificial hard substrate as a habitat for hard bottom benthic assemblages in the southern part of the Baltic Sea-a preliminary study. *Oceanological and Hydrobiological Studies*, *45*(1), 121. DOI:10.1515/ohs-2016-0012

Byrne, M. (1991). Reproduction, development and population biology of the Caribbean ophiuroid *Ophionereis olivacea*, a protandric hermaphrodite that broods its young. *Marine Biology*, *111*(3), 387-399.

Byrne, M., Cisternas, P., O'Hara, T. D., Sewell, M. A., & Selvakumaraswamy, P. (2024). Evolution of Maternal Provisioning and Development in the Ophiuroidea: Egg Size, Larval Form, and Parental Care. *Integrative and Comparative Biology*, *64*(6), 1536-1555. https://doi.org/10.1093/icb/icae048

Chausson, F. (2001). *Adaptation au milieu hydrothermal profond: étude comparative de l'écophysiology respiratoire des crustacés décapodes des dorsales Pacifique et Atlantique* (Doctoral dissertation, Paris 6).

Comtet, T., & Desbruyeres, D. (1998). Population structure and recruitment in mytilid bivalves from the Lucky Strike and Menez Gwen hydrothermal vent fields (37° 17\'N and 37° 50\'N on the Mid-Atlantic Ridge). *Marine Ecology Progress Series*, *163*, 165-177. https://doi.org/10.3354/meps163165

Convention on Biological Diversity. (2012). *Special places in the ocean: The ecologically or biologically significant marine areas (EBSAs)*. Secretariat of the Convention on Biological Diversity. https://www.cbd.int/marine/ebsa/booklet-ebsa-impact-en.pdf

Copley, J. T. P., Tyler, P. A., Murton, B. J., & Van Dover, C. L. (1997). Spatial and interannual variation in the faunal distribution at Broken Spur vent field (29 N, Mid-Atlantic Ridge). *Marine Biology*, *129*, 723-733. https://doi.org/10.1007/s002270050215

Corliss, J. B., Dymond, J., Gordon, L. I., Edmond, J. M., von Herzen, R. P., Ballard, R. D., ... & van Andel, T. H. (1979). Submarine thermal springs on the Galapagos Rift. *Science*, *203*(4385), 1073-1083. https://doi.org/10.1126/science.203.4385.1073

Cruz, M., Le Bris, N., & Colaço, A. (2022). Reproductive traits of the vent crab *Segonzacia mesatlantica* (Guinot, 1989) from the Mid-Atlantic Ridge. *Frontiers in Marine Science*, *9*, 900990. https://doi.org/10.3389/fmars.2022.900990

Desbruyères, D., Almeida, A., Biscoito, M., Comtet, T., Khripounoff, A., Le Bris, N., ... & Segonzac, M. (2000). A review of the distribution of hydrothermal vent communities along the northern Mid-Atlantic Ridge: dispersal vs. environmental controls. *In Island, Ocean and Deep-Sea Biology: Proceedings of the 34th European Marine Biology Symposium, held in Ponta Delgada (Azores), Portugal, 13–17 September 1999* (pp. 201-216). Springer Netherlands. https://doi.org/10.1023/A:1004175211848

Desbruyères, D., Biscoito, M., Caprais, J. C., Colaço, A., Comtet, T., Crassous, P., ... & Vangriesheim, A. (2001). Variations in deep-sea hydrothermal vent communities on the Mid-Atlantic Ridge near the Azores plateau. *Deep Sea Research Part I: Oceanographic Research Papers*, *48*(5), 1325-1346. https://doi.org/10.1016/S0967-0637(00)00083-2

Desbruyères, D., Hashimoto, J., & Fabri, M. C. (2006). Composition and biogeography of hydrothermal vent communities in western Pacific back-arc basins. *Geophysical monograph series*, *166*, 215-234. DOI: 10.1029/166GM11

Dobson, W. E., & Turner, R. L. (1989). Morphology and histology of the disc autotomy plane in *Ophiophragmus filograneus* (Echinodermata, Ophiurida). *Zoomorphology*, *108*(6), 323-332. https://doi.org/10.1007/BF00312273

Dover, C. L. V. (1995). Ecology of mid-Atlantic ridge hydrothermal vents. *Geological Society, London, Special Publications*, *87*(1), 257-294. https://doi.org/10.1144/GSL.SP.1995.087.01.21

Duarte, C. M., Chapuis, L., Collin, S. P., Costa, D. P., Devassy, R. P., Eguiluz, V. M., ... & Juanes, F. (2021). *The soundscape of the Anthropocene ocean. Science*, *371*(6529), eaba4658. DOI: 10.1126/science.aba4658

Eichsteller, A., Taylor, J., Stöhr, S., Brix, S., & Martìnez Arbizu, P. (2022). DNA barcoding of cold-water coral-associated ophiuroid fauna from the North Atlantic. *Diversity*, *14*(5), 358. https://doi.org/10.3390/d14050358

Escartin, J. and Andreani, M. and the Arc-en-Sub Science Party: Diversity and dynamics of ultramafic-hosted hydrothermal activity at mid-ocean ridges : first results from the Arc-en-Sub oceanographic cruise, Rainbow Massif, 36°14'N MAR, EGU General Assembly 2023, Vienna, Austria, 24–28 Apr 2023, EGU23-13265, 10.5194/egusphere-egu23-13265

Gage, J. D., & Tyler, P. A. (1982). Growth and reproduction of the deep-sea brittlestar *ophiomusiu lymani* wyville thomson. *Oceanologica acta*, *5*(1), 73-83.

Gage, J. D., & Tyler, P. A. (1991). *Deep-sea biology: a natural history of organisms at the deep-sea floor*. Cambridge University Press.

Gebruk, A. V., Galkin, S. V., Vereshchaka, A. L., Moskalev, L. I., & Southward, A. J. (1997). Ecology and biogeography of the hydrothermal vent fauna of the Mid-Atlantic Ridge. In *Advances in Marine Biology* (Vol. 32, pp. 93-144). Academic Press. https://doi.org/10.1016/S0065-2881(08)60016-4

Gebruk, A. V., Chevaldonné, P., Shank, T., Lutz, R. A., & Vrijenhoek, R. C. (2000). Deep-sea hydrothermal vent communities of the Logatchev area (14 45′ N, Mid-Atlantic Ridge): Diverse biotopes and high biomass. *Journal of the Marine Biological Association of the United Kingdom*, *80*(3), 383-393. https://doi.org/10.1017/S0025315499002088

Gebruk, A., Fabri, M. C., Briand, P., & Desbruyeres, D. (2010, January). Community dynamics over a decadal scale at Logatchev, 14 degrees 45'N, Mid-Atlantic Ridge. In *Cahiers de biologie marine* (Vol. 51, No. 4, pp. 383-388). Station biologique de Roscoff.

Georgieva, M. N., Little, C. T., Maslennikov, V. V., Glover, A. G., Ayupova, N. R., & Herrington, R. J. (2021). The history of life at hydrothermal vents. *Earth-Science Reviews*, *217*, 103602. https://doi.org/10.1016/j.earscirev.2021.103602

German, C. R., Yoerger, D. R., Jakuba, M., Shank, T. M., Langmuir, C. H., & Nakamura, K. I. (2008). Hydrothermal exploration with the autonomous benthic explorer. *Deep Sea Research Part I: Oceanographic Research Papers*, *55*(2), 203-219. https://doi.org/10.1016/j.dsr.2007.11.004

Glowka, L., Burhenne-Guilmin, F., Synge, H., McNeely, J. A., & Gündling, L. (1994). A guide to the convention on biological diversity.

Glowka, L. (2003). Putting marine scientific research on a sustainable footing at hydrothermal vents. *Marine Policy*, *27*(4), 303-312. https://doi.org/10.1016/S0308-597X(03)00042-3

Gollner, S., Colaço, A., Gebruk, A., Halpin, P. N., Higgs, N., Menini, E., ... & Van Dover, C. L. (2021). Application of scientific criteria for identifying hydrothermal ecosystems in need of protection. *Marine Policy*, *132*, 104641. https://doi.org/10.1016/j.marpol.2021.104641

Grange, L. J., Tyler, P. A., Peck, L. S., & Cornelius, N. (2004). Long-term interannual cycles of the gametogenic ecology of the Antarctic brittle star *Ophionotus victoriae*. *Marine Ecology Progress Series*, *278*, 141-155. https://doi.org/10.3354/meps278141

Grassle, J. F. (1985). Hydrothermal vent animals: distribution and biology. *Science*, *229*(4715), 713-717. https://doi.org/10.1126/science.229.4715.713

Greene, H. G., Yoklavich, M. M., Starr, R. M., O'Connell, V. M., Wakefield, W. W., Sullivan, D. E., ... & Cailliet, G. M. (1999). A classification scheme for deep seafloor habitats. *Oceanologica acta*, *22*(6), 663-678. https://doi.org/10.1016/S0399-1784(00)88957-4

Falkner, I., & Byrne, M. (2003). Reproduction of *Ophiactis resiliens* (Echinodermata: Ophiuroidea) in New South Wales with observations on recruitment. *Marine Biology*, *143*(3), 459-466. https://doi.org/10.1007/s00227-003-1066-z

Falkner, I., Sewell, M. A., & Byrne, M. (2015). Evolution of maternal provisioning in ophiuroid echinoderms: characterisation of egg composition in planktotrophic and lecithotrophic developers. *Marine Ecology Progress Series*, *525*, 1-13. https://doi.org/10.3354/meps11217

Jannasch, H. W. (1985). Review Lecture-The chemosynthetic support of life and the microbial diversity at deep-sea hydrothermal vents. *Proceedings of the Royal society of London*. *Series B. Biological sciences*, *225*(1240), 277-297. https://doi.org/10.1098/rspb.1985.0062

Juniper, S. K., Tunnicliffe, V., & Southward, E. C. (1992). Hydrothermal vents in turbidite sediments on a Northeast Pacific spreading centre: organisms and substratum at an ocean drilling site. *Canadian Journal of Zoology*, *70*(9), 1792-1809. https://doi.org/10.1139/z92-247

Konn, C., Charlou, J. L., Holm, N. G., & Mousis, O. (2015). The production of methane, hydrogen, and organic compounds in ultramafic-hosted hydrothermal vents of the Mid-Atlantic Ridge. *Astrobiology*, *15*(5), 381-399. https://doi.org/10.1089/ast.2014.1198

Halpern, B. S., Walbridge, S., Selkoe, K. A., Kappel, C. V., Micheli, F., d'Agrosa, C., ... & Watson, R. (2008). A global map of human impact on marine ecosystems. *science*, *319*(5865), 948-952. https://doi.org/10.1126/science.1149345

Hamoda, A. M., Fayed, B., Ashmawy, N. S., El-Shorbagi, A. N. A., Hamdy, R., & Soliman, S. S. (2021). Marine sponge is a promising natural source of anti-SARS-CoV-2 scaffold. *Frontiers in pharmacology*, *12*, 666664. https://doi.org/10.3389/fphar.2021.666664

Harris, P. T. (2020). Anthropogenic threats to benthic habitats. In *Seafloor geomorphology as benthic habitat* (pp. 35-61). Elsevier. https://doi.org/10.1016/B978-0-12-814960-7.00003-8

Hendler G (1991) Echinodermata: Ophiuroidea. In: Giese A, Pearse JS, Pearse VB (eds) *Reproduction of marine invertebrates,Vol VI: echinoderms and lophophorates*. Boxwood Press, Pacific Grove, CA, p 351−511

Hendler, G., & Tran, L. U. (2001). Reproductive biology of a deep-sea brittle star *Amphiura carchara* (Echinodermata: Ophiuroidea). *Marine Biology*, *138*, 113-123. https://doi.org/10.1007/s002270000446

Hinrichs, K. U., & Boetius, A. (2002). The anaerobic oxidation of methane: new insights in microbial ecology and biogeochemistry. *Ocean margin systems*, 457-477.

Hoagland, P., Beaulieu, S., Tivey, M. A., Eggert, R. G., German, C., Glowka, L., & Lin, J. (2010). Deep-sea mining of seafloor massive sulfides. *Marine Policy*, *34*(3), 728-732. https://doi.org/10.1016/j.marpol.2009.12.001

Holden, J. F., Breier, J. A., Rogers, K. L., Schulte, M. D., & Toner, B. M. (2012). Biogeochemical processes at hydrothermal vents: microbes and minerals, bioenergetics, and carbon fluxes. *Oceanography*, 25(1), 196-208. https://www.jstor.org/stable/24861158

Huang, Z., Brooke, B. P. et Harris, P. T. (2011). A new approach to mapping marine benthic habitats using physical environmental data. *Continental Shelf Research*, *31*(2), S4-S16. http://dx.doi.org/10.1016/j.csr.2010.03.012

Joydas, T. V., & Borja, A. N. G. E. L. (2019). Benthic ecosystems (soft and hard substrata). *Ecosystems and biodiversity of the Arabian Gulf: fifty years of scientific research. Saudi Aramco & King Fahd University of Petroleum & Minerals, Dhahran,* 222-253.

Fisher, C. R., Childress, J. J., Arp, A. J., Brooks, J. M., Distel, D. L., Dugan, J. A., ... & Soto, T. (1988). Variation in the hydrothermal vent clam, Calyptogen magnifica, at the Rose Garden vent on the Galapagos spreading center. *Deep Sea Research Part A. Oceanographic Research Papers*, *35*(10-11), 1811-1831. https://doi.org/10.1016/0198-0149(88)90051-9

Fisher, C. R., Takai, K., & Le Bris, N. (2007). Hydrothermal vent ecosystems. *Oceanography*, *20*(1), 14-23. https://www.jstor.org/stable/24859970

Laming, S. R., Christodoulou, M., Martinez Arbizu, P., & Hilário, A. (2021). Comparative reproductive biology of deep-sea ophiuroids inhabiting polymetallic-nodule fields in the Clarion-Clipperton Fracture Zone. *Frontiers in Marine Science*, *8*, 663798. https://doi.org/10.3389/fmars.2021.663798

Le Bris, N., & Gaill, F. (2007). How does the annelid *Alvinella pompejana* deal with an extreme hydrothermal environment?. *Reviews in Environmental Science and Bio/Technology*, *6*, 197-221. https://doi.org/10.1007/s11157-006-9112-1

Lecours, V., Devillers, R., Schneider, D. C., Lucieer, V. L., Brown, C. J., & Edinger, E. N. (2015). Spatial scale and geographic context in benthic habitat mapping: review and future directions. *Marine Ecology Progress Series*, *535*, 259-284. https://doi.org/10.3354/meps

Levin, L. A., Baco, A. R., Bowden, D. A., Colaco, A., Cordes, E. E., Cunha, M. R., ... & Watling, L. (2016). Hydrothermal vents and methane seeps: rethinking the sphere of influence. *Frontiers in Marine Science*, *3*, 72. https://doi.org/10.3389/fmars.2016.00072

Lin, T. H., Chen, C., Watanabe, H. K., Kawagucci, S., Yamamoto, H., & Akamatsu, T. (2019). Using soundscapes to assess deep-sea benthic ecosystems. *Trends in Ecology & Evolution*, *34*(12), 1066-1069.

Loh, T. L., Archer, S. K., & Dunham, A. (2019). Monitoring program design for data-limited marine biogenic habitats: A structured approach. *Ecology and Evolution*, *9*(12), 7346-7359. https://doi.org/10.1002/ece3.5261

Lough, A. J. M., Tagliabue, A., Demasy, C., Resing, J. A., Mellett, T., Wyatt, N. J., & Lohan, M. C. (2022). The impact of hydrothermal vent geochemistry on the addition of iron to the deep ocean. *Biogeosciences Discussions, 2022*, 1-23. https://doi.org/10.5194/bg-20-405-2023, 2023.

MacNeil, C., Baker, M., Copley, J., Tyler, P., Hilario, A., & Ramirez-Llodra, E. (2025). Reproductive biology of two hydrothermal vent Cocculinidae species (Mollusca: Gastropoda) from the Arctic and Southern Ocean. *Marine Biology*, *172*(7), 114. https://doi.org/10.1007/s00227-025-04648-x

Macpherson, E., Jones, W., & Segonzac, M. (2005). A new squat lobster family of Galatheoidea (Crustacea, Decapoda: Anomura) from the hydrothermal vents of the Pacific-Antarctic Ridge.

Märkel, K., & Röser, U. (1985). Comparative morphology of echinoderm calcified tissues: Histology and ultrastructure of ophiuroid scales (Echinodermata, Ophiuroida). *Zoomorphology*, *105*(3), 197-207. https://doi.org/10.1007/BF00312157

Marticorena, J., Matabos, M., Sarrazin, J., & Ramirez-Llodra, E. (2020). Contrasting reproductive biology of two hydrothermal gastropods from the Mid-Atlantic Ridge: implications for resilience of vent communities. *Marine Biology*, *167*(8), 109. https://doi.org/10.1007/s00227-020-03721-x

McIntyre, A. (Ed.). (2010). *Life in the world's oceans: Diversity, distribution, and abundance*. John Wiley & Sons.

Menini, E., & Van Dover, C. L. (2019). An atlas of protected hydrothermal vents. *Marine Policy*, *108*, 103654. https://doi.org/10.1016/j.marpol.2019.103654

Mora, C., & Sale, P. F. (2011). Ongoing global biodiversity loss and the need to move beyond protected areas: a review of the technical and practical shortcomings of protected areas on land and sea. *Marine ecology progress series*, *434*, 251-266. https://doi.org/10.3354/meps

Mullineaux, L. S., Metaxas, A., Beaulieu, S. E., Bright, M., Gollner, S., Grupe, B. M., ... & Won, Y. J. (2018). Exploring the ecology of deep-sea hydrothermal vents in a metacommunity framework. *Frontiers in Marine Science*, *5*, 49. https://doi.org/10.3389/fmars.2018.00049

Murton, B. J., Klinkhammer, G., Becker, K., Briais, A., Edge, D., Hayward, N., ... & Parson, L. (1994). Direct evidence for the distribution and occurrence of hydrothermal activity between 27 N–30 N on the Mid-Atlantic Ridge. *Earth and Planetary Science Letters*, *125*(1-4), 119-128. https://doi.org/10.1016/0012-821X(94)90210-0

Murton, B. J., Van Dover, C., & Southward, E. (1995). Geological setting and ecology of the Broken Spur hydrothermal vent field: 29 10′ N on the Mid-Atlantic Ridge. *Geological Society, London, Special Publications*, *87*(1), 33-41. https://doi.org/10.1144/GSL.SP.1995.087.01.

Nesbitt, R. W., & Murton, B. J. (1995). Chimney Growth Rates and Metal Deposition at the Broken Spur Vent Field, 29N MAR: a Correction and Further Speculation. *BRIDGE Newsletter*, (9), 38-41.

Nye, V., Copley, J. T., & Tyler, P. A. (2013). Spatial variation in the population structure and reproductive biology of *Rimicaris hybisae* (Caridea: Alvinocarididae) at hydrothermal vents on the Mid-Cayman Spreading Centre. *PLoS One*, *8*(3), e60319. https://doi.org/10.1371/journal.pone.0060319

O'Hara, T. D., England, P. R., Gunasekera, R. M., & Naughton, K. M. (2014). Limited phylogeographic structure for five bathyal ophiuroids at continental scales. *Deep Sea Research Part I: Oceanographic Research Papers*, *84*, 18-28. https://doi.org/10.1016/j.dsr.2013.09.009

O'Mullan, G. D., Maas, P. A. Y., Lutz, R. A., & Vrijenhoek, R. C. (2001). A hybrid zone between hydrothermal vent mussels (Bivalvia: Mytilidae) from the Mid-Atlantic Ridge. *Molecular Ecology*, *10*(12), 2819-2831. https://doi.org/10.1046/j.0962-1083.2001.01401.x

Pearson, H. C., Savoca, M. S., Costa, D. P., Lomas, M. W., Molina, R., Pershing, A. J., ... & Roman, J. (2023). Whales in the carbon cycle: can recovery remove carbon dioxide?. *Trends in Ecology & Evolution*, *38*(3), 238-249.

Radziejewska, T., Błażewicz, M., Włodarska-Kowalczuk, M., Jóźwiak, P., Pabis, K., & Węsławski, J. M. (2022). Benthic biology in the Polish exploration contract area of the Mid-Atlantic Ridge: The knowns and the unknowns. A review. *Frontiers in Marine Science*, *9*, 898828. https://doi.org/10.3389/fmars.2022.898828

Rakka, M. (2024). *Histological processing of octocoral tissue* (Version 1). protocols.io. dx.doi.org/10.17504/protocols.io.81wgbx38nlpk/v1

Llodra, E. R. (2002). Fecundity and life-history strategies in marine invertebrates. https://doi.org/10.1016/S0065-2881(02)43004-0

Ramirez-Llodra, E., Brandt, A., Danovaro, R., De Mol, B., Escobar, E., German, C. R., ... & Vecchione, M. (2010). Deep, diverse and definitely different: unique attributes of the world's largest ecosystem. *Biogeosciences*, *7*(9), 2851-2899. https://doi.org/10.5194/bg-7-2851-2010

Ramirez-Llodra, E., Tyler, P. A., Baker, M. C., Bergstad, O. A., Clark, M. R., Escobar, E., ... & Van Dover, C. L. (2011). Man and the last great wilderness: human impact on the deep sea. *PLoS one*, *6*(8), e22588. https://doi.org/10.1371/journal.pone.0022588

Resing, J. A., Sedwick, P. N., German, C. R., Jenkins, W. J., Moffett, J. W., Sohst, B. M., & Tagliabue, A. (2015). Basin-scale transport of hydrothermal dissolved metals across the South Pacific Ocean. *Nature*, *523*(7559), 200-203. https://doi.org/10.1038/nature14577

Richer de Forges, B., Koslow, J. A., & Poore, G. C. B. (2000). Diversity and endemism of the benthic seamount fauna in the southwest Pacific. *Nature*, *405*(6789), 944-947. https://doi.org/10.1038/35016066

Ritchie, H., & Roser, M. (2021). Fish and overfishing. *Our World in Data*.

Roberts, J. M. (2009). *Cold-water corals: the biology and geology of deep-sea coral habitats*. Cambridge University Press.

Rodrigues, C. F., Paterson, G. L., Cabrinovic, A., & Cunha, M. R. (2011). Deep-sea ophiuroids (Echinodermata: Ophiuroidea: Ophiurida) from the Gulf of Cadiz (NE Atlantic). *Zootaxa*, *2754*(1), 1-26. https://doi.org/10.11646/zootaxa.2754.1.1

Rogers, A. D., Tyler, P. A., Connelly, D. P., Copley, J. T., James, R., Larter, R. D., ... & Zwirglmaier, K. (2012). The discovery of new deep-sea hydrothermal vent communities in the Southern Ocean and implications for biogeography. *PLoS biology*, *10*(1), e1001234. https://doi.org/10.1371/journal.pbio.1001234

Rona, P., Guard, C. C., & Sector, O. (2010). *Photo credits.* In Fisheries and Oceans Canada (DFO), *Endeavour Hydrothermal Vents Marine Protected Area Management Plan 2010–2015* (pp. 1–43).

Saeed, A. F., Su, J., & Ouyang, S. (2021). Marine-derived drugs: Recent advances in cancer therapy and immune signaling. *Biomedicine & Pharmacotherapy*, *134*, 111091. https://doi.org/10.1016/j.biopha.2020.111091

Santos, R. S., Colaço, A., & Christiansen, S. (2003). *Planning the management of deep-sea hydrothermal vent fields MPA in the Azores Triple Junction*.

Sardà, F., Company, J. B., Bahamón, N., Rotllant, G., Flexas, M. M., Sánchez, J. D., ... & Espino, M. (2009). Relationship between environment and the occurrence of the deep-water rose shrimp *Aristeus antennatus* (Risso, 1816) in the Blanes submarine canyon (NW Mediterranean). *Progress in Oceanography*, *82*(4), 227-238. https://doi.org/10.1016/j.pocean.2009.07.001

Schander, C., Rapp, H. T., Kongsrud, J. A., Bakken, T., Berge, J., Cochrane, S., ... & Pedersen, R. B. (2010). The fauna of hydrothermal vents on the Mohn Ridge (North Atlantic). *Marine Biology Research*, *6*(2), 155-171. https://doi.org/10.1080/17451000903147450

Schmidt, L. A., Brix, S., Rossel, S., Forster, S., & Eichsteller, A. (2024). Unveiling ophiuroid biodiversity across North Atlantic habitats via an integrative perspective. *Scientific Reports*, *14*(1), 20405. https://doi.org/10.1038/s41598-024-71178-9

Schwarz, G. (1978). Estimating the dimension of a model. *The annals of statistics*, 461-464. https://www.jstor.org/stable/2958889

Segonzac, M., & Desbruyères, D. (1997). Handbook of deep-sea hydrothermal vent fauna.

Selvakumaraswamy, P., & Byrne, M. (1995). Reproductive cycle of two populations of *Ophionereis schayeri* (Ophiuroidea) in New South Wales. *Marine Biology*, *124*(1), 85-97. https://doi.org/10.1007/BF00349150

Sevgen, S., Le Bris, N., & Yücel, M. (2025). The control of end-member iron-to-sulfide ratios on hydrothermal plume geochemistry at the Rainbow, Broken Spur, and Lost City vent fields in the Mid-Atlantic Ridge. *Geochemistry, Geophysics, Geosystems*, *26*(7), e2025GC012370. https://doi.org/10.1029/2025GC012370

Shanks, A. L. (2009). Pelagic larval duration and dispersal distance revisited. *The biological bulletin*, *216*(3), 373-385.

Smirnov, A. V., Gebruk, A. V., Galkin, S. V., & Shank, T. (2000). New species of holothurian (Echinodermata: Holothuroidea) from hydrothermal vent habitats. J*ournal of the Marine Biological Association of the United Kingdom, 80*(2), 321-328. https://doi.org/10.1017/S0025315499001897

Spalding, M. D., Agostini, V. N., Rice, J., & Grant, S. M. (2012). Pelagic provinces of the world: A biogeographic classification of the world's surface pelagic waters. *Ocean & Coastal Management*, *60*, 19-30. https://doi.org/10.1016/j.ocecoaman.2011.12.016

Stohr, S., & Segonzac, M. (2006). Two new genera and species of ophiuroid (Echinodermata) from hydrothermal vents in the East Pacific. *Species diversity*, *11*(1), 7-32. https://doi.org/10.12782/specdiv.11.7

Sumida, P. Y. G., Tyler, P. A., Lampitt, R. S., & Gage, J. D. (2000). Reproduction, dispersal and settlement of the bathyal ophiuroid *Ophiocten gracilis* in the NE Atlantic Ocean. *Marine Biology*, *137*, 623-630. https://doi.org/10.1007/s002270000376

Thatje, S., Marsh, L., Roterman, C. N., Mavrogordato, M. N., & Linse, K. (2015). Adaptations to hydrothermal vent life in *Kiwa tyleri*, a new species of yeti crab from the East Scotia Ridge, Antarctica. *PLoS One*, *10*(6), e0127621. https://doi.org/10.1371/journal.pone.0127621

Tunnicliffe, V. (1991). The biology of hydrothermal vents: ecology and evolution. *Oceanogr Mar Biol Annu Rev*, *29*, 319-407.

Turner, P. J., Thaler, A. D., Freitag, A., & Collins, P. C. (2019). Deep-sea hydrothermal vent ecosystem principles: identification of ecosystem processes, services and communication of value. *Marine Policy*, *101*, 118-124. https://doi.org/10.1016/j.marpol.2019.01.003

Tyler, P. A., Paterson, G. J. L., Sibuet, M., Murton, B. J., & Segonzac, M. (1995). A new genus of ophiuroid (Echinodermata: Ophiuroidea) from hydrothermal mounds along the Mid-Atlantic Ridge. *Journal of the Marine Biological Association of the United Kingdom*, *75*(4), 977-986. https://doi.org/10.1017/S0025315400038303

Tyler, P. A., & Young, C. M. (1999). Reproduction and dispersal at vents and cold seeps. *Journal of the Marine Biological Association of the United Kingdom*, *79*(2), 193-208. https://doi.org/10.1017/S0025315499000235

Tyler, P. A. (Ed.). (2003). *Ecosystems of the deep oceans* (Vol. 28). Elsevier.

Tyler, P. A., Pendlebury, S., Mills, S. W., Mullineaux, L., Eckelbarger, K. J., Baker, M., & Young, C. M. (2008). Reproduction of gastropods from vents on the East Pacific Rise and the Mid-Atlantic Ridge. *Journal of Shellfish Research*, *27*(1), 107-118. https://doi.org/10.2983/0730-8000(2008)27[107:ROGFVO]2.0.CO;2

Tyler, P. A., Baker, M., & Ramirez-Llodra, E. (2016). Deep-sea benthic habitats. *Biological sampling in the deep sea*, 1-15. https://doi.org/10.1002/9781118332535.ch1

Van Dover, C. L., Fry, B., Grassle, J. F., Humphris, S., & Rona, P. A. (1988). Feeding biology of the shrimp *Rimicaris exoculata* at hydrothermal vents on the Mid-Atlantic Ridge. *Marine Biology*, *98*, 209-216. https://doi.org/10.1007/BF00391196

Van Dover, C. L., Berg Jr, C. J., & Turner, R. D. (1988). Recruitment of marine invertebrates to hard substrates at deep-sea hydrothermal vents on the East Pacific Rise and Galapagos spreading center. *Deep Sea Research Part A. Oceanographic Research Papers*, *35*(10-11), 1833-1849. https://doi.org/10.1016/0198-0149(88)90052-0

Van Dover, C. L., German, C. R., Speer, K. G., Parson, L. M., & Vrijenhoek, R. C. (2002). Evolution and biogeography of deep-sea vent and seep invertebrates. *science*, *295*(5558), 1253-1257. https://doi.org/10.1126/science.1067361

Van Dover, C. L., & Doerries, M. B. (2005). Community structure in mussel beds at Logatchev hydrothermal vents and a comparison of macrofaunal species richness on slow-and fast-spreading mid-ocean ridges. *Marine Ecology*, *26*(2), 110-120. https://doi.org/10.1111/j.1439-0485.2005.00047.x

Van Dover, C. L. (2014). Impacts of anthropogenic disturbances at deep-sea hydrothermal vent ecosystems: a review. *Marine environmental research*, *102*, 59-72. https://doi.org/10.1016/j.marenvres.2014.03.008

Van Dover, C. L., Arnaud-Haond, S., Gianni, M., Helmreich, S., Huber, J. A., Jaeckel, A. L., ... & Yamamoto, H. (2018). Scientific rationale and international obligations for protection of active hydrothermal vent ecosystems from deep-sea mining. *Marine Policy*, *90*, 20-28. https://doi.org/10.1016/j.marpol.2018.01.020

Viegas, C., Juliano, M., & Colaço, A. (2024). Larval dispersal and physical connectivity of *Pheronema carpenteri* populations in the Azores. Frontiers in Marine Science, 11, 1393385. https://doi.org/10.3389/fmars.2024.1393385

Vinogradova, N. G. (1979). The geographical distribution of the abyssal and hadal (ultra-abyssal) fauna in relation to the vertical zonation of the ocean. *Sarsia*, *64*(1-2), 41-50. https://doi.org/10.1080/00364827.1979.10411361

Vivian, O. O., Kelechi, I. N., Ademola, L., Victory, O. K., Victor, A., Chukwudalu, E., & Chinazaepkere, A. M. (2023). Submarine canyon: A brief review. *Authorea Preprints*. https://doi.org/10.22541/essoar.167591083.32767863/v1

Von Damm, K. L. (1995). Controls on the chemistry and temporal variability of seafloor hydrothermal fluids. *Seafloor hydrothermal systems: Physical, chemical, biological, and geological interactions*, *91*, 222-247. https://doi.org/10.1029/GM091p0222

Wilkie, I. C. (2016). Functional morphology of the arm spine joint and adjacent structures of the brittlestar *Ophiocomina nigra* (Echinodermata: Ophiuroidea). *PLoS One*, *11*(12), e0167533. https://doi.org/10.1371/journal.pone.0167533

Williams, A., Schlacher, T. A., Rowden, A. A., Althaus, F., Clark, M. R., Bowden, D. A., ... & Kloser, R. J. (2010). Seamount megabenthic assemblages fail to recover from trawling impacts. *Marine Ecology*, *31*, 183-199. https://doi.org/10.1111/j.1439-0485.2010.00385.x

Wolff, T. (2005). Composition and endemism of the deep-sea hydrothermal vent fauna. *CBM-Cahiers de Biologie Marine., 46*(2), 97-104.

Won, Y., Hallam, S. J., O'mullan, G. D., & Vrijenhoek, R. C. (2003). Cytonuclear disequilibrium in a hybrid zone involving deep-sea hydrothermal vent mussels of the genus Bathymodiolus. *Molecular Ecology, 12*(11), 3185-3190. https://doi.org/10.1046/j.1365-294X.2003.01974.x

Yamaguchi, R., Kouketsu, S., Kosugi, N., & Ishii, M. (2024). Global upper ocean dissolved oxygen budget for constraining the biological carbon pump. *Communications Earth & Environment*, *5*(1), 732. https://doi.org/10.1038/s43247-024-01886-7